APAE-23

REACTORS—POWER

UNITED STATES ATOMIC ENERGY COMMISSION

APPR-1: DESIGN, CONSTRUCTION AND OPERATION

November 20, 1957

Alco Products, Inc.
Schenectady, New York

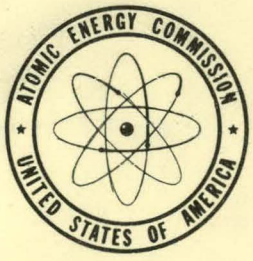

Technical Information Service Extension, Oak Ridge, Tenn.

DISCLAIMER

Printed in USA. Price $3.00. Available from the Office of Technical Services, Department of Commerce, Washington 25, D. C.

AEC Technical Information Service Extension
Oak Ridge, Tennessee

APAE-23

APPR - 1

DESIGN, CONSTRUCTION & OPERATION

CONTRACT NO. AT (11-1)-318

Issued November 20, 1957

ALCO PRODUCTS, INC.
POST OFFICE BOX 414
SCHENECTADY, NEW YORK

THIS PAGE

WAS INTENTIONALLY

LEFT BLANK

TABLE OF CONTENTS

APPR-1 PLANT DESIGN AND CONSTRUCTION

BY

K. Kasschau, Alco Products, Inc.

C. T. Chave, Stone and Webster Engineering Corp.

This document includes papers covering technical problems involved in the design, construction and operation of the APPR-1. These papers were presented at the second winter meeting of the American Nuclear Society on October 28, 1957 in New York City.

Presented at the Second Winter Meeting of The American Nuclear Society on October 28, 1957 in New York City.

LIST OF FIGURES

APPR-1 DESIGN AND CONSTRUCTION

I. Introduction

The Army Package Power Reactor concept was originated by Oak Ridge National Laboratory. The basic idea of a reactor plant which could be built at a remote location by transportation of the components, as distinguished from a strictly portable plant, was embodied in the Oak Ridge concept, as was the preliminary design of the reactor and the power plant steam cycle. All of this was set forth in Document No. ORNL-1613, which was made available to organizations desiring to bid on the construction of such a plant at Fort Belvoir, Virginia.

Construction at the Fort involved the concept of vapor containment and other special safety features which may or may not be considered necessary in a remote location. Alco and Stone & Webster worked on these problems from the outset, through the proposal, design, construction and preliminary operation stages. As you know, the plant has, in the summer of 1957, completed the 700-hr test.

The APPR-1 in many respects was a pioneering job in which ideas were generated both at the Stone & Webster and Alco engineering establishments which have been repeated elsewhere. While we do not claim to be the originators of these ideas and say that others have copied them, as often happens, thoughts occur to a great many designers almost simultaneously, and in late 1954 and early 1955 these ideas were being discussed under security regulations with many cleared engineers. Through the progress of the design and construction,

the new concepts, or at least those which were new to Alco and Stone & Webster, had to be developed, modified and put into practice. It represents part of an evolution of thinking, at least on the part of the Stone & Webster organization, which has resulted in some of today's designs, which are in many respects markedly different from the APPR and in many respects the same.

II. Discussion

The first problem was to contain the nuclear reactor and primary loop in a safe manner. We had seen many ideas of containment, including placing the entire plant in a sphere or some type of vaportight Quonset hut, or a rectangular box designed mostly of concrete but which is supposed to be pressuretight, but they did not attract us.

When we started on the Alco job we had already developed a concept of containment for the Pressurized Water Reactor at Shippingport, which involved a number of horizontal bullets. During the development of this job, we acquired or evolved (we can't remember which) certain ideas. These included leaktight containment in pressure vessels, consideration of missile protection of the vapor container, means for testing with tracers such as helium or Freon gas, means for calculating the volume and design pressure of the containment, and economic means for shielding.

Referring to Figure 1, which is an artist's cutaway of the power plant at Fort Belvoir, Virginia, you see that the reactor, steam generator, primary circulating pumps and pressurizer are housed in a vertical bullet. The APPR-1 gave us a fine opportunity to second-guess the PWR. We therefore used a

vertical bullet instead of a horizontal bullet, which was justified on the grounds that the plant being smaller, the difficulties encountered in constructing a tall vertical cylinder of large diameter were removed. In order to aid further in achieving this, a vertical steam generator was proposed. For small plants, we think that this approach has now become standard. The EBWR at Argonne National Laboratories is also contained in a vertical bullet. Stone & Webster has proposed a similar arrangement for Carolinas Virginia, whose proposal is now before the Atomic Energy Commission.

We currently think horizontal vapor containers are apt to be a mess, especially due to secondary stresses induced at supports and the need for stiffening rings just to keep them round.

The vertical steam generator has also become fairly standard. It lends itself far more readily to a confined space where there is ample vertical clearance. Four such steam generators will be used in the Yankee Atomic Electric Company plant, and we note that similar steam generators are being used on the Dresden power plant.

Looking further at Figure 1, we see that the interior of the steel bullet is lined with concrete and, as a matter of fact, so is a portion of the exterior. This interior concrete lining provides for protection against missiles resulting from a rupture of the pressure parts, and is designed to stop a missile weighing 50 lb. and traveling at 700 fps. There are difficulties with a design of this kind which must be realized. Unless the concrete lining can be made to work with the steel shell when the pressure is imposed, severe cracking and disintegration will result, and as we got into the design work we developed rather heavy

reinforcing and the expense was higher than expected. The inner lining had 1 1/4 in. bars on 6 in. centers both ways, forming two concentric "birdcages." In the future, we would attempt to separate the concrete lining from the shell, and this has been done on the designs with spherical vapor containers, such as for Yankee.

To do this probably required that access space should be provided between the concrete and the shell to permit decontamination, and may mean a larger shell for a small reactor plant. Another approach is to put all of the biological shielding on the outside, but this eliminates missile protection. Serious thought is being given to means for anchoring and restraining potential missiles rather than trying to stop the flying pieces. Such a design might permit the bullet to be partly buried where subsoil and water conditions permit, thur saving much expensive concrete.

APPR-1 is especially elegant in regard to the protection of the interior concrete, which is lined throughout with a thin steel liner. We thought this was a good idea, but would probably never repeat it. This inner shell, furnished by Posey Iron Works, had to be erected in lifts along with the interior concrete, and served as formwork. It was a tricky job, particularly in the hemispherical head, and made it necessary to pump the concrete. On PWR, Amercoat is used. The question to be considered is, how much insurance should we take out against the owner's property damage caused by an incident whose likelihood is considered remote?

May I say right here that vapor containment is a serious obstacle to competitive nuclear power, and we should all be putting our minds on means to reduce the cost, if not dispense with it entirely. I am convinced that much of the security it offers is specious.

You see outside of the bullet a spent fuel pit. This communicates with the vapor container through an inclined chute, and the water level in the pit is carried right up to the level in the fuel handling cavity inside the shield tank and over the reactor. With this arrangement, individual fuel elements can be removed from the reactor under water and transferred through the inclined tube to the external fuel pit. The chute is plugged during operation.

This was an important concept. The entire Shippingport design, with its multiple containers and large fuel canals, evolved solely around the requirement that a complete core be removable from the reactor. Elimination of this requirement for the removal of a complete core resulted in great simplification of the spent fuel handling facilities. This idea is carried on through several current designs, and is one of the basic concepts of the Yankee design, although here we have had to modify the idea of having the water levels equal and will use a hydraulic lift mechanism in the inclined tube which will permit the transfer of fuel, with the water level in the spent fuel pit considerably lower than the water level above the opened reactor.

Having referred to Yankee several times, see Figure 2, which is a cross section of the container, to show how the design has evolved with us. Here we see the APPR-1 shield and missile protection structure supported independently inside a bare sphere. Because of the remote location, we have dispensed

with the biological shielding outside the sphere which would otherwise protect those close by in case of an incident.

The ideas expressed here were largely generated on APPR-1.

It was recognized early in the program that the erection sequence for the vapor container would have to be planned carefully. To pressure test and leak test the container successfully, it was essential to test the empty shell before any interior work could be initiated. Otherwise, detection and repair of leaks would become almost impossible.

Figure 3 shows the actual construction sequence followed. The shell was built first and, after testing, the concrete work was resumed inside to form the equipment foundation and the missile protection lining. The latter required seven lifts, each one setting for seven days before the next lift could be poured. The interim period was used for doing outside concrete work and raising the inner steel liner which served as the inner form, as well as forming the impervious inner lining considered desirable to prevent contamination penetration.

Once the inner concrete work was completed, installation of the equipment could proceed. The access hatch, at grade level, was not large enough to pass most of the equipment. For this reason, an equipment loading hatch at the top of the container had been provided. All major components, including the reactor vessel, were hoisted by crane some 80 ft in the air and lowered through the hatch to their final position.

The shell was given a hydrostatic test, followed by a helium leak test. The hydrostatic test gives one a good feeling, but it can not be made on large vapor containers. If consistency has any virtue, except as the last refuge of a scoundrel, vapor container design is most lacking in this virtuous quality.

The helium or a Freon leak test makes much more sense to us than a pressure reduction test. Temperature changes so mask the effects of leakage that the results of pressure readings are inconclusive. The only sound way to detect small leaks in a large vessel is with a tracer.

Turning our attention to the shield tank surrounding the reactor, this design had to be special because of the necessity to transport it. In plants designed for easy access, we would normally build such a shield tank using an annular tank containing about 2 ft of water surrounded by a cylinder of concrete, probably 5 ft thick. This concept is getting to be standard. It should be observed in passing that concrete alone will not work because of the heat absorption and that a tank of water or some other effective method of cooling is a necessity.

Referring, however, to Figure 4, we see that on the APPR-1 no concrete was used. A number of concentric cylinders of steel are employed to absorb gamma radiation and transfer the heat to the surrounding water. This design then permits the steel plates to be transported to a remote side and the entire shield tank to be field erected around the reactor.

The secondary plant, consisting of a steam turbine generator operating at 200 psi and 25 F superheat, contains nothing truly remarkable, but there are some features which are worthy of mention.

In the first place, an evaporator, as disclosed in ORNL-1613, is used to handle raw make-up water, as opposed to a demineralizer, and this was selected after considerable discussion and analysis. We think this choice is correct for a plant which is likely to go into almost any location and for which the design must be standarized. Unlike the Oak Ridge concept, we used a deaerating condenser instead of a deaerating heater. This allowed us to pump boiler feed directly from the hot well to the steam generator.

An important feature which is introduced into this plant, and which has been proposed for many plants since, is a direct by-pass from the steam generator to the condenser. This eases the control problem in regard to dropping load. It also permits the reactor to be operated at low load without the need to operate the generating equipment. As a part of this system, we used a steam turbine driven boiler feed pump, which can allow the reactor to coast down while still pumping feed water to the steam generators. On a small plant like this, it removes the need for special shutdown cooling apparatus.

Another feature of this APPR-1 is a low pressure primary coolant purification system, in which the pressurizer is bled through reducing valves to an outside tank from which feed water may be returned to the reactor. In the case of APPR-1, the bled stream flowed through ion exchangers. On a larger plant such as Yankee, there might be a separate circuit for circulating water from the low pressure water surge tank through the ion exchanger. This low pressure surge tank offers a comvenient point in which to inject hydrogen into the system, and by maintaining hydrogen under moderate pressure the hydrogen concentration can be kept at from 15-25 cc per liter.

II. Conclusion

There is not time to describe in detail construction and operating experience with the plant, except to say that construction was accomplished without major difficulty and that the plant works essentially as it was designed to do. I won't claim there were no hitches. It is only the lad who is there the first time who expects a construction and plant start-up job to go off click-click-click. These things we accomplished by continuous planning, contriving and striving. The two companies had the men to do it, and that is why the job is successful.

Figure 5 shows the finished job. Greater detail will be presented by the subsequent speakers.

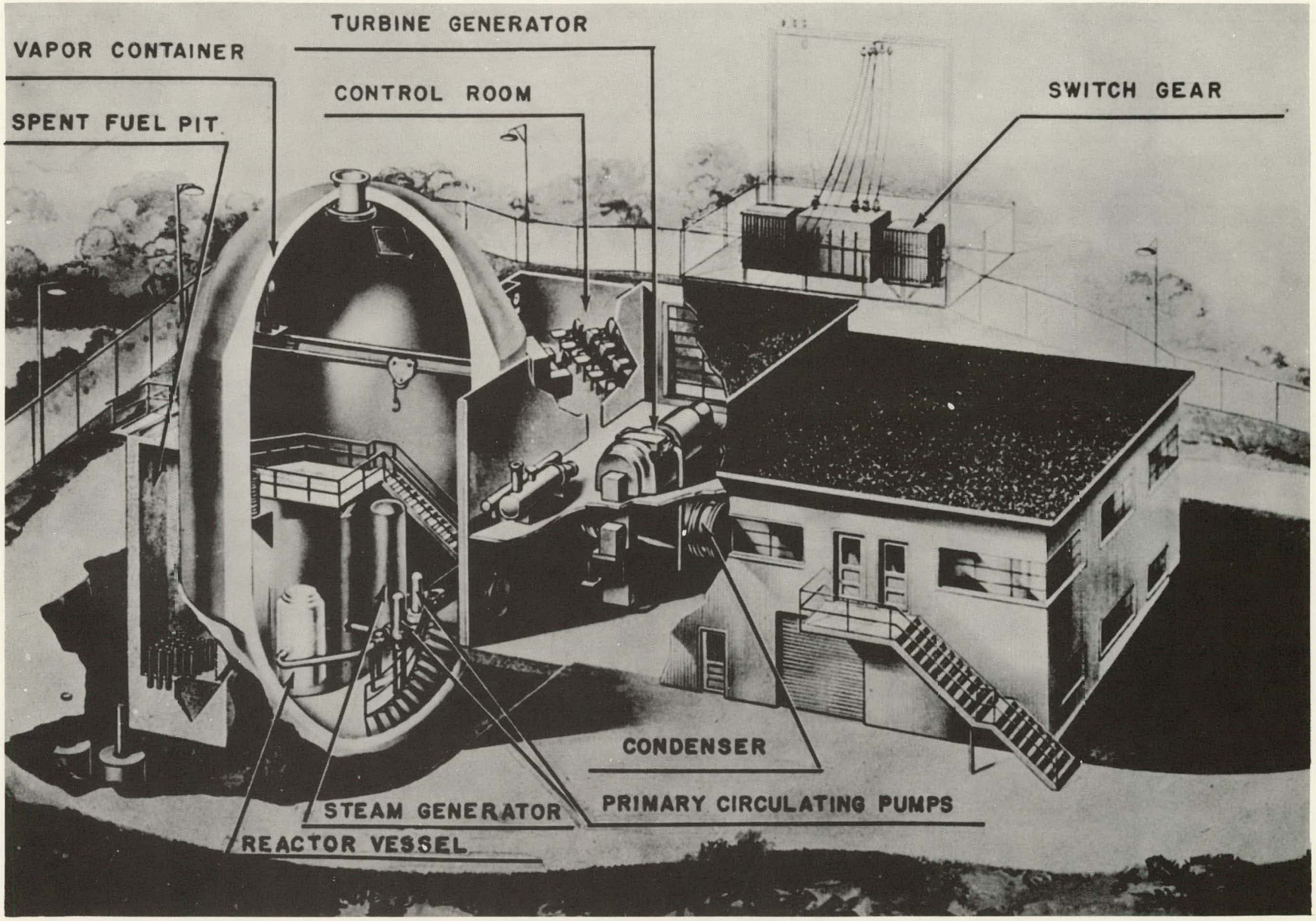

Fig. 1 Cutaway of the APPR-1

Fig. 2 Elevation of the Yankee Atomic Electric Plant

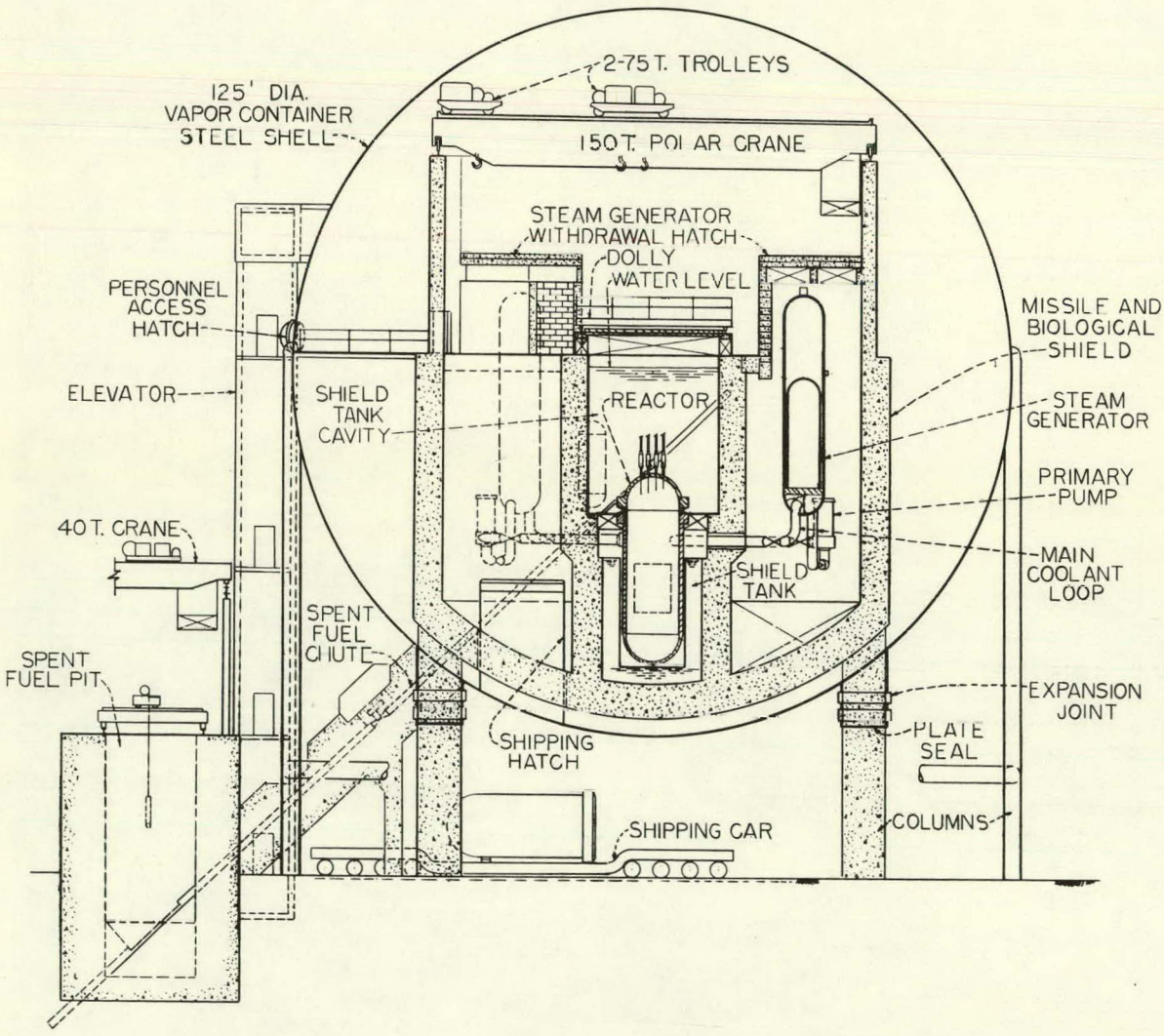

Fig. 3 Vapor Container and Primary Piping Sequence

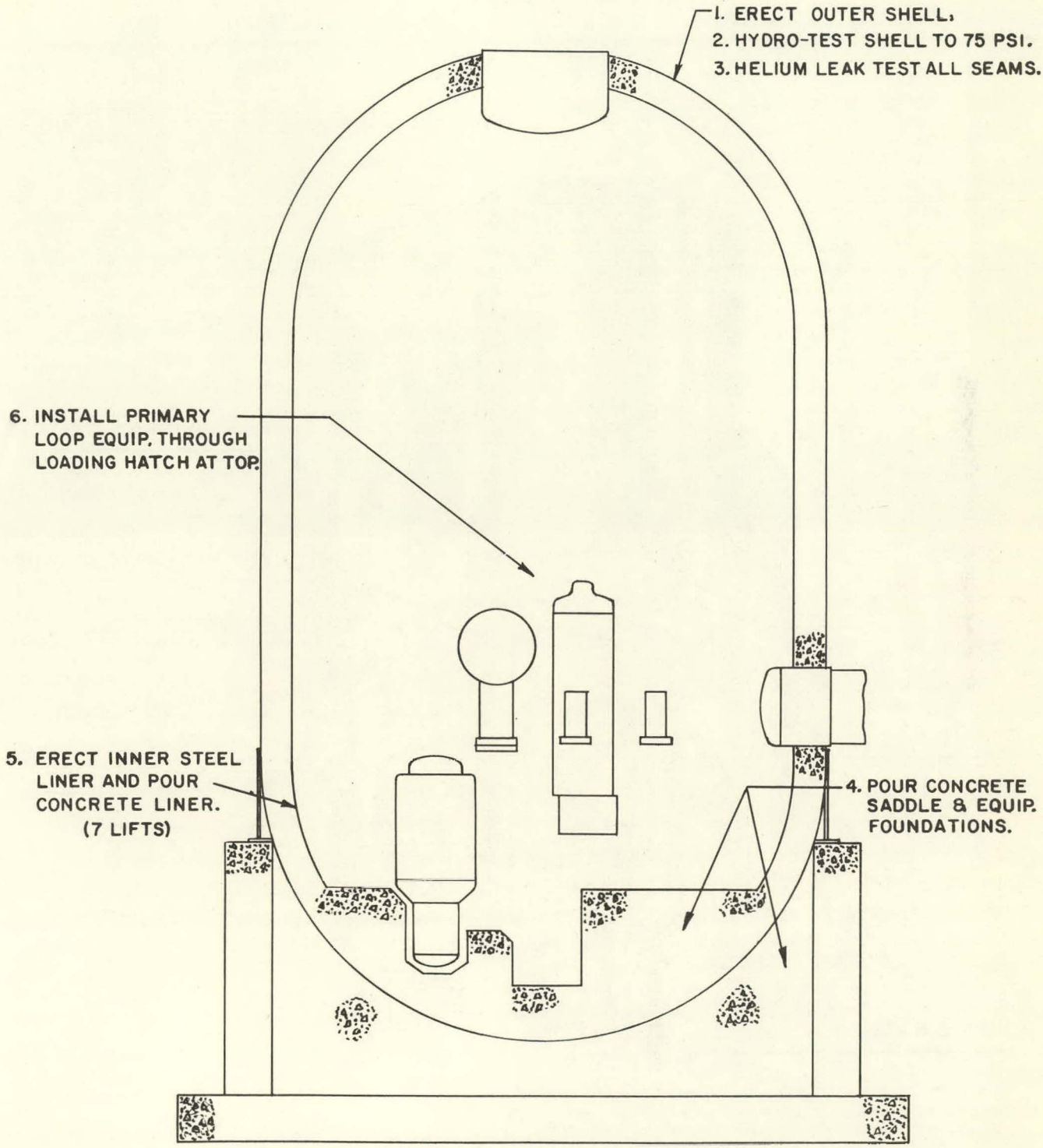

Fig. 4 Reactor Core, Pressure Vessel and Shield

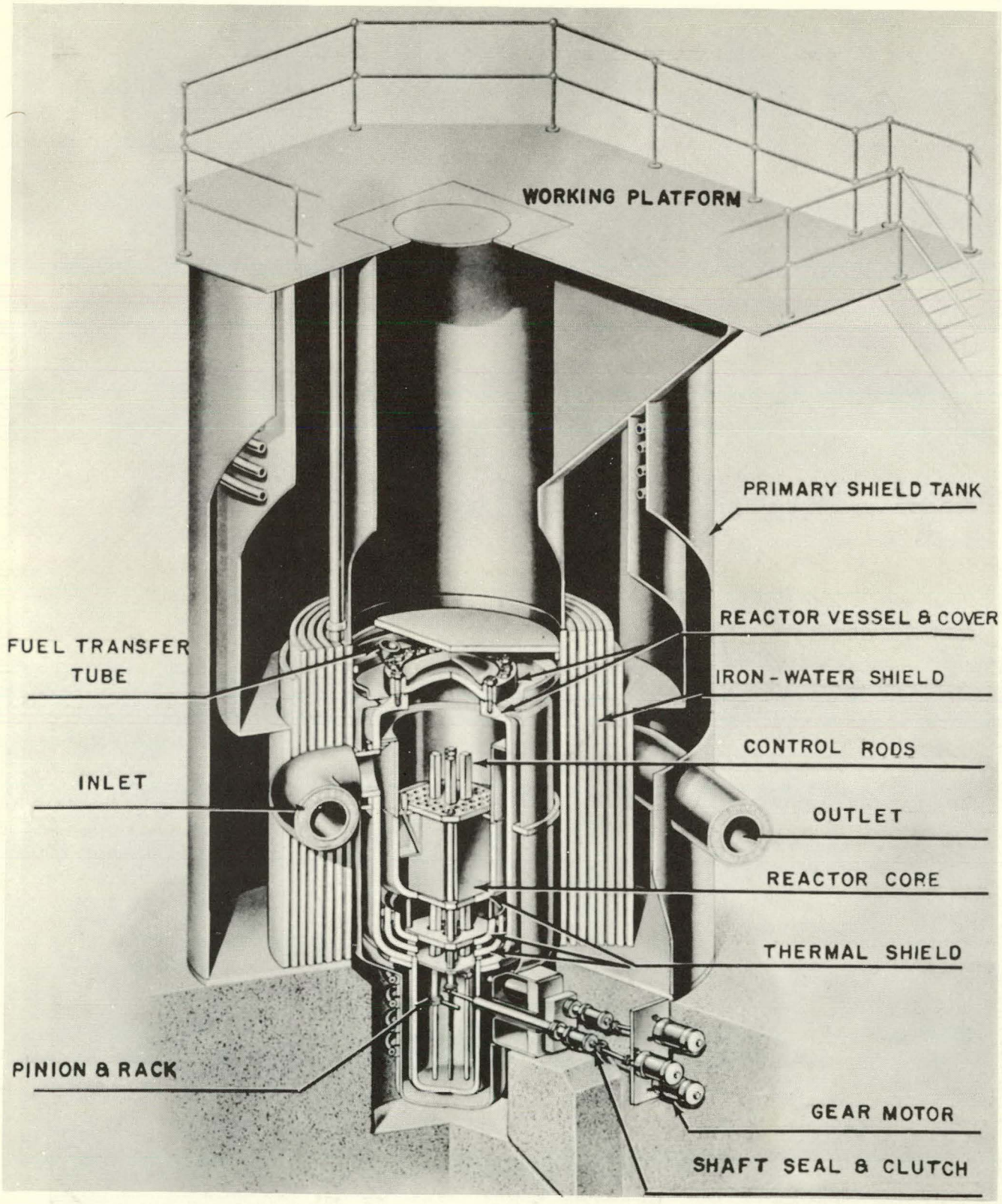

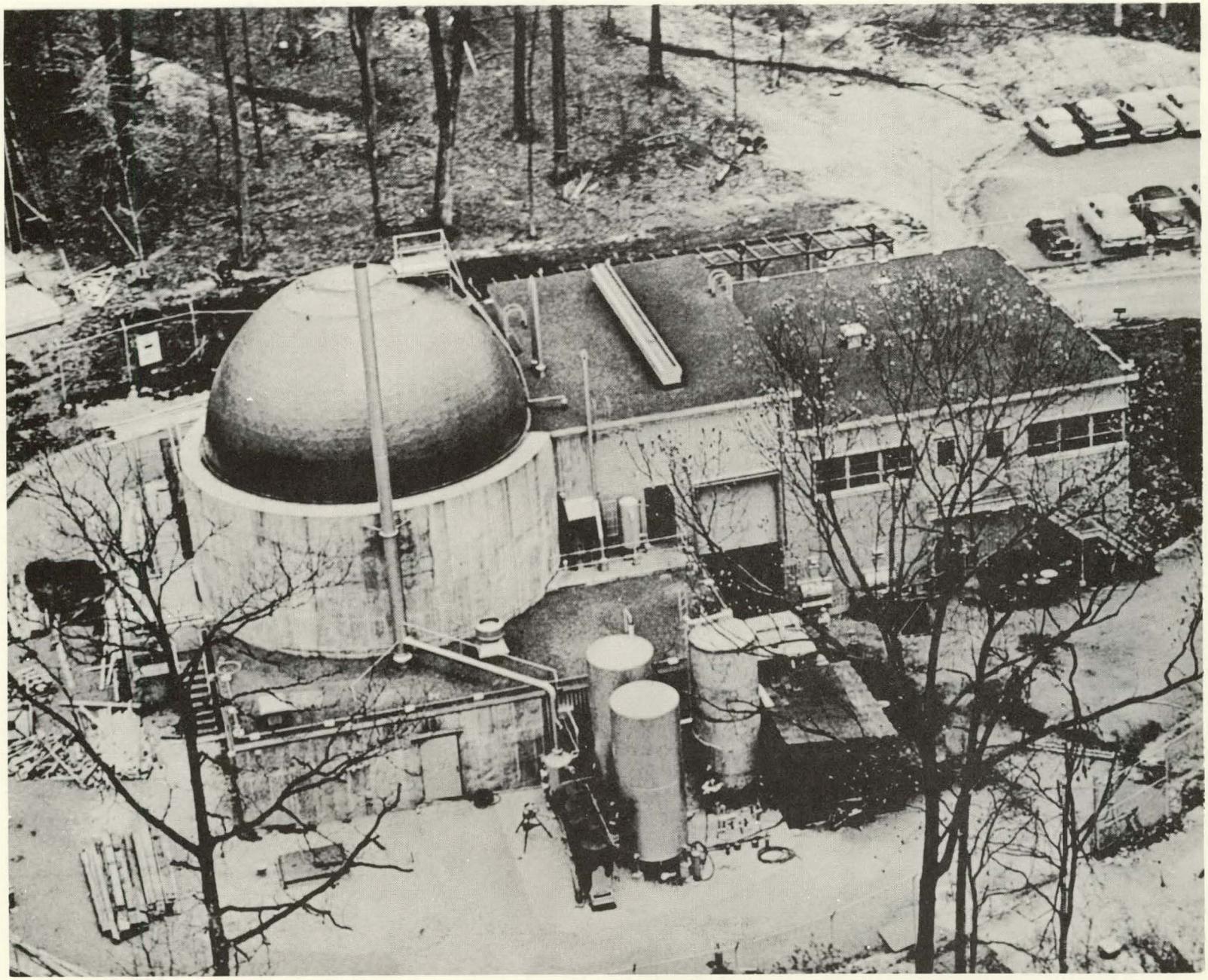

Fig. 5 Photograph of Completed Plant

APPR-1 CORE LOADING CALCULATIONS AND EXPERIMENTS

BY

H. W. Giesler

F. B. Fairbanks

P. V. Oby

J. G. Gallagher

Presented at the Second Winter Meeting of The American Nuclear Society on October 28, 1957 in New York City.

LIST OF FIGURES

APPR-1 CORE LOADING CALCULATIONS AND EXPERIMENTS

I. Introduction

This paper summarizes the APPR-1 core loading calculations and compares the predicted performance with the experimental measurements. Before beginning a description of the core loading calculations the contract specifications (A) will be reviewed. The core design and loading for the APPR-1 was affected by the following contract specifications.

1. A pressurized water cooled and moderated reactor using highly enriched uranium.
2. Stainless steel-clad fuel elements arranged in convenient sub-assemblies.
3. Burnout poisons in fuel elements.
4. A negative temperature coefficient of reactivity of $10^{-4}/^{o}F$ or better.
5. A minimum number of control rods such that the core can be shut down at any time with 80% of the control rods.
6. Non-boiling conditions in the primary coolant loop during steady state operation at full power.
7. The core to be designed for a 15 MW core life.
8. The core to be designed for operation on the line 95% of the time.

During the course of the core design a stipulation was made that the U^{235} loading should not exceed 22.5 kg. This left boron content and number of control rods as the most important core variables.

II. Schedule

It is of interest to quickly review the schedule on which the APPR-1 core design and experiments were carried out. Figure 1 shows the schedule. The very tight time schedule from signing of the original contract to required date for completion of the 700 hour test definitely placed a sense of urgency on calculations and experiments. An important decision regarding number of control rods had to be made in December of 1955 in order not to delay pressure vessel fabrication. A decision was made to employ seven control rods. There existed only two weeks between the last critical experiment measurement and fixing core boron content.

III. ORNL Critical Experiment[B]

As part of the original contract between Alco Products and the U.S.A.E.C., Oak Ridge National Laboratory was committed to perform a critical experiment for the APPR-1. Without the full cooperation of ORNL on this critical experiment it would have been impossible to meet the very tight time schedule of the APPR-1. The design of a critical experiment which will permit measurements of critical mass for various boron contents, control rod worth measurements and flux distribution is in itself no easy task. This was accomplished by ORNL with the cooperation of Alco.

The most important decision that affected the critical experiment design was to keep metal water ratio and core diameter constant in all the experiments. As a result of this decision the inner cell material distribution varied widely between the experiments containing no boron and those containing boron. In order to give flexibility to the experiment it was decided to employ separate fuel plates, boron steel plates and stainless steel plates. Figure 2 shows a fuel box for this experiment. With these three types of plates a wide range of of compositions of fuel and boron could be obtained at constant metal water ratio. This decision to use separate plates would certainly be carefully scrutinized in any future critical experiments for reactors of this type.

The effect of the employment of separate fuel and steel plates is shown in Figure 3. This Figure shows an inner cell traverse in the direction perpendicular to the fuel and steel plates. The flux peaking in the side plate region was of such a magnitude that the flux on the side plate was 1.3 times the value at the center of the fuel element when measured with dysprosium foils.

The extreme variation of inner cell flux distribution was a matter of considerable concern in interpreting the critical experiments. The approach used at Alco to calculate thermal utilization was to consider the measured inner cell distributions to obtain the relative flux on the various constituents. This approach was handicapped by the variation of plate arrangement with core boron content and the difficulty of obtaining inner cell distributions. As an aid in resolving this question of heterogeneity of the critical experiment, special elements resembling the APPR-1 elements were substituted in a single position within the core and reactivity differences measured.

IV. Calculation of Critical Experiment (C) (D)

The general approach used to calculate the various critical configurations was to employ 2-group theory modified to include above thermal absorptions and fissions. The important equations used are shown in Figure 4 along with the equation for K_{eff} of the equivalent bare reactor. The equations used to calculate resonance multiplication and resonance escape probability are given on Figure 5. All the calculations employed the equivalent bare model. The buckling for the core at room temperature was found by least squared fittings of gross flux distributions. The resulting buckling of the core is 0.0072 cm^2 at 68° F. The other factors in the critical equation, that is K_{th}, K_f, p and L^2, were calculated. In order to get the modified 2-group theory results to agree with the experiment the neutron age was adjusted until K_{eff} equaled 1.0.

It was possible by using this approach to calculate the clean critical experiment with no boron and 10.4 Kg of U^{235} and a second experiment with 21.1 Kg U^{235} and 255 gms of boron with a neutron age of 38.7 cm^2. This same calculation model was used to check flux distributions, the percentage thermal fissions and fuel reactivity with good agreement. In addition, calculations of homogeneous APPR's agreed with the critical mass values inferred from substitution of a homogeneous fuel element. This adjusted two group theory gave reasonable good agreement with all the critical experiment measurements and it was then employed to establish the APPR-1 core loading.

V. Calculation of APPR-1 Loading (C) (D)

The geometrical and material differences between the APPR-1 core and the critical experiment are tabulated in Figure 6. The first geometrical

difference shown in Figure 6 was treated by interpreting the weighing factors made in the critical experiment and on a special APPR-1 element substituted in the critical experiment. Items 2 and 3 were neglected. Allowances for Items 4 and 5 were treated by interpreting a special critical experiment measurement which attempted to account for these differences in terms of a uniform poison added to the APPR-1. The important material differences in Items 1 and 2 were felt to be properly allowed for by the self-shielding factor used within the fuel plates. A uniform Σ_p was included to compensate for the braze material.

The important muclear parameters that were assumed invariant in the transition from the critical experiment to the APPR-1 were the neutron age and the geometrical buckling. Using modified 2-group theory and a U^{235} loading of 22-1/2 kg, a range of boron contents were investigated. The principal concern in the Boron-10 addition was the fear of over-poisoning the core so that the core could not obtain full power with peak xenon. For operational flexibility, it was decided to design the core to have a K_{eff} of at least 1.02 at 450° F with equilibrium Xe and Sm. The confidence in the calculated reactivity was affected by the uncertainty associated with the following:

1. Braze content in the core because of the variation in fillet radii.
2. Allowance to be made for reduced fuel and boron content and added steel content at 7 control rod positions.
3. Dimensional tolerances on the fuel plates.
4. Boron content was estimated to be uncertain to plus 1% and minus 6% at that time.

An examination of the reactor analysis uncertainty as well as the mechanical uncertainties indicated that K_{eff} could be uncertain to plus 2.3% and minus 3.3%.

The material contents for the APPR-1 core as fabricated are given in Figure 7.

VI. Comparison of Analysis with Experiment (E, F, G)

The final APPR-1 loading was analyzed using the window shade model for treatment of partially inserted shim bank. A comparison between the expected and experimental determined shim bank withdrawals are shown in Figure 8. The experimental data is shown from both the APPR-1 ZPE and Ft. Belvoir operation. The difference between initial and predicted shim bank insertions when interpreted with the experimentally determined control rod calibration indicated that the calculations under-estimated the reactivity in the APPR-1 core by 5.05% at 68°F and 4.31% at 450°F. The predicted temperature coefficient at 450°F was $-3.2 \times 10^{-4}/^{o}F$ compared with the measured value of $-2.3 \times 10^{-4}/^{o}F$. A final resolution of the calculated and measured reactivity has not been made. Information now available indicates that the following are the principal causes of the discrepancy.

1. The final stainless steel content of the APPR-1 was 1.34% by volume less than that used in the calculations. This was due to the fact that the fuel element plates were not rolled to 100% theoretical density assumed in the calculation. This difference in steel content explains about 0.9% of the reactivity difference and 1/2-inch of shim bank insertion.

2. Inner cell measurements on the APPR-1 indicate that the core is more homogeneous than interpreted from the critical experiment measurements.

3. Measurements in the ZPE #2 (H) indicate that the core age is less than that inferred from the ORNL critical experiments.

The information available to date on the APPR-1 burnout characteristics is summarized in Figure 9. The calculated curves were those made following the ZPE at room temperature. Present indications are that the core will be good for 15 MW years of life (about 13,000 efph). It is hoped to present more detailed analysis and results on the APPR-1 core burnout and behavior at operating temperature in a subsequent paper.

VII. Acknowledgements

The design of the ORNL critical experiment was directed by A.L. Boch, Package Reactor Group, Oak Ridge National Laboratory. The critical experiment itself was carried out under the direction of Dr. A. D. Callihan. Without their complete cooperation the schedule could not have been met on the APPR-1. In the interpretation of ORNL critical experiments, aid was received from Dr. A.M. Perry, Oak Ridge National Laboratory, and Dr. R.L. Murray, North Carolina State University. A sub-contract with Walter Kidde Nuclear Laboratories under the immediate direction of Karl H. Puechl, was employed to investigate special problems in interpreting the critical experiments.

The aid of all these individuals is gratefully acknowledged. However, responsibility for the final decisions in regard to the APPR-1 core loading must rest with Alco Products, Inc. The overall supervision of this work was by Dr. J.L. Meem, whose guidance is gratefully acknowledged.

References

A. Contract No. AT (11-1)-318

B. D. V. Williams et al, "Army Package Power Reactor Critical Experiment", ORNL 2128, August 21, 1956

C. J. G. Gallagher, "Reactor Analysis for the Army Package Power Reactor No. 1", APAE-7, May 29, 1956

D. F. B. Fairbanks, "Predicted Core Performance for the Army Package Power Reactor No. 1", APAE 11, August 31, 1956

E. J. L. Meem, "Initial Operation and Testing of the Army Package Power Reactor APPR-1", APAE No. 18, August 9, 1957

F. Alco Products, Inc., "Results and Analysis of the APPR-1 Zero Power Experiments Part 1", AP Memo No. 61 November 7, 1956

G. Alco Products, Inc., "Phase III Report Army Package Power Reactor Field Unit No. 1 APPR-1a Design Analysis", Vol. 1 APAE 17 Supplement 1, July 31, 1957

H. Alco Products, Inc., "Extended Zero Power Experiments for the APPR", ZPE-2, to be published.

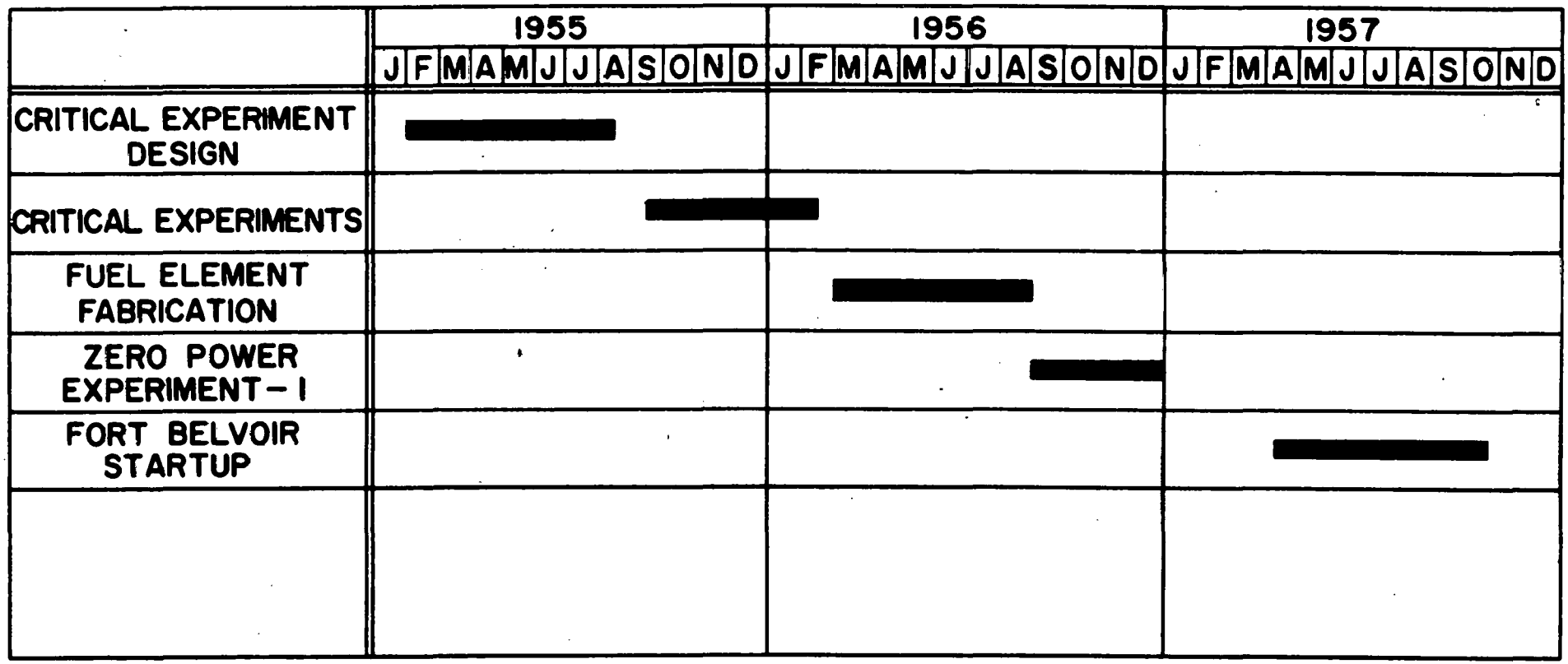

Fig. 1 Schedule

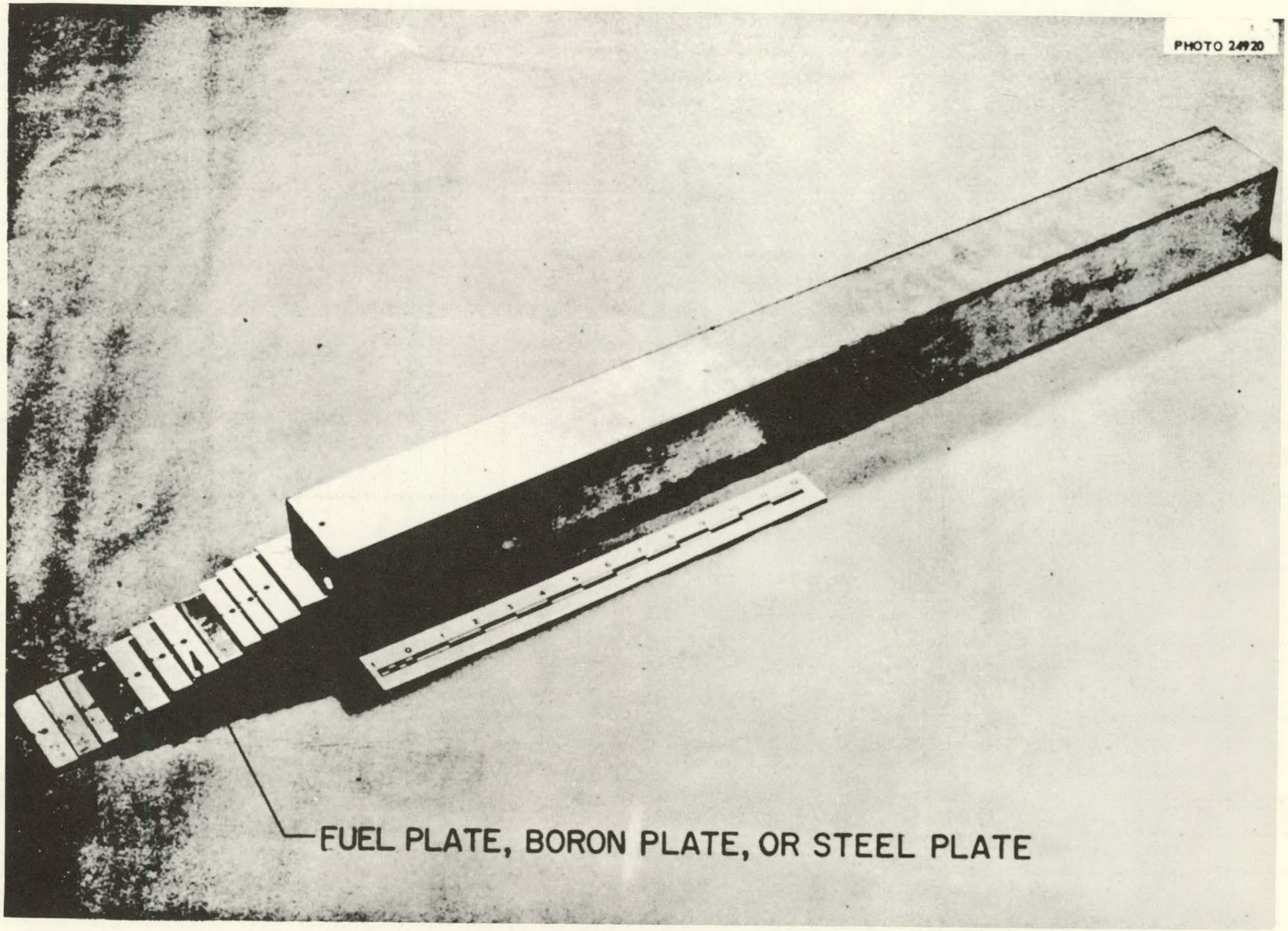

Fig. 2 Fuel Box Partially Loaded with Fuel and Stainless Steel Plates

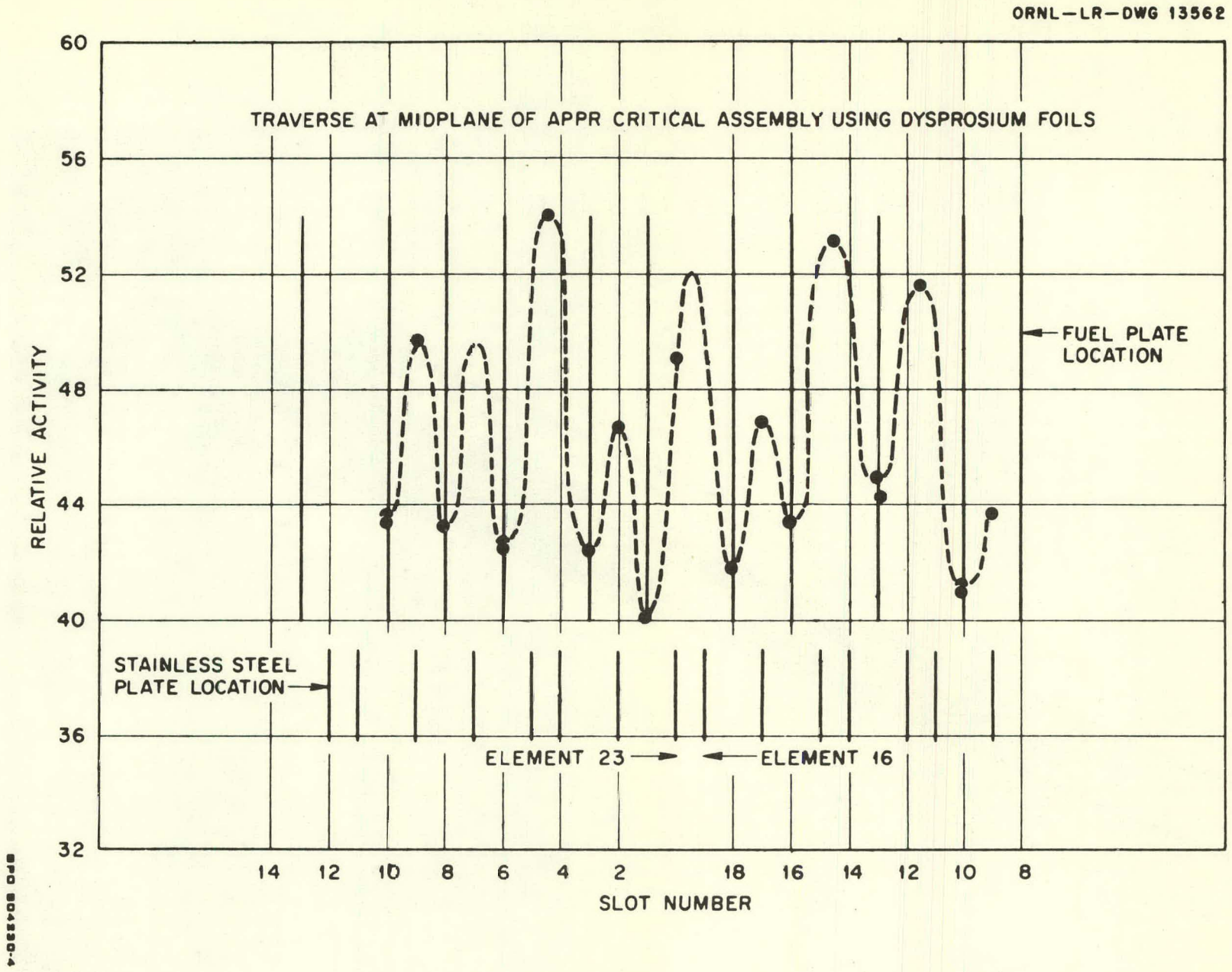

Fig. 3 Microscopic Flux Traverse in Clean Reactor, Perpendicular to Fuel

Fig. 4 Equations for Modified Two Group and K Effective

$$-D_1 \nabla^2 F(\vec{r}) + \Sigma_1 F(\vec{r}) = (1-p) K_f \Sigma_1 F(\vec{r}) + K_m \Sigma_{a2} \phi(\vec{r})$$

$$-D_2 \nabla^2 \phi(\vec{r}) + \Sigma_{a2} \phi(\vec{r}) = p \Sigma_1 F(\vec{r})$$

$$K_{eff} = \frac{\nu}{\lambda} = \frac{(1-p)K_f}{(1+\tau B^2)} + \frac{p K_m}{(1+L^2 B^2)(1+\tau B^2)}$$

Fig. 5 Equations for the Resonance Multiplication and K Fast

$$p = EXP\left[-\int_{u=0}^{u=18} \frac{\Sigma_a^T(u)}{\Sigma_s^N(u) + \Sigma_a^T(u)}\, du\right]$$

$$K_f = \frac{\nu \int_{u=0}^{u=18} \Sigma_f^{25}(u)\, du}{\int_{u=0}^{u=18} \Sigma_a^T(u)\, du}$$

		Critical Experiment	APPR-1
Geometrical Differences			
Plates		18 + 2 end plates	18
Cell Size	in.	2.952 x 2.9000	2.9375
Core Lateral Dimensions	in.	20.7 x 20.3	20.6 x 20.6
Fixed Element Position	% Metal	19.8	20.33
Material Differences			
		Separate Plates	Composite Plates
		U Foil clad in steel B in iron Steel	UO_2, B_4C in steel

Fig. 6 Differences between Critical Experiment and APPR-1

Material content:		
U-235	kg	22.5
B-10	gm	19.516
SS	kg	208.92
Fixed element:		
U-235	gm	515.16
B-10	gm	.4468
Control rod element:		
U-235	gm	417.76
B-10	gm	.3627

Fig. 7 Material Content of APPR-1 Core

			Calculated	Measured
Five Rod Bank Withdrawal				
Initial Startup	68°F	in.	8.0	3.7
Initial Startup	440°F	in.	12.9	6.85
Reactivity in core at startup	68°F	%	10.35	15.42
Temperature Coefficient		$\Delta K/^{o}F$	-3.2×10^{-4}	-2.3×10^{-4}
Core Lifetime		MWYR	12.1	---

Fig. 8 Calculated and Measured Values

Fig. 9 Five Rod Shim Bank Position Vs Lifetime

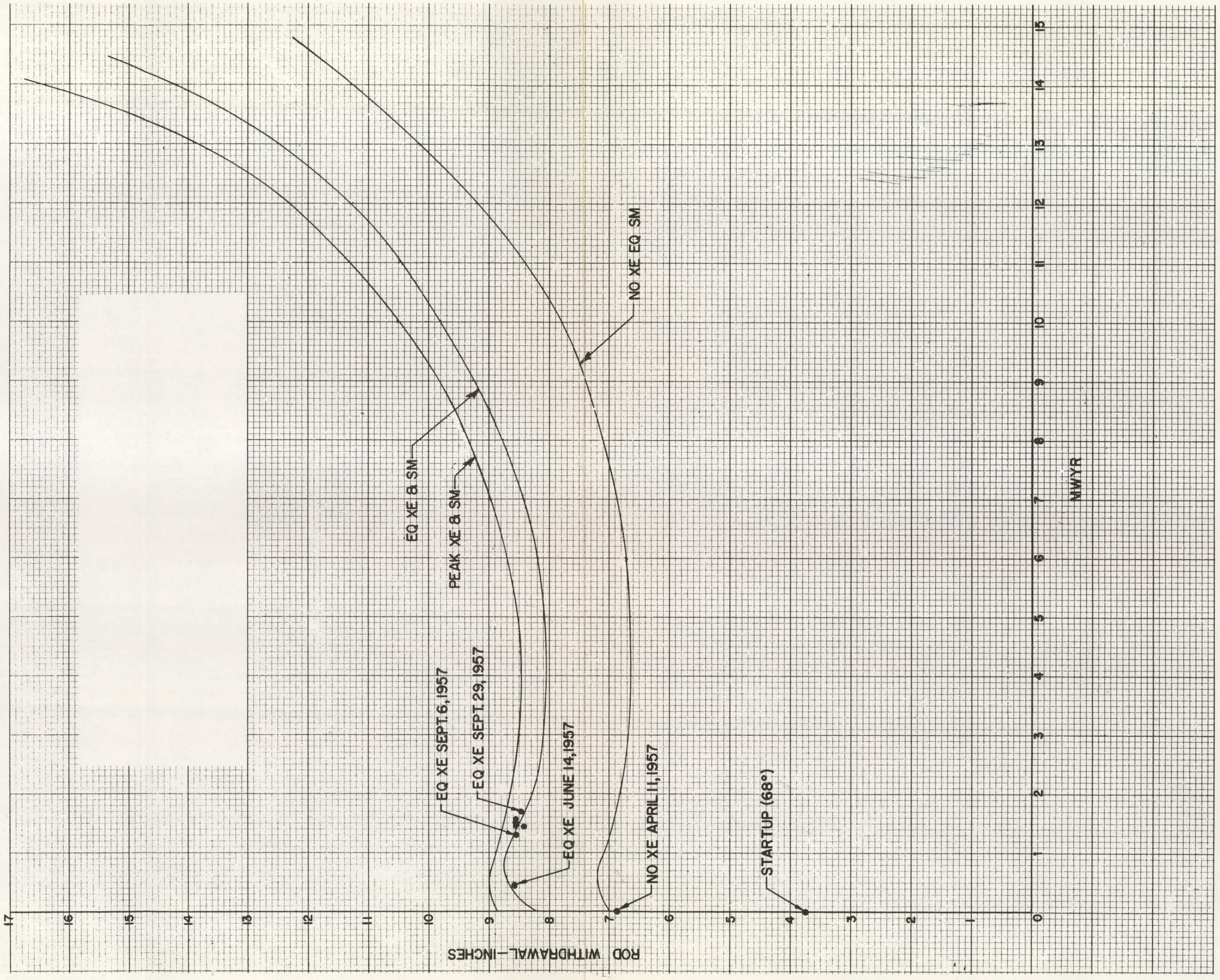

APPR-1 ZERO POWER EXPERIMENTS

BY

J. W. Noaks

W. R. Johnson

S. D. McKay

Presented at the Second Winter Meeting of The American Nuclear Society on October 28, 1957 in New York City.

LIST OF FIGURES

APPR-1 ZERO POWER EXPERIMENTS

I. Introduction

The Alco Products Criticality Facility was designed originally for the APPR Zero Power Experiment. Since our start-up date in August 1956, a continuing program of facility modifications and improvements has increased the laboratories versatility to permit accomodation of a variety of critical experiments. We are therefore currently accepting invitations to bid on the performance of critical experiments in addition to those required through our own company efforts.

The material for this paper is derived in its entirety from document APAE No. 8 and the figure numbers on the following slides correspond to the figures presented in that report.

Your speaker has made an attempt to extract material from APAE No. 8 that would be representative of the type of experiments performed and at the same time emphasizing problems peculiar to the APPR-1 system.

The experimental techniques used during the course of this work are well known and quite standard to the art.

1: Criticality Facility

The Alco Criticality Facility contains roughly 2500 square feet of floor area, 1200 of which is devoted to a test cell. The balance of the facility contains a control room, office area, counting room etc. The building, Fig. 1, is constructed of from one to five feet reinforced concrete, depending upon shielding requirements. The test cell itself is so constructed as to contain the pressures that would result from a maximum credible accident on the APPR-1 system.

2: Reactor and Reactor Tank

Fig. 2 shows the 2500 gallon reactor tank which was used for these experiments. The tank is fed by a 50 gallon/min. pump from a 3500 gallon storage tank. A six inch dump line with quick acting butterfly valve is provided for rapid dumping of the water moderator. This slide also shows the lower control rod drives which penetrate an extension attached to the bottom of the reactor tank.

3: APPR-1 Core

This view of the APPR-1 core in the reactor tank, Fig. 3, shows clearly the control rod caps, stationary fuel elements, instrument tubes, and immersion heaters (which were used for the temperature coefficient measurements).

4: Control Rod Assembly

The control rod assembly, Fig. 4, is clearly shown by this slide. The basket, control rod fuel element, absorber section and cap are shown in the disassembled state.

5: Stationary Fuel Element With Plates Exposed

During the course of the experiments use was made of several APPR fuel elements that were supplied to us with detachable end boxes. Fig. 5 shows clearly the structure of the APPR fuel elements.

6: Core Lattice Designations

For experimental convenience, the various fuel element positions were located by means of the numbering system displayed in Fig. 6. The relative positions of the neutron source and start-up chambers are also shown.

7: Position of the 5 Rod Bank Versus Number of Elements

The minimum number of stationary and control rod fuel elements for criticality was 17. Fig. 7 shows the position of the 5 rod bank as the remaining elements were added to the core. With rods A and B fully withdrawn the 5 rod bank rod position is seen to be 3. 7 inches.

8: Boron Content Versus Bank Position

In order to aid in the determination of the system excess K, Boron-stainless steel strips were added uniformly to the system until the control rods were essentially withdrawn. The quantity of contained B^{10} added to fully withdraw the rods was estimated to be 33. 5 grams.

9: Calibration of the 5 Rod Bank

In order to determine the excess K in the APPR-1 core the 5 rod bank was calibrated at several positions during the addition of the Boron-stainless steel strips. Fig. 9 shows this calibration and Fig, 10 shows the integral rod bank value versus position. The experimental excess K determined by this means is seen to be 16. 6%. In order to convert this value to the common analytical expression for ρ the following expression was used:

$$\rho = 1 - e^{-\int \frac{\partial \rho}{\partial x} dx}$$

where $\frac{\partial \rho}{\partial x}$ is the aforementioned calibration curve.

The value for ρ so computed is 15. 4%.

11: Temperature Coefficient Versus Temperature

Temperature coefficient from 68° to 180°F was determined by heating the moderator with two 15 KVA immersion heaters. The value of temperature

coefficient at 180°F is approximately -1.0 cents/°F or -0.75 x 10^{-4} $\frac{\Delta K}{K}$/°F. The "bump" in this coefficient was due to the use of fresh water that had not been previously heated. The dissolved air accumulated along the fuel plates during heating resulting in an apparent severe negative effect. As the temperature was further increased, these air bubbles left the fuel plates and resulted in an apparent positive component. (See Fig. 11.)

12: Relative Activity Versus Position

Fig. 12 illustrates a typical axial neutron flux distribution in the stationary fuel elements with the 5 rod bank withdrawn 3.7 inches. The bare gold activities shown are normalized to the core average (= 1).

13: Average Activity Per Element

The average bare gold activity of elements relative to the core average of one is shown by Fig. 13.

14: Relative Activity Versus Radial Position

Fig. 14 depicts a radial bare gold traverse taken 6.5 inches above the bottom of the core and therefore approximately three inches above the plane of the 5 rod bank (3.7 inches). The flux depression at the absorber faces and the flux peaking within the absorber section is shown.

15: Relative Activity Versus Position

The neutron flux peaking in the end reflectors is shown by this bare gold traverse, Fig. 15. The displacement of the gross axial flux peak due to the deep bank insertion is striking though understandable.

16: Control Rod Fuel Element With Suppressors

This photograph of a control rod fuel element, Fig. 16, clearly shows

its structure. The handle is used to facilitate loading and unloading. The metal comb in place at the upper end of the element is the subject of the next slide.

17: Relative Activity Versus Vertical Position

The bare gold traverses shown here, Fig. 17, demonstrate vividly the effect on flux peaking of the water hole separation between the control rod fuel and absorber sections.

Since this water hole flux peak is roughly 4 times the core average at the point of its intersection with the leading edge of the fuel section, there was concern about the temperatures that might be developed at that point.

By making use of suppressor combs of Haynes alloy 25 it was possible to reduce this peak effect to about 3 times core average. Combs of design similar to the one shown in the previous slide were fabricated and included in the APPR-1 at Fort Belvoir.

II Conclusion

Additional experiments on the APPR-1 system have just been completed under separate contract with the AEC and the Army. The results of these Extended Zero Power Experiments will be issued shortly as APAE No. 21.

Fig. 1 Criticality Facility

Fig. 2 Reactor and Reactor Tank

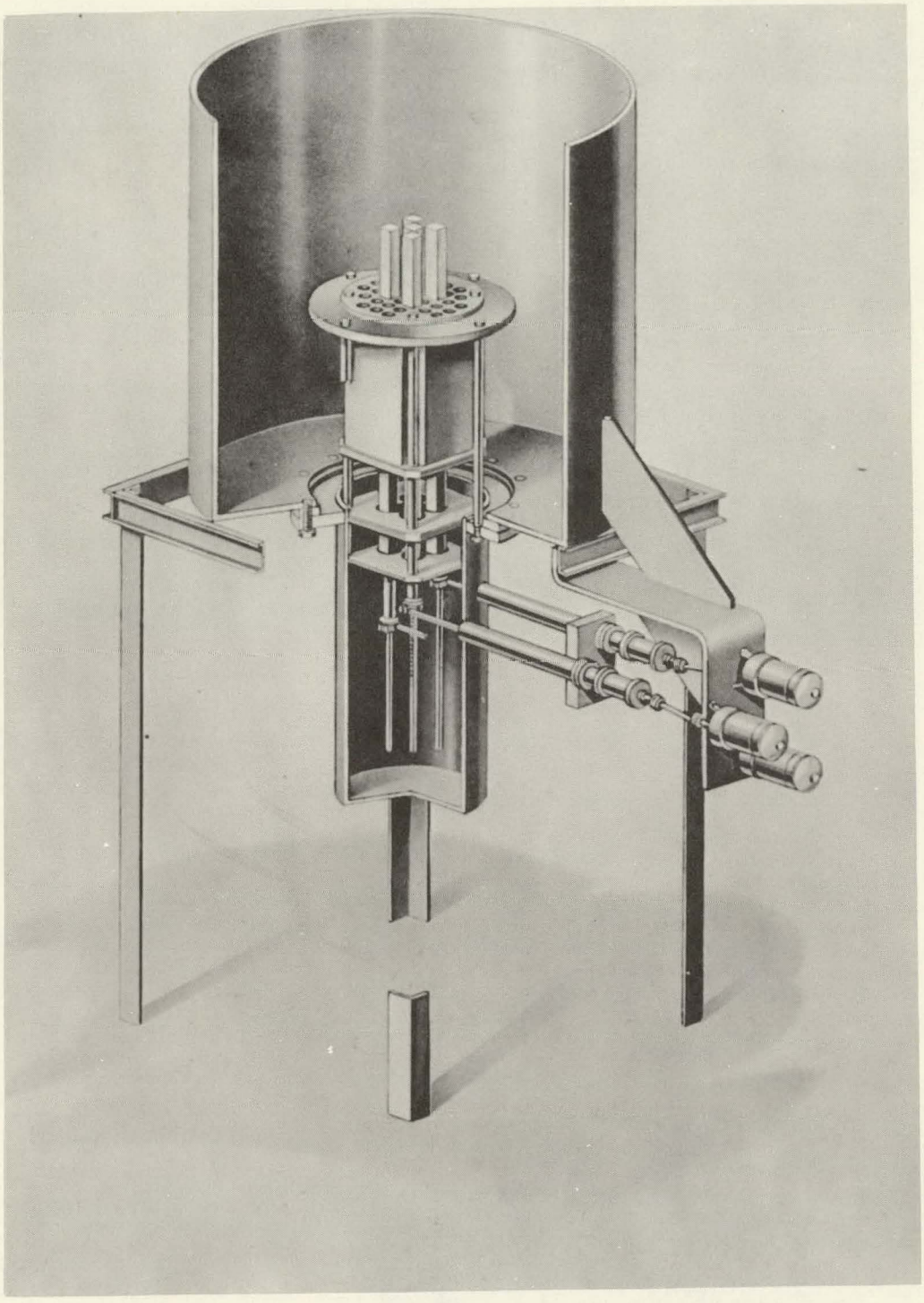

Fig. 3 APPR-1 Core

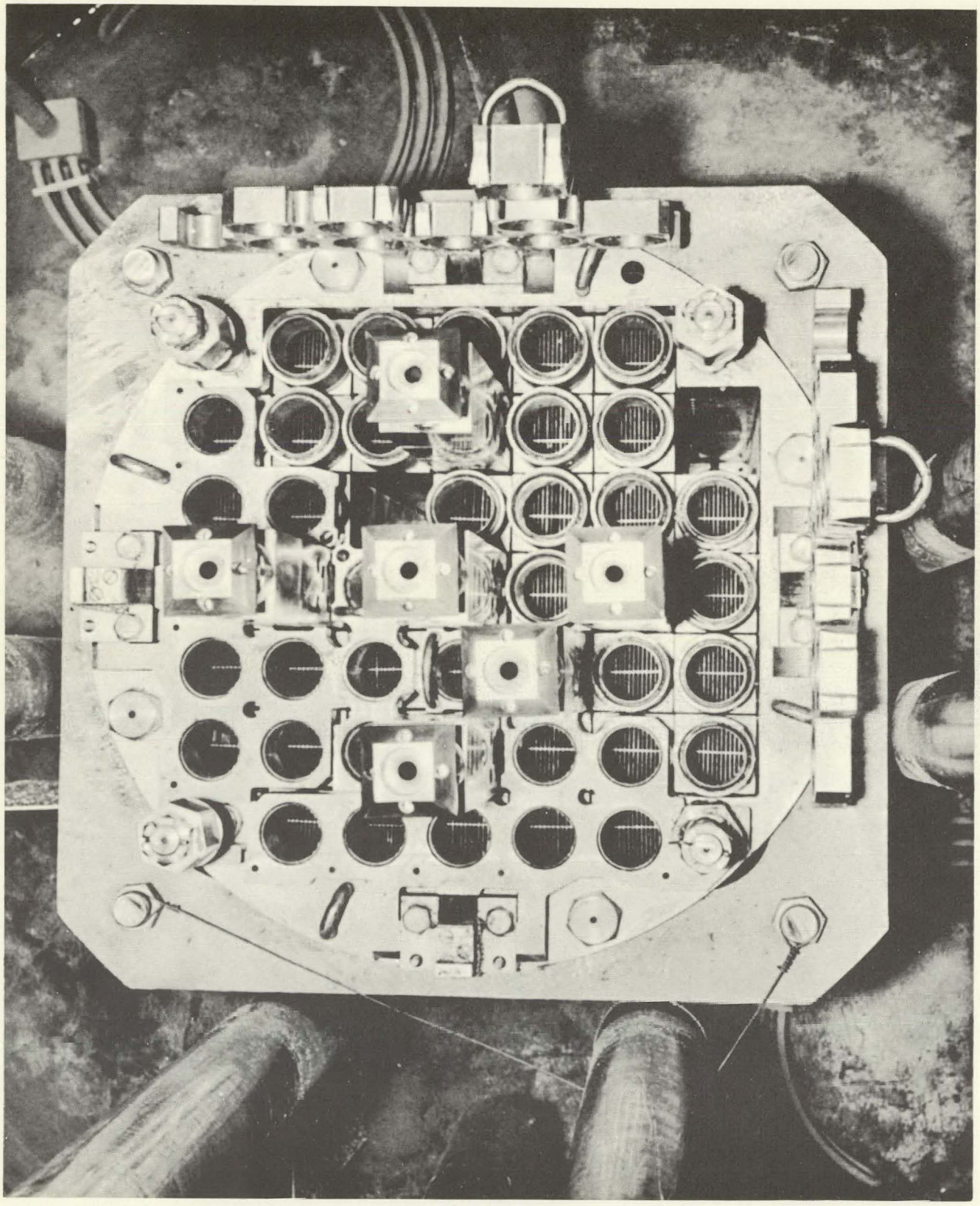

Fig. 4 Control Rod Assembly

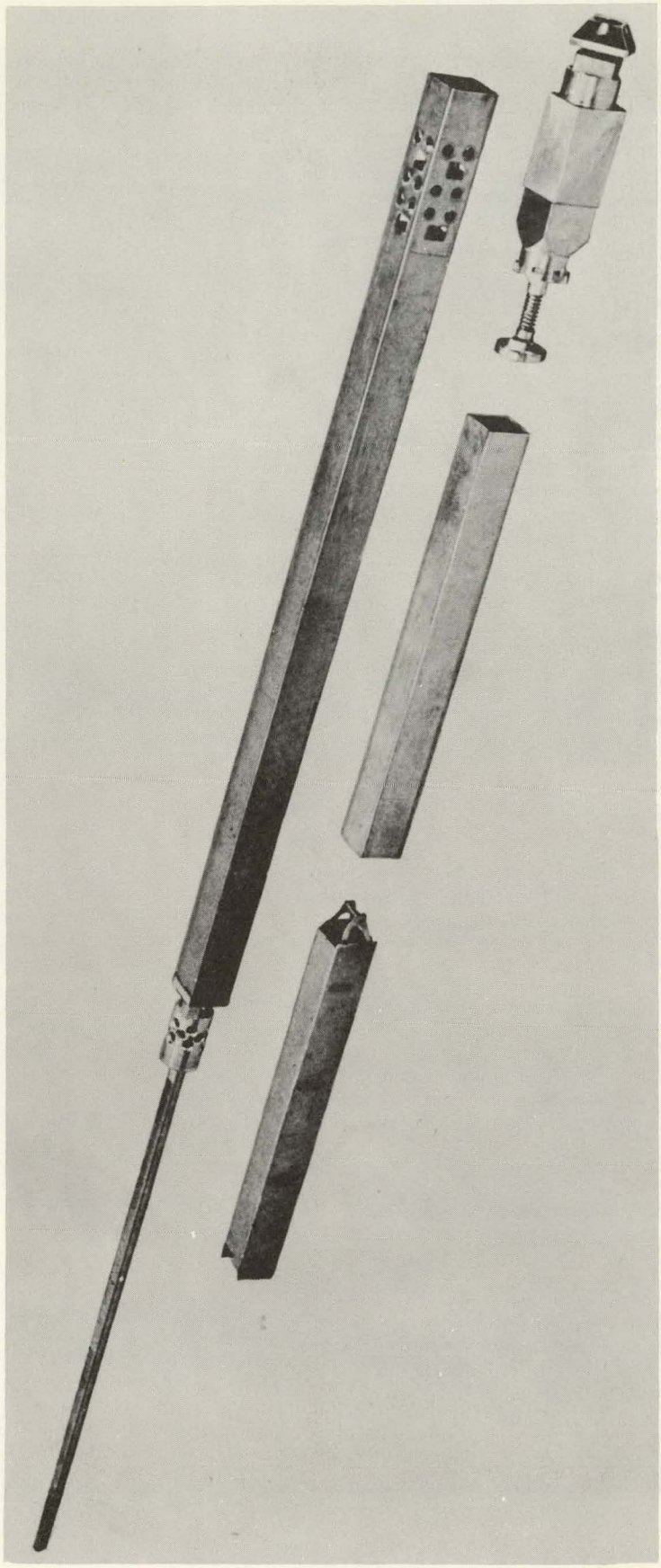

Fig. 5 Stationary Fuel Elements with Plates Exposed

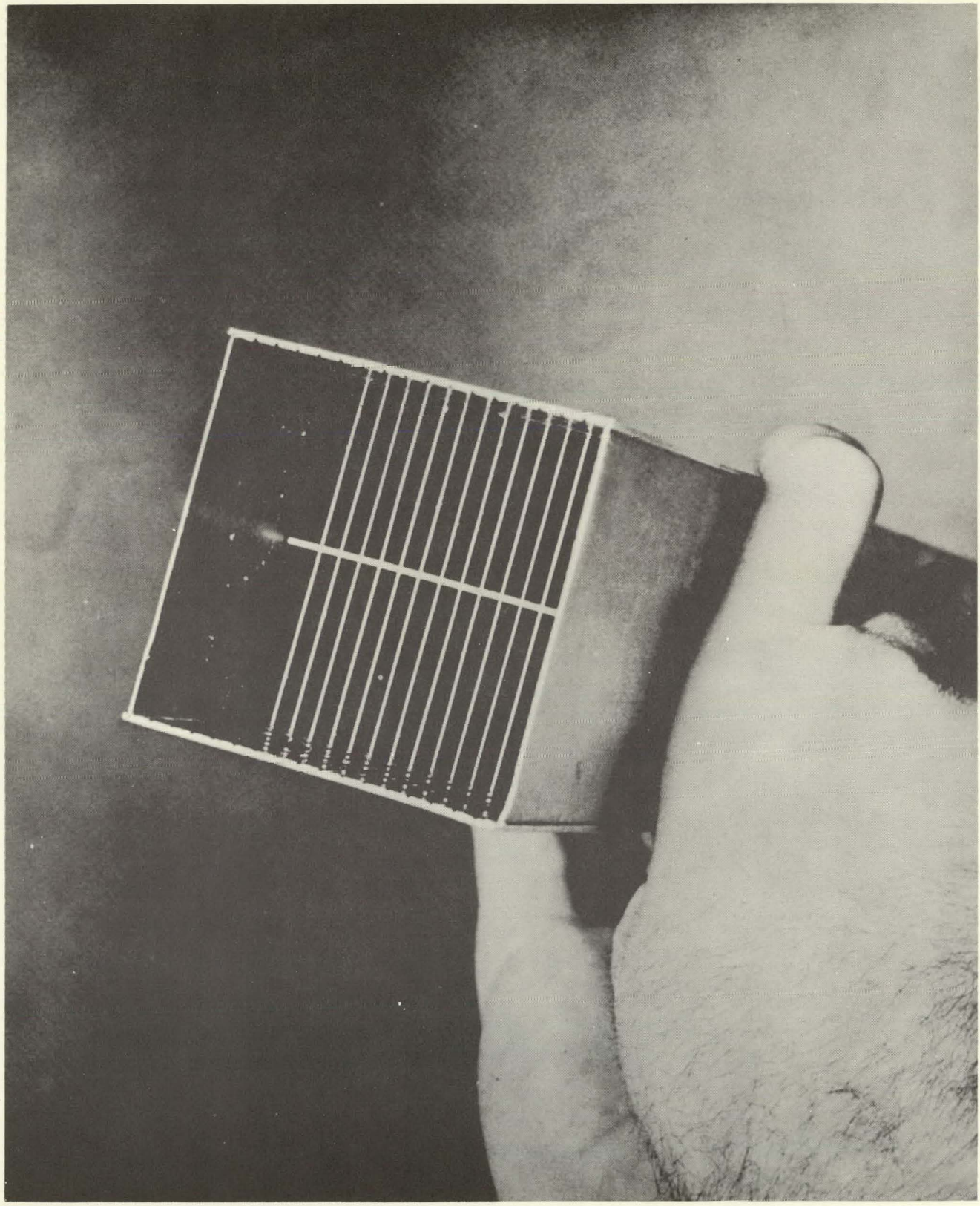

Fig. 6 Core Lattice Designations

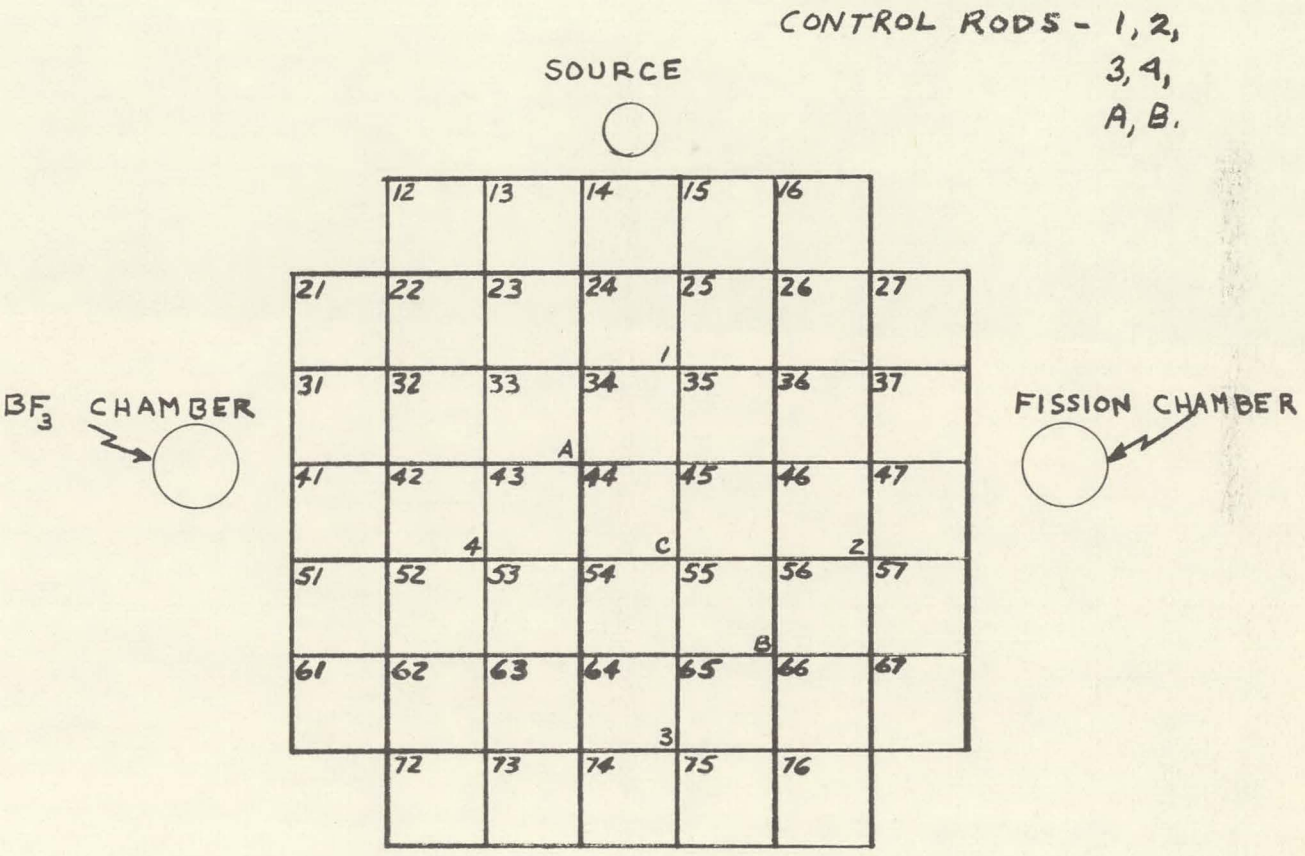

Fig. 7 Position of the 5 Rod Bank Versus Number of Elements

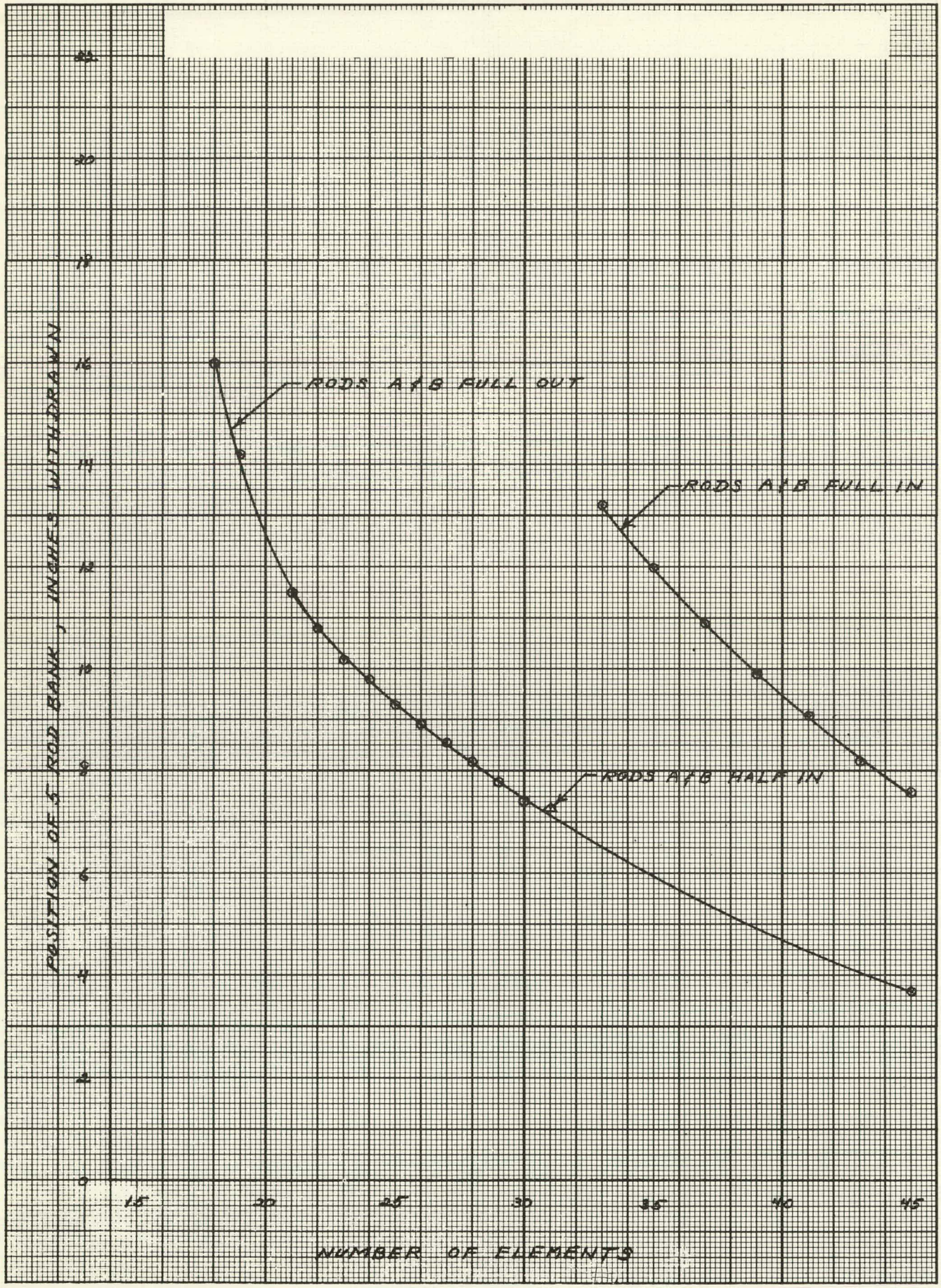

Fig. 8 Boron Content Versus Bank Position

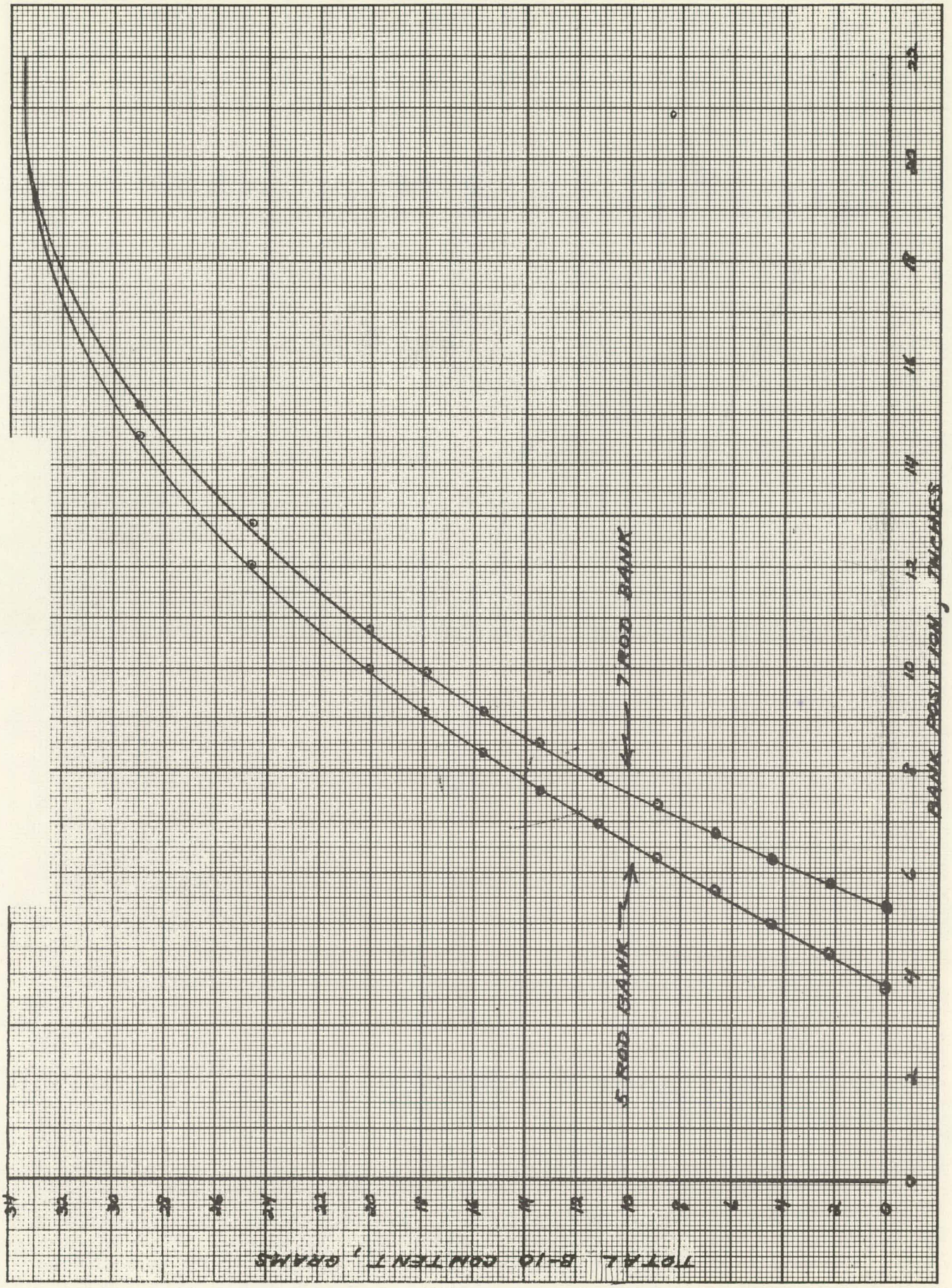

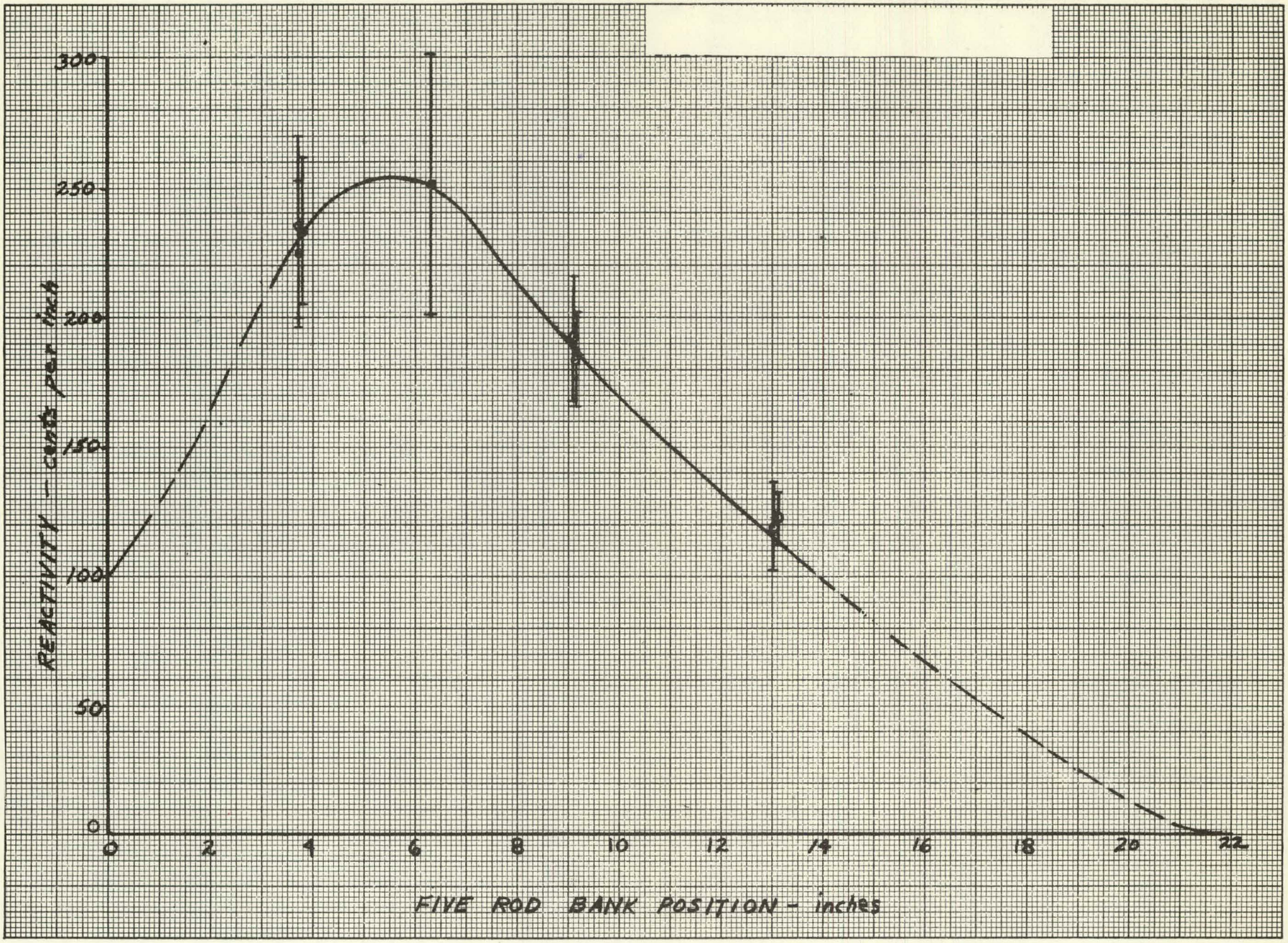

Fig. 9 Calibration of the 5 Rod Bank

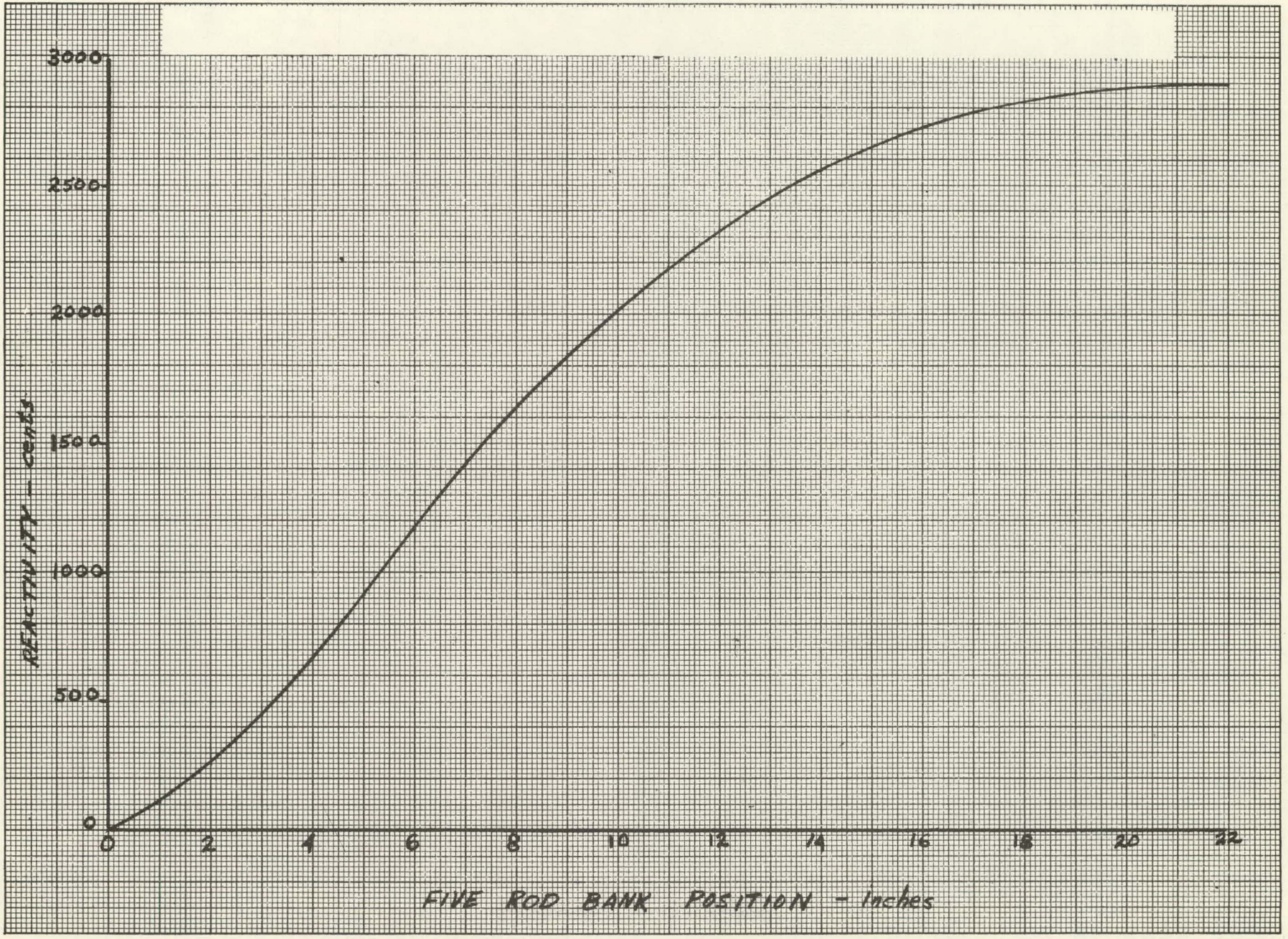

Fig. 10 Integral Rod Bank Value Versus Position

Fig. 11 Temperature Coefficient Versus Temperature

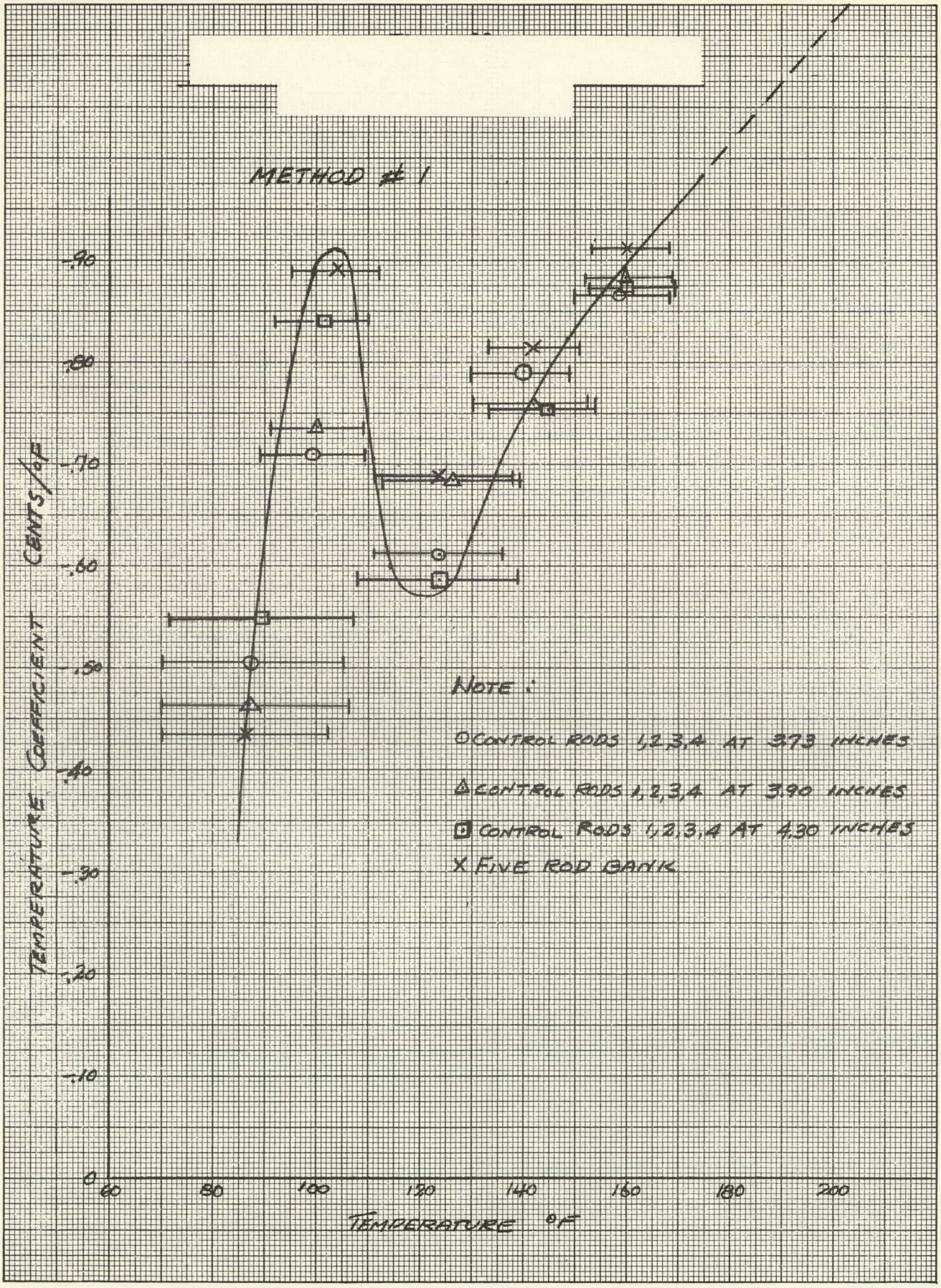

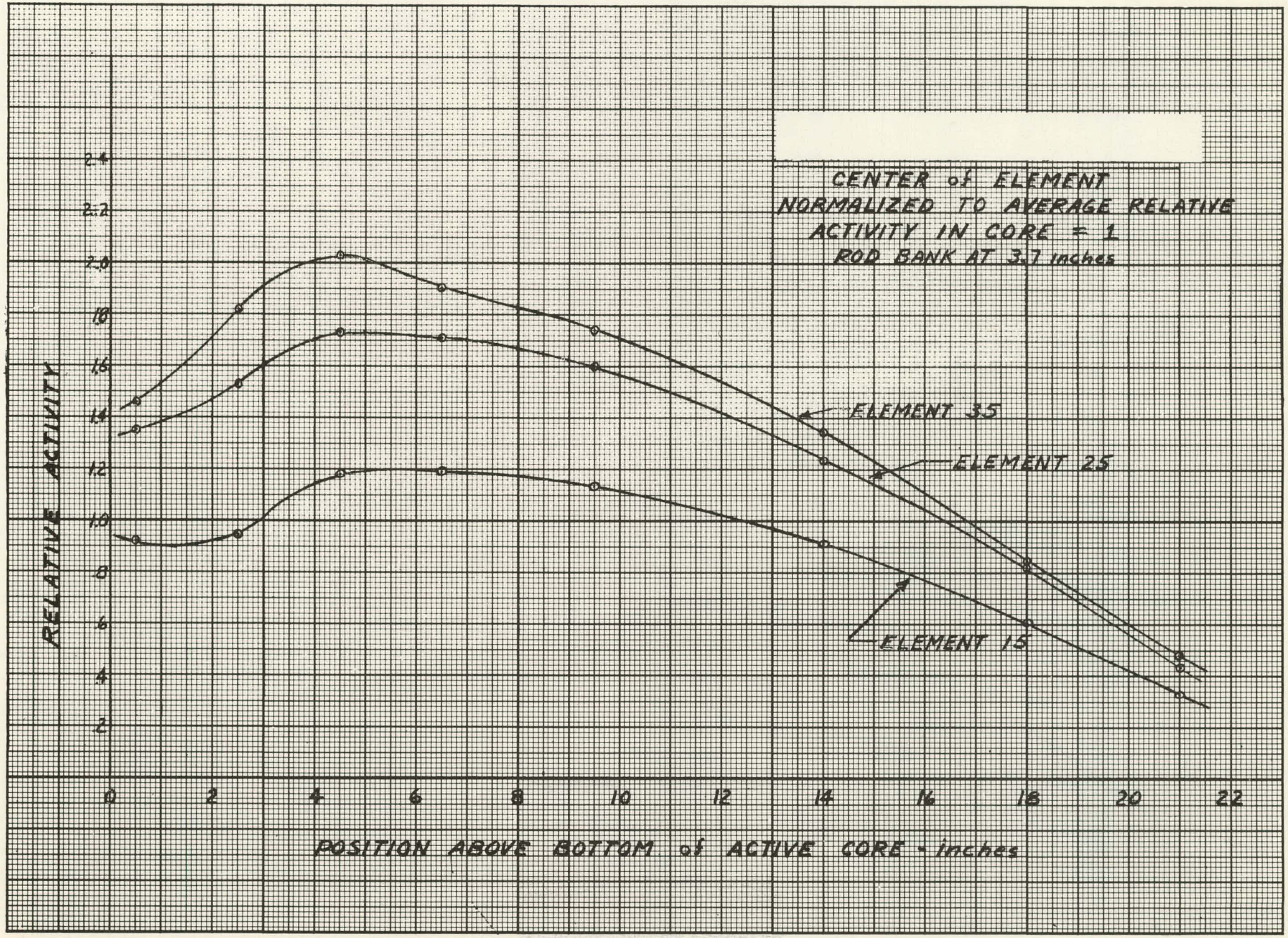

Fig. 12 Relative Activity Versus Position

Fig. 13 Average Activity Per Element

ROD BANK AT 3.7"

MEASURED WITH BARE GOLD AXIAL TRAVERSES IN THE CENTER OF ELEMENTS 14, 15, 16, 25, 26, 34, 35 AND CONTROL RODS 1 & C. NORMALIZED TO AVERAGE REACTOR ACTIVITY = 1 PER ELEMENT.

	12 .778	13 .899	14 .836	15 .899	16 .778	← ELEMENT # ← RELATIVE ACTIVITY
21 .778	22 1.298	23 1.277	24 .352 [1]	25 1.277	26 1.298	27 .778
31 .899	32 1.277	33 1.414 [A]	34 1.324	35 1.414	36 1.277	37 .899
41 .836	42 .352 [4]	43 1.324	44 .471 [C]	45 1.324	46 .352 [2]	47 .836
51 .899	52 1.277	53 1.414	54 1.324	55 1.414 [B]	56 1.277	57 .899
61 .778	62 1.298	63 1.277	64 .352 [3]	65 1.277	66 1.298	67 .778
	72 .778	73 .899	74 .836	75 .899	76 .778	

Fig. 14 Relative Activity Versus Radial Position

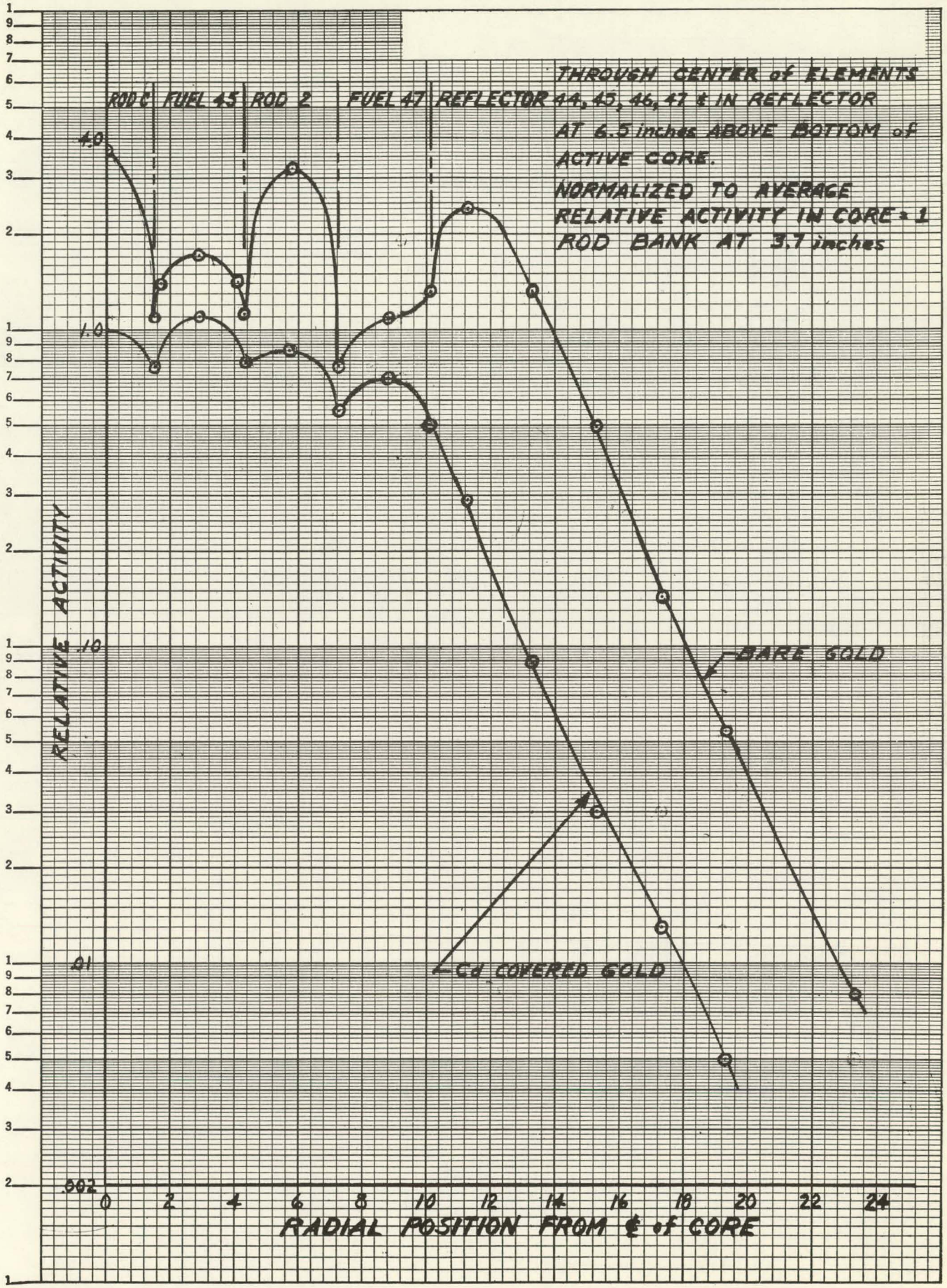

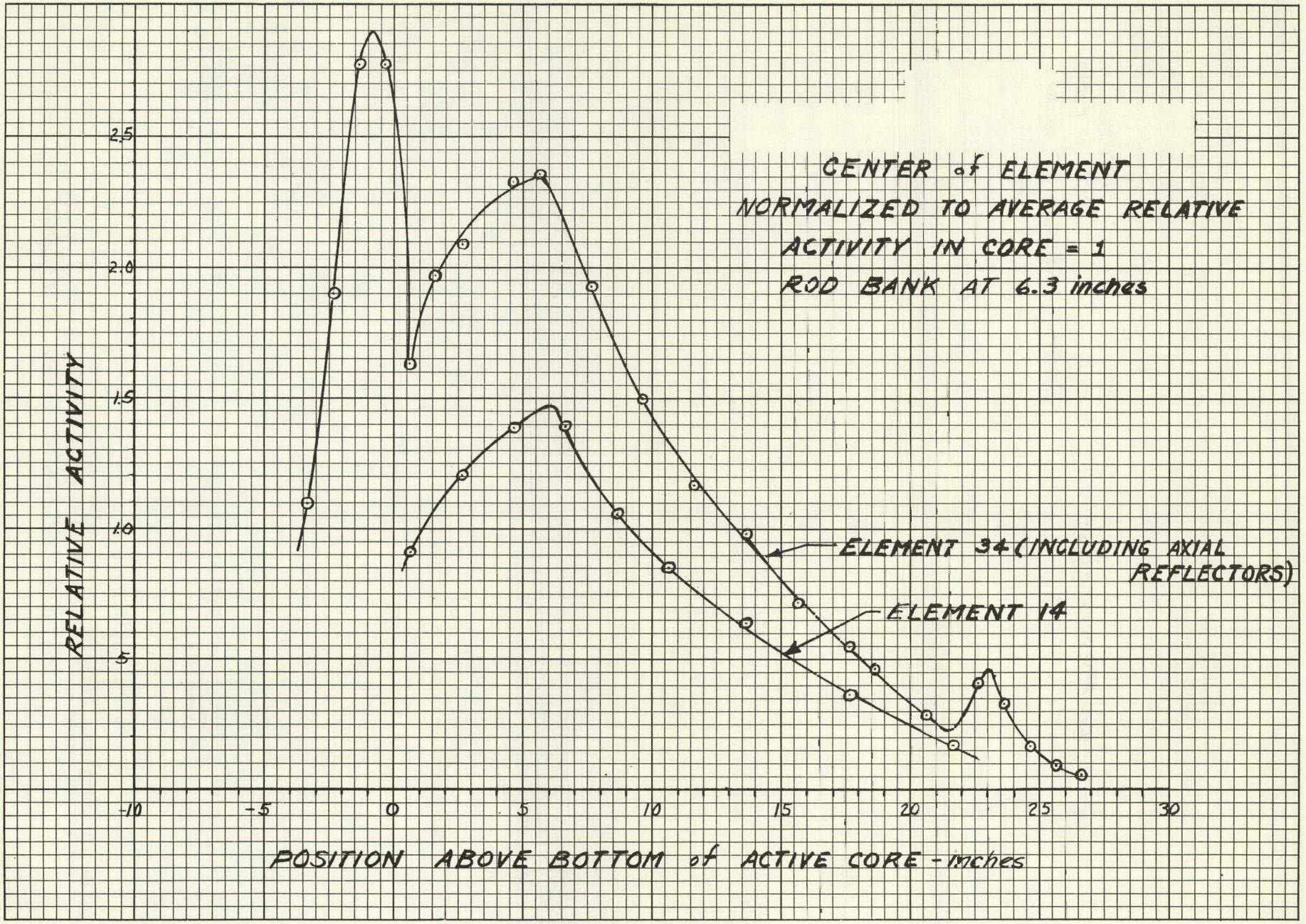

Fig. 15 Relative Activity Versus Position

Fig. 16 Control Rod Fuel Element with Suppressors

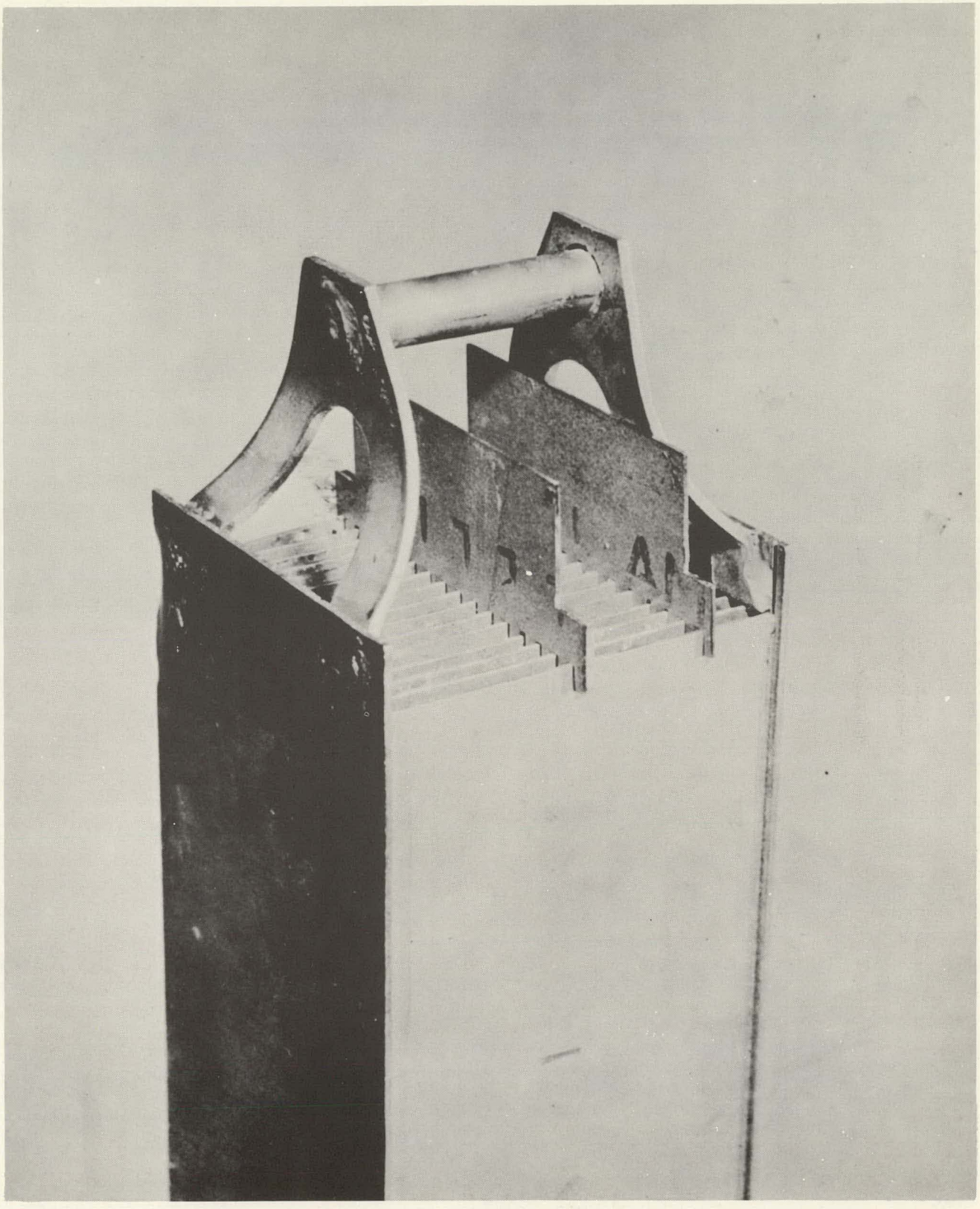

Fig. 17 Relative Activity Versus Vertical Position

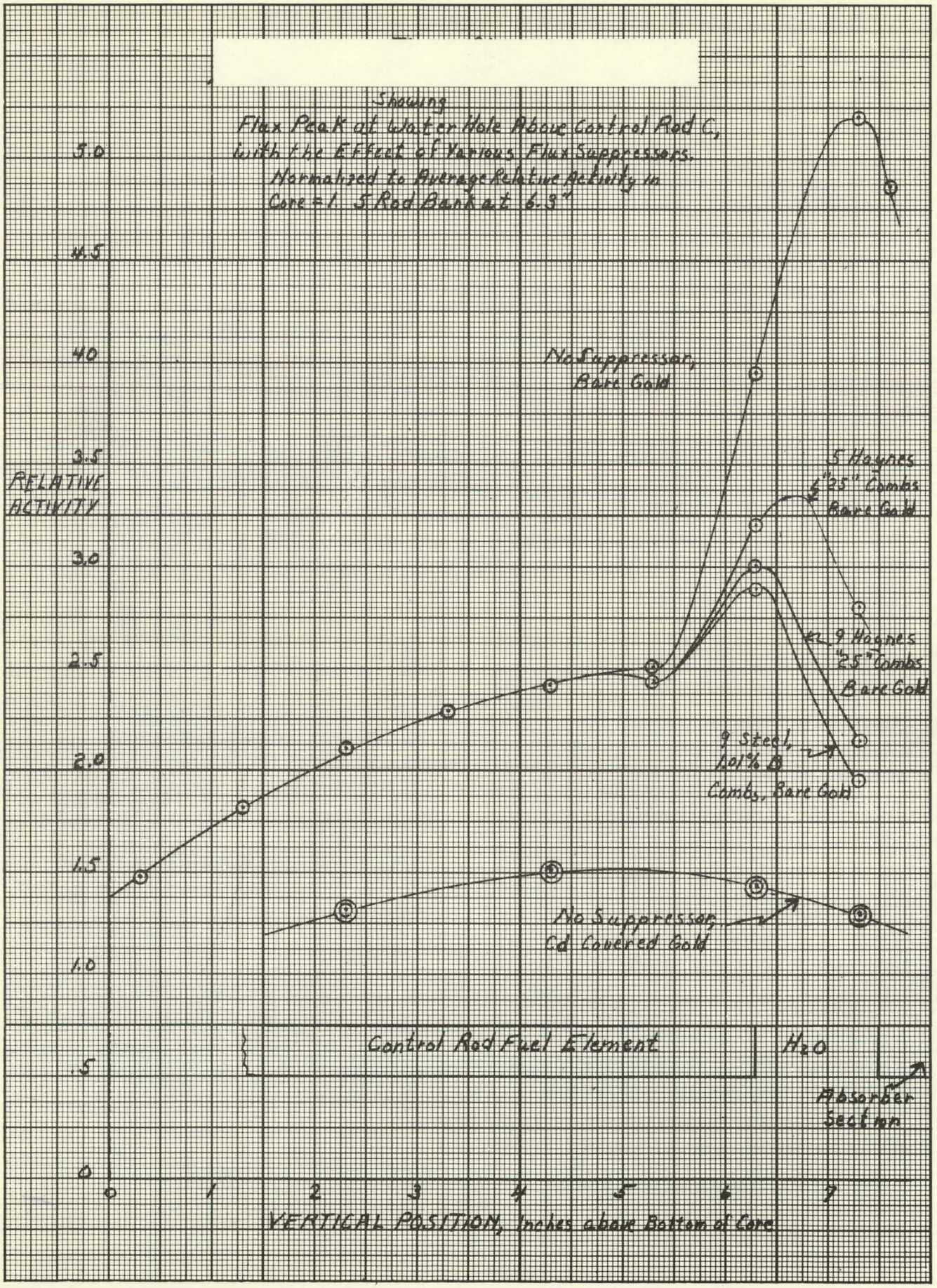

APPR-1 HEAT REMOVAL CALCULATIONS AND EXPERIMENTS

BY

W. M. S. Richards

C. H. Harvey

S. M. Ingeneri

Presented at The Second Winter Meeting of The American Nuclear Society on October 28, 1957 in New York City.

LIST OF FIGURES

APPR-1 HEAT REMOVAL CALCULATIONS AND EXPERIMENTS

I. Introduction

The APPR-1 core, from its original concept at ORNL, has been designed to operate with positively no boiling of the primary since this results in a very stable, self-regulating reactor. The basic purpose of the work described in this part of the paper was to make sure that at every point throughout the reactor core the water would be cool enough and flowing fast enough to satisfy this requirement by preventing the occurrence, anywhere in the core, of plate surface temperatures above the boiling point of the coolant.

The rate of nuclear energy release in a pressurized water reactor is not uniform throughout the core but varies in both the radial and axial directions. If the coolant flow velocity is uniform across a given core cross section, the peak metal surface temperature will vary from passage to passage along the core radius, the highest temperatures occurring along the central passage where the rate of heat release is greatest. Accordingly a further objective was to optimize the flow distribution of the coolant so that maximum surface temperatures in each channel would be as nearly equal as possible. This was done in order to achieve the greatest possible margin between peak surface temperature and the saturation temperature of the pressurized water, thus providing the maximum capacity for overload operation. The method of controlling the distribution of the flow was to apply the proper degree of restriction to each passage, in the form of varying sizes of orifice holes in a thin plate fastened to the lower surface of the bottom support plate of the core. Thus, in order to achieve interchangeability, it is the positions and not the units themselves which are orificed.

II. Analytical Treatment

1. Source Data and Basic Computations

The first step in the analytical approach to this problem was to determine the axial power distribution through each of the parallel flow passages through the core. In the APPR-1 there are 38 stationary fuel elements and 7 movable control rods, but the flux symmetry in the core makes it necessary to use only the flux measurements in 6 stationary elements, and 2 control rods since the safety rods are equivalent to fuel elements in this respect. The axial power distribution in each of these passages was obtained by making neutron flux measurements at zero power in Alco's Criticality Facility. The neutron flux values at various points along the core axis, in each passage, were normalized to the average in the core and, since the neutron flux is proportional to the heat flux, the normalized neutron flux curve was used as a normalized heat flux curve.

The next step was to calculate the axial metal surface temperature pattern in the central control rod fuel-element section using the appropriate normalized axial heat flux curve. For this calculation, the average coolant velocity through the core was used. The central control rod was selected because the region of highest flux and greatest heat release lies very nearly along the core centerline. Figure 1 shows the curve of metal surface temperature versus axial location within the central control rod flow passage up to the point where the peak temperature occurs. Although in this brief presentation there will be no discussion of the evaluation and application of hot channel factors, it should be understood that at every point in this and the next figure, and wherever peak temperatures are cited throughout this paper, they are calculated on the basis that all identifi-

Fig. 1 Fuel Plate Surface Temperature Versus Axial Position

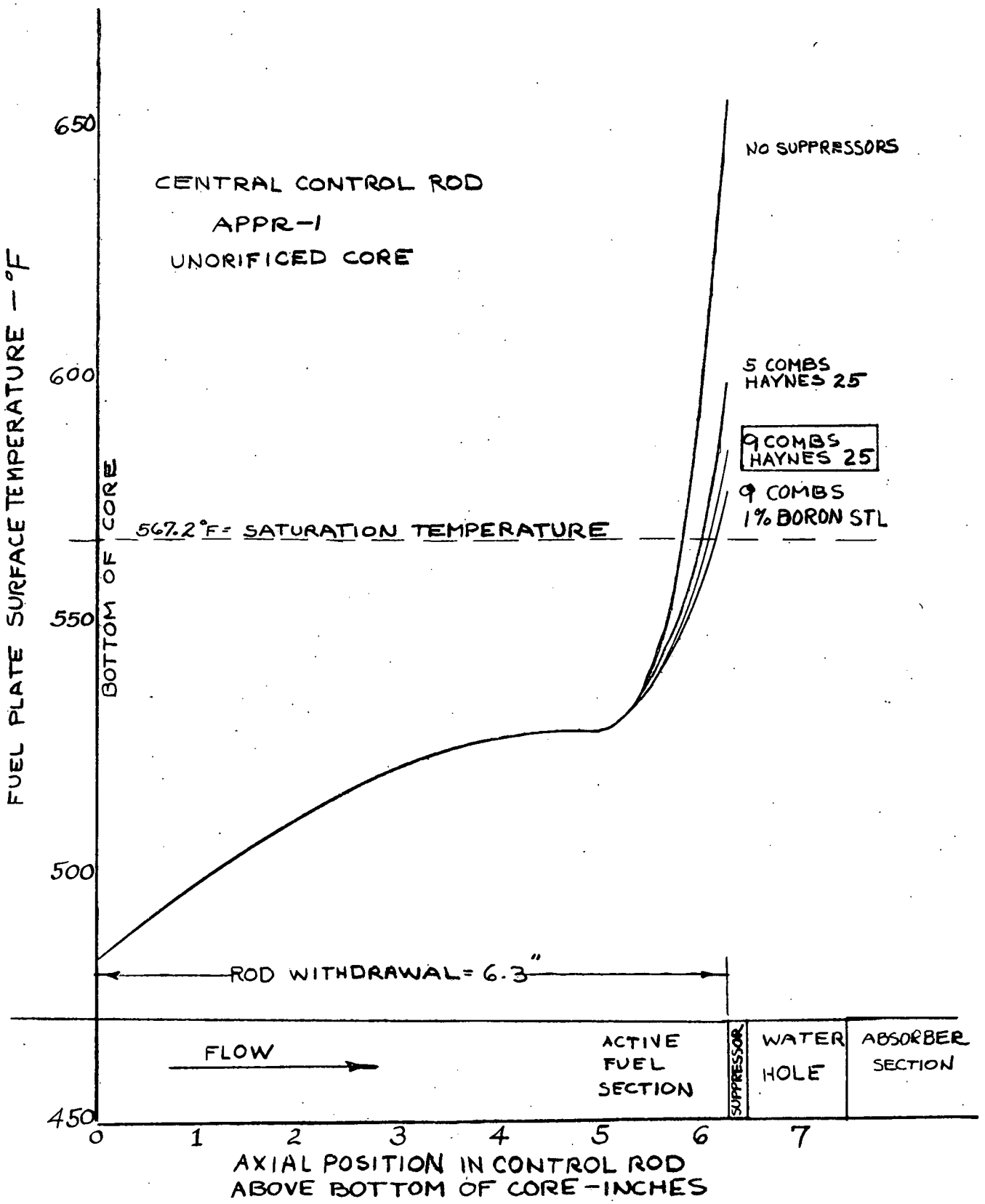

able hot channel factors were simultaneously at their worst in the particular channel and at the point in question. For this study the core burnout is assumed to be 5.4 MW yr., and the fuel to contain equilibrium samarium and no xenon. According to nuclear calculations, these conditions represent the worst to be expected and occur when the rods have been withdrawn so that the fuel-bearing portion extends 6.3 inches into the core to compensate for the 5.4 MW yr. burnout.

2. Water Hole Flux Peaking

The upper half of each APPR-1 control rod contains a neutron absorbing medium and the lower half contains an assembly of parallel fuel plates. At the junction of these two sections there is a relatively large volume of coolant water in which the neutron absorber is not fully effective and in which fast fission neutrons are slowed to thermal energies and reflected back to the fuel plates. The increased thermal neutron density at the upper tips of the fuel plates results in a very high rate of fission heat release in this region and is referred to as the "water hole flux peaking". The sharp rise in temperature at the upper end of the curve shows this effect.

To prevent the occurrence of boiling in the reactor, the metal surface temperatures in the region of the water hole are controlled by means of small, neutron-absorbing plates which are attached to the upper ends of the fuel plates. The highest curve shows the rise in surface temperature which would occur if no "flux suppressors" were used. The other curves show the effect on the surface temperature of inserting different types and configurations of flux suppressors. The flux suppressors are shaped like combs and are placed in the water hole at

right angles to the fuel plates, spaced evenly, with their teeth inserted between the upper ends of the plates. The suppressor combination outlined by the box was chosen for reasons of fabrication and durability.

Having established the peak surface temperature for the centerline flow passage, the peak surface temperature of all other flow passages could now be computed. The calculation was based on the assumption that the maximum metal surface temperature in each parallel passage occurs at the same distance from the inlet to the core, that is, the maxima lie in the same transverse plane. The Z. P. E. flux measurements showed that the axial positions of these maxima deviate from a common transverse plane by only 3/4 of an inch.

3. Preparation of Working Charts

The rise in bulk water temperature from the inlet of each flow passage to the point of maximum surface temperature was then computed by applying the ratio of the integrated heat flux along the passage to the integrated heat flux along the central control rod passage. The temperature drop across the film, from the metal surface to the bulk cooling water at the point of maximum surface temperature was then calculated by applying the ratio of the local fluxes at that point. These calculations were carried out for all fuel element passages for the average coolant flow velocity of 4. 12 ft/sec. Since the heat transfer coefficient varies very closely with the velocity raised to the . 8 power, a plot of maximum surface temperature versus coolant flow velocity for each element could be made as shown in Figure 2. Each curve is labeled to identify it with the proper flow passage shown in the schematic core cross section. It is apparent that, for a given flow velocity, the highest temperatures occur near the center of the core.

Fig. 2 Metal Surface Temperature Versus Coolant Flow Velocity

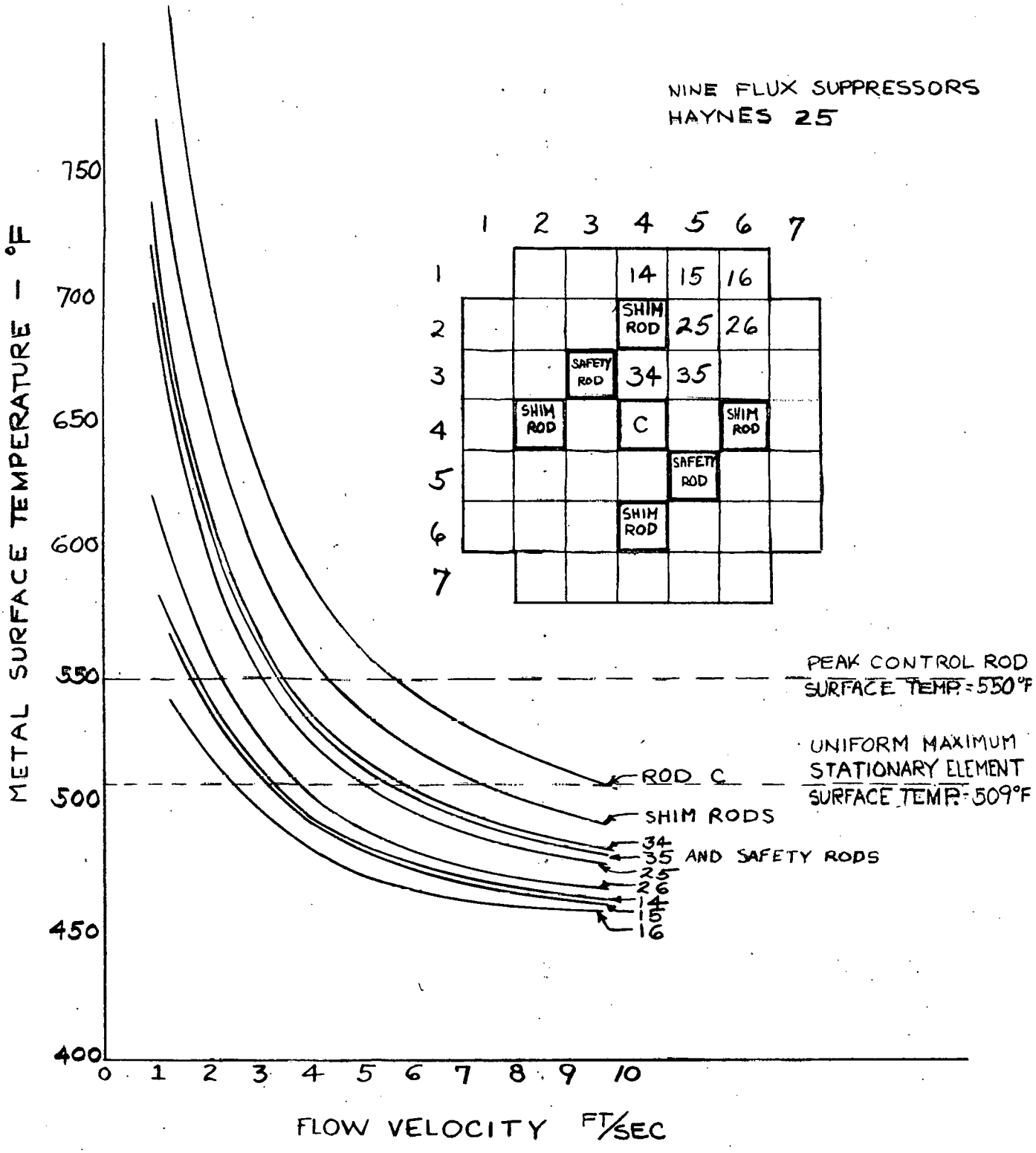

The coolant flow through the various control rods cannot conveniently be regulated individually, so it was postulated for this program that the velocity through all seven rods should be the same. It should be noted that only the central control rod and the four shim rods operate at intermediate positions and are moved in any way during normal operation of the reactor. The two safety rods are always at the fully withdrawn position during normal operation, so that, thermally, they can be considered as normal stationary elements.

4. Calculation of Desired Flow Distribution

The final step in calculating the desired velocity distribution was to determine a common maximum surface temperature for all flow passages such that the sum of the volume flows through all passages should be equal to the overall coolant design flow rate of the power plant. This required a trial and error solution. Recall that Figure 1 showed a high local peaking of surface temperature adjacent to the water hole in the central control rod. Similar peaking, but at lower levels, is experienced by the four shim rods which also operate at a partially withdrawn position. This flux peak is an extremely localized condition, occurring only at the downstream tips of these fuel plates where the spacing tolerance is held within closer limits than usual by these suppressor combs. Accordingly at this point the hot channel factors used for the core as a whole are excessive. For these reasons it was decided that a proper balance would be achieved by giving the control rods sufficient flow to hold the peak temperature in the central control rod at $550^{\circ}F$, 17° below saturation. This led to a trial and error calculation of the combination of common maximum surface temperature and schedule of individual flow passage

velocities which would satisfy the total flow requirements.

5. Prediction of Results

The final results of this analysis showed that a peak control rod temperature of 550°F, could be obtained at 4000 GPM if the velocity distribution shown in Figure 3 was imposed on the core by the successful execution of the development program which is described below.

We believe that the actual cooling of the reactor as built, while completely satisfactory, does not fully match the performance just cited for the stationary elements, for three reasons:

(a) In the calculation of the desired flow distribution, each fuel element was treated on the basis of its center-line flux level. It was estimated that the obvious discrepancy between this value and the side or corner of the element nearest the axial core center-line would be sufficiently small to make this the most desirable treatment. Later analysis revealed that when rigorously applied this descrepancy amounted to a significant correction for the eight outer-most corner elements.

(b) Flow distribution in the lattice cannot be significantly tailored because of the absence of separate, continuous channels. Furthermore, in the experimental work the calibration of the equipment used to measure flow in the lattice proved more difficult than anticipated, and not of sufficient importance to warrant an expensive program to refine it. Accordingly, in the final design it was necessary to allow a slightly disproportionate amount of coolant to flow through the lattice, thus depriving all intra-unit passages of a fraction of their anticipated flow.

Fig. 3 Coolant Flow Velocity Profile

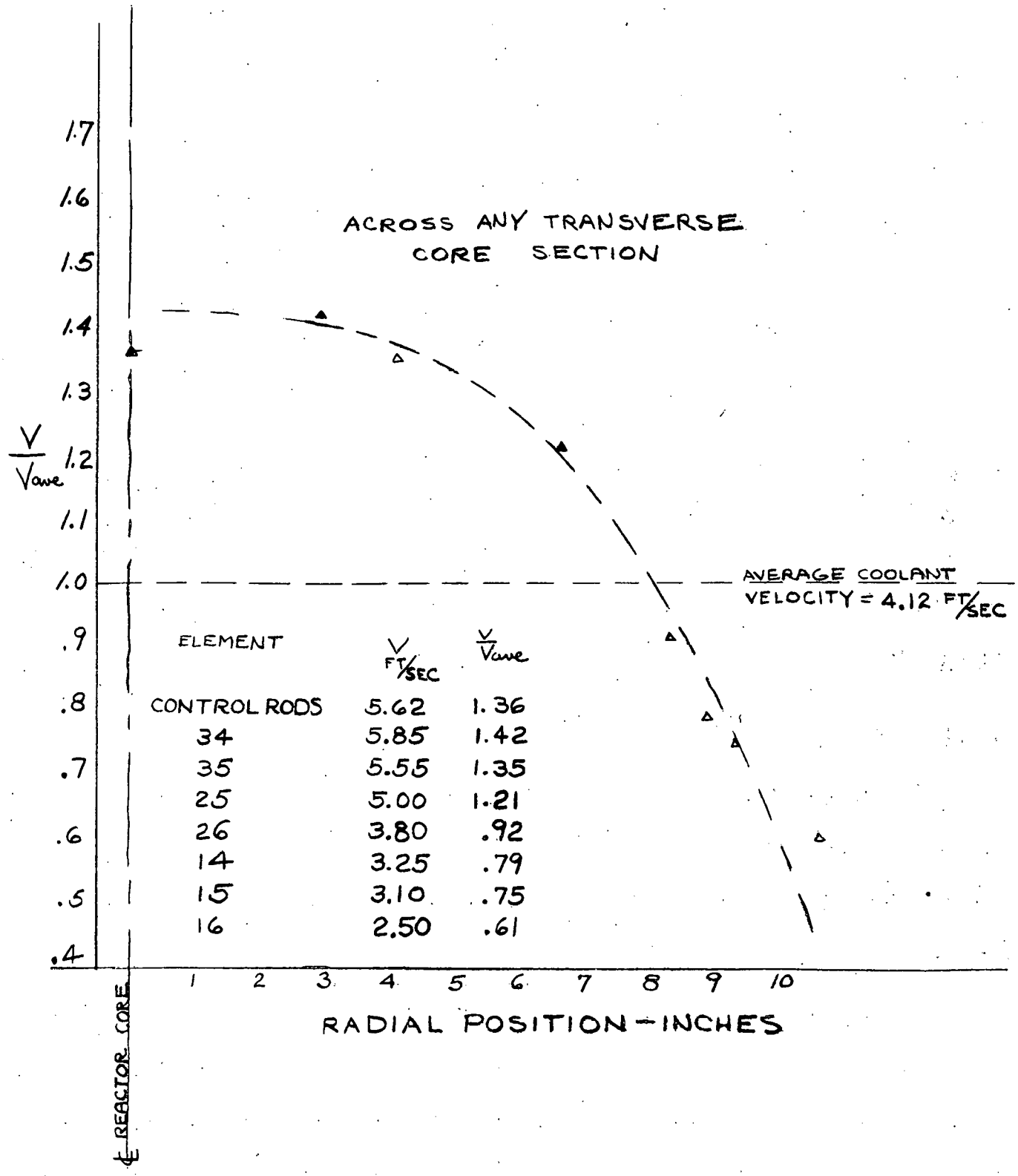

(c) As a whole, the matching of the primary coolant circulating pump head to the system (including the back flow through the Y-valve to keep the inactive pump leg warm), as revealed when the completed plant was first operated, appears to have been gratifyingly close. Nevertheless the actual head required, including the effect of this orificing program and of the back-flow, exceeded the specification prepared for the pumps a year and a half earlier by several percent. The two alternate pumps differ in head at the design flow rate by about the same percentage and thus it turns out that with the lower head pump the net flow through the core is about 3-1/2% below the design value.

The net result is that our present calculation of the maximum possible surface temperature in the fuel elements ranges from 523°F to 551° F, due principally to this radial gradient within individual outer elements taken rigorously at full face value.

III Experimental Operations

Because of the irregular and non-symmetrical conditions in the upper and lower plenum chambers, and of numerous other complications, it was very early decided that control of the flow distribution would have to be worked out experimentally, on a test model.

Turning now to this experimental phase of the program, Figure 4 is a cross-sectional view of the model used. The coolant enters the vessel in the annulus between a shroud and the vessel wall, spreads around that annulus and flows down into the lower plenum chamber. There it turns and passes up through the orifice plate, into the core and up into the upper plenum chamber and out through the nozzle leading through the annulus. The two plenum chambers are

not free and clear as indicated by this drawing, but significantly obstructed by the control rods. Although water is the coolant in the real reactor it was decided that the use of air as the test fluid in the rig would yield adequate simulation and tremendous savings in cost compared to handling large volumes of water. The air velocities used were far below the range at which compressibility becomes a factor, but high enough to provide a Reynolds Number in the turbulent regime.

As was noted earlier, the coolant velocities through the core were tailored, to match the schedule determined from the calculations just described, by a multi-orifice plate fastened to the bottom of the reactor core. Obviously these orifices also had to eradicate all random variations in flow velocity resulting from non-uniform conditions in the plenum chamber just below the core. Because of the 10^{o} rotation of the core structure in relation to vessel inlet and outlet, combined with the assymmetrical arrangement of seven control rods, it was necessary to build a model of the complete reactor, not just a fraction of it, to simulate these flow characteristics. The necessity of measuring these effects upon the flow in individual channels with actual widths of 0.133 inch required making the model the same size or even larger than the real reactor. As shown in figures to follow, the final choice here was to make the model exactly full scale.

1. Design of Flow Rig

The guiding principle was the simulation of all shapes and dimensions of surfaces exposed to the coolant with whatever degree of precision was warranted for the passage involved. Accordingly, the shell of the model, for instance, was made from 1/8 inch steel to the correct inside diameter. The parts of the thermal shield which were all thick and which had surfaces forming flow

Fig. 4 General Cross-Sectional View of APPR-1 Flow Test Rig

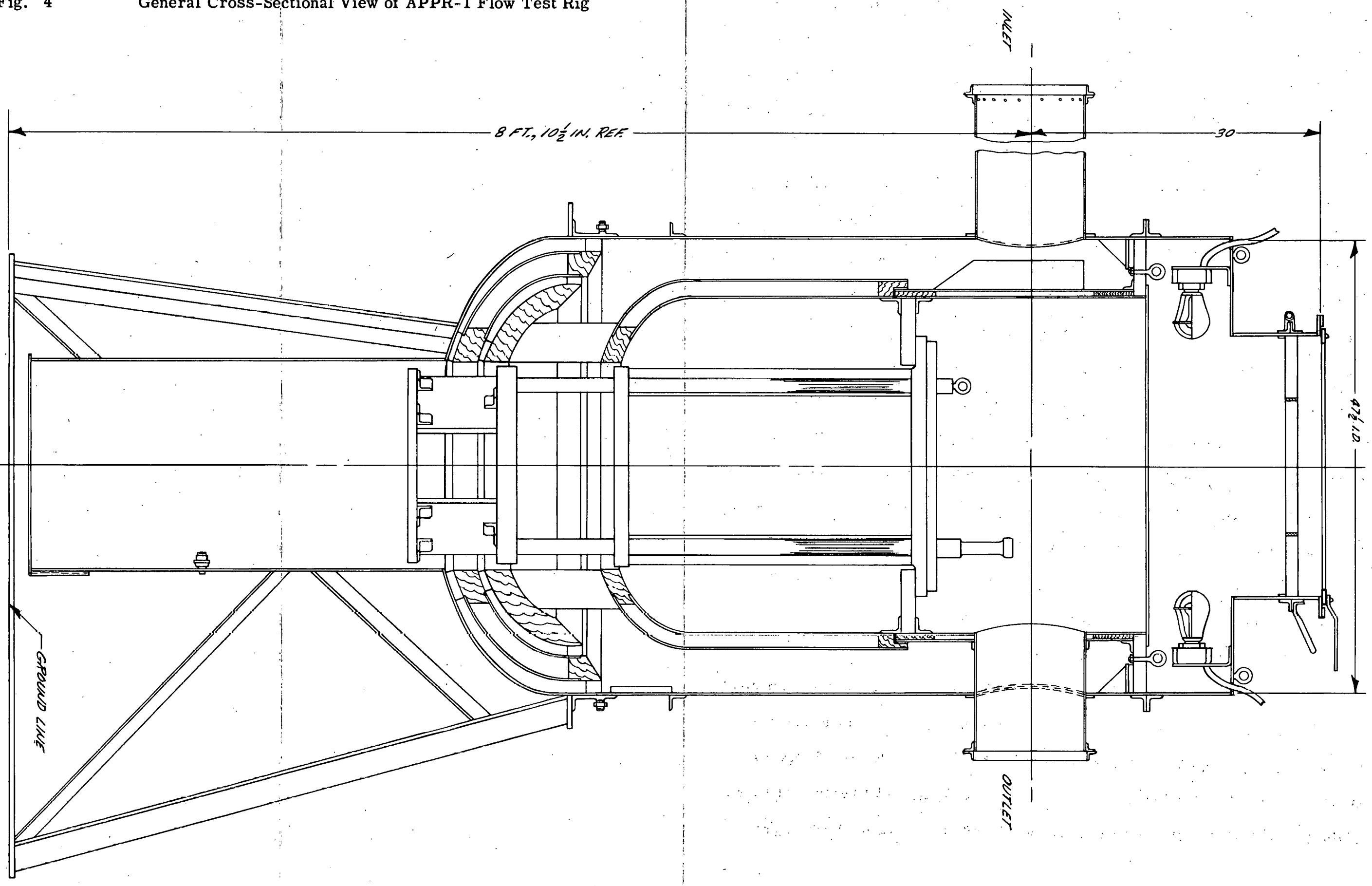

channels, were simulated either by a sandwich construction or by large wooden sections prepared in the pattern shop. Aluminum spinnings were used to simulate the dished shapes except that steel was used in the one case where it was necessary to be able to mount an instrument anywhere on that surface by magnetic feet.

Looking first at the cross-sectional view of the assembled test rig, Figure 4, the orifice plate, the specifications for which were the entire objective of this program, is mounted on the lower face of the main bottom core support plate. The control rods, not shown in this drawing, move up and down through the entire core, including this plate, so that full square clearance holes must be provided for each rod in this plate. This means that in keeping with the principle of orificing the position and not the unit, there can be no direct regulation of the flow through the rods, only indirect regulating by the combined effect of all the other orifices, which operate directly on the stationary fuel elements and the latticework of passages between elements and rods. This is possible because the three portions of the coolant flow -- through rods, through stationary elements and through the lattice -- all operate in parallel, with a common pressure drop from the lower plenum chamber to the upper plenum chamber.

Considering now just a few of the features of the rig as a piece of test equipment, it is apparent that the far corners of the upper and lower plenum chambers have been simplified to the maximum extent practical since they could have no significant effect on the flow distribution. Parting flanges have been located to suit testing convenience. The entire rod drive mechanism, even the portions within the reactor vessel, have been omitted, with the exception of

wooden shafts to simulate the racks on the rods. In the real reactor the assembly of foundation shields supports and locates the pinions and back-up rollers for the control rod drives and is, therefore, rigidly and accurately fastened to the central portion of the support structure by the thru-bolts. In this rig, in order to facilitate access to the orifice plate and to instruments which we had planned to use in the lower plenum chamber if the experimental results required it, the entire lower portion of the central assembly was supported from the foundation shields. These in turn rested on the outer shell. The lower portion of the thermal shield, instead of being fastened to the spacers below it and having its weight carried through the foundation shields to the bottom of the main vessel, was suspended in the rig from the upper portion of the thermal shield. This provided a parting plane requiring no attachments at the outer surface of the thermal shield nor at the lower surface of the orifice plate.

Immediately above the associated parting flanges were three sets of plastic windows and access doors. In order to provide light in this lower plenum chamber, the tubes simulating the lower thru-bolt spacing columns, but actually serving only as mock-ups in the rig, were made of clear plastic with a flourescent bulb installed in each one. The ordinary lights clearly indicated in the drawing provided generous illumination in the upper plenum chamber and this region was observed through the top window which was also clear plastic. The grid immediately below this window served to suspend the control rods at any desired height, since there was no mechanism for positioning them from below. Lifting eyes with threaded adapters as shown on the left side of the drawing, were replaced during operation by wooden imitations of the upper extension of the thru-

bolts and the door-closing nuts and travel-limiting nuts, as shown on the right. For the basic testing, which consisted of comparative surveys of velocity heads of the discharge from the various fuel elements, a set of holes was drilled in the top window, one each at nine different radii, and all but the one currently occupied by the probe were plugged with ordinary chemistry lab rubber stoppers. This window was free to rotate so as to bring the holes to any desired position.

Dimensionally accurate replicas of the ends and four sides of the stationary fuel elements and of the control rods were procured. For economy's sake, only one of each kind contained accurately simulating parts inside them. For the stationary fuel elements, these comprised dummy fuel plates. For the control rod, as shown in Figure 5, a dummy absorber section, fuel plate bundle and cap and locking mechanism were fabricated. The schematic plan view of the rig and reactor cores in Figure 2 shows the relative positions of the fuel elements and controls. The coolant entry nozzle, not shown, is located on the right 10^{o} below the horizontal centerline of this top view. The exit nozzle is directly opposite it. Figure 6 shows how the elements and rods look when fitted into the model reactor core.

In order to use the fuel elements and control rods which did not have any interior parts, preliminary calibrations of flow versus pressure drop were run on the two complete units. By analysis, followed by two or three experimental tries for each, the correct diameters were determined for orifices installed inside the incomplete units to make their pressure drop curves match almost exactly those of the complete units. The discharge from each control rod must divide and turn in order to exit through 24 holes in the side of the rod near the

Fig. 5 The Simulating Control Rod With Its Components, With the Total Pressure Tube Installed

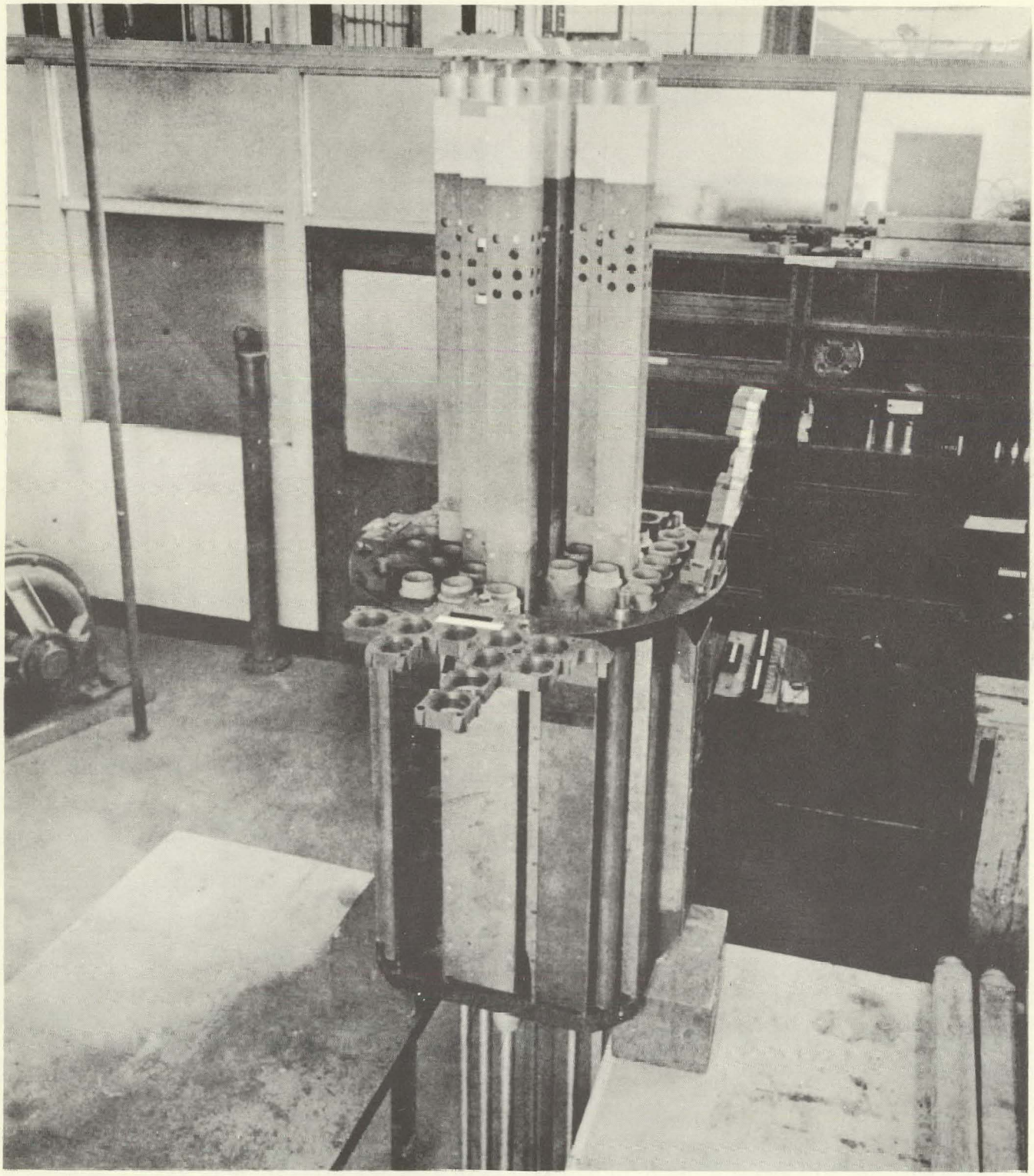

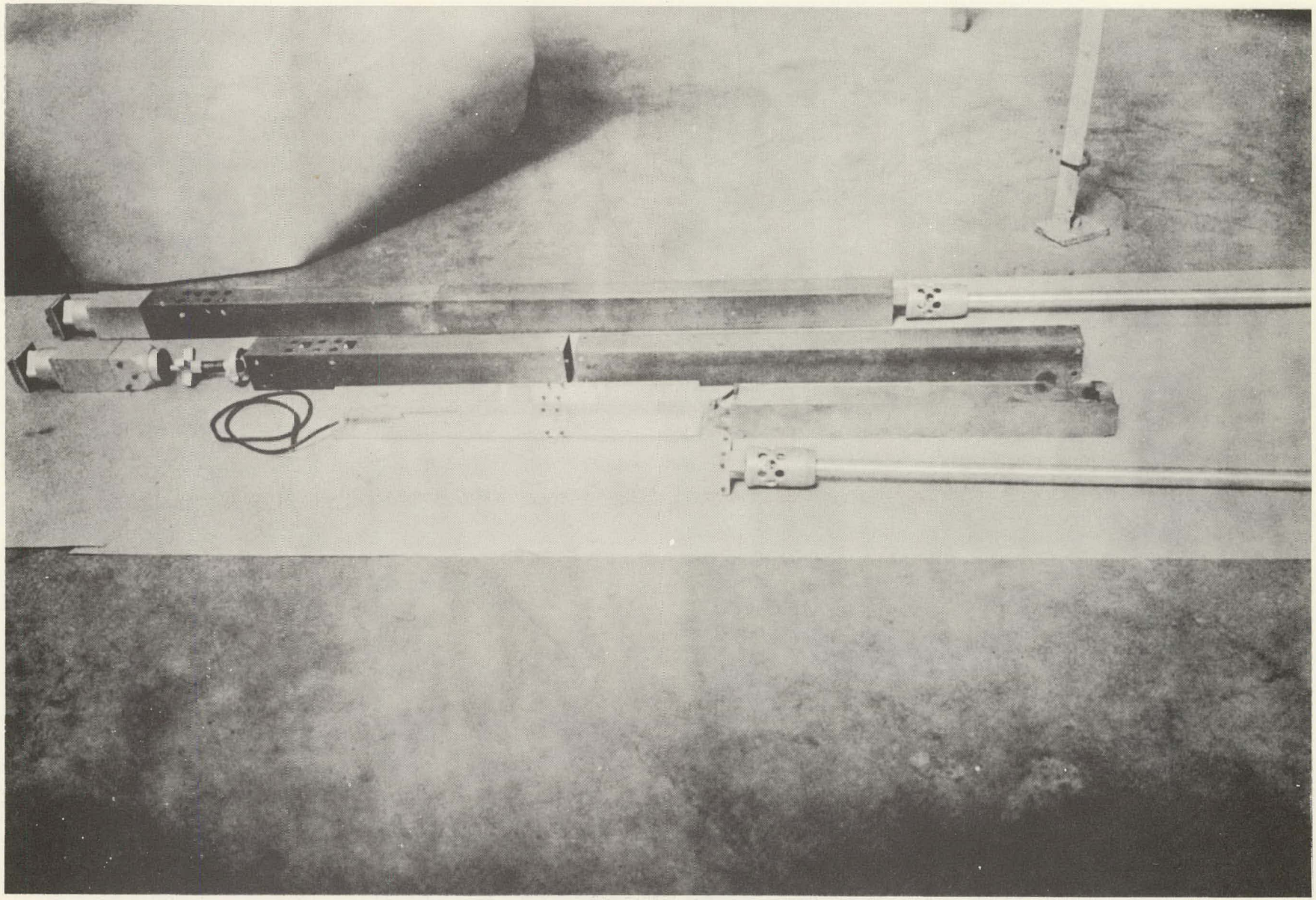

Fig. 6 View of Flow Rig Core Containing Stationary Fuel Elements and Control Rods

upper end. This prevented a simple measurement of flow through the rods by any instrument operating in either plenum chamber, and required the use of a pitot-static tube permanently installed in the absorber region of a rod. This instrument also required preliminary calibration in a basic air flow measuring facility. It seemed advisable to use only the rod with fully simulated parts for this measurement, especially since the use of additional lines would have required correspondingly more manometer hoses inside the rig. This involved the disadvantage that the one rod had to be placed successively in all seven positions in order to complete a survey, each shift requiring opening of the top of the rig. By contrast, the discharge from the stationary fuel elements is in the form of a single, cylindrical stream flowing axially, which made comparative observations of velocity head quite easy, and permitted taking measurements on all 38 units without shifting them around.

The method used to measure the flow velocities in any single channel between the fuel plates, either inside or between fuel elements, was basically that of the hot wire anemometer. We departed from normal practice, however, in that in order to be able to pinpoint the location of our measurement in these fairly small passages, and also to get a high ratio of measuring element resistance to complete circuit resistance, thermistors were used in place of the hot wire filaments. Figure 7 shows how the thermistors were installed. A second program of preliminary testing was necessary to obtain calibrations for these thermistors. In order not to have the electrical leads from them interfere with the normal airflow, these leads were in the form of copper ribbons .010 inch thick, imbedded flush in the imitation fuel plates.

Fig. 7 Installation of Thermistors on Plastic Simulating Fuel Plate

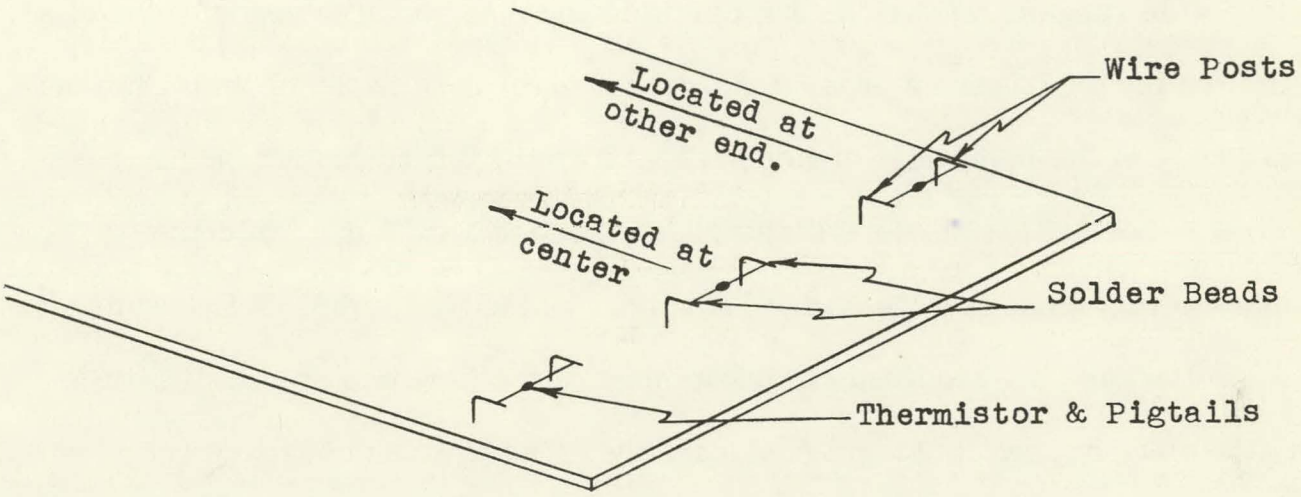

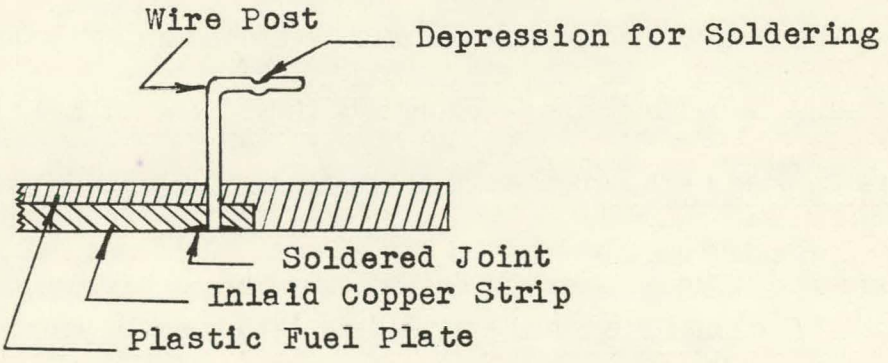

2. Basic Test Program

In the testing with the full rig, the initial survey of flow rates for each stationary element and control rod position, presented in Figure 8, showed a fairly wide range of variations due partly to the dissymmetry described earlier, partly to the obstructions presented by the control rods in the plenum chambers and partly to the inherently higher pressure drop characteristics of the rods. A first set of orifice diameters was computed to meet the dual objective of counteracting these factors and of providing the desired radial distribution.

Because the required rearrangement of the flow was so drastic, this orifice plate missed its target considerably. The test of the second set of orifice diameters showed great improvement, but was still not quite close enough to the target, so a third plate was cut, which proved generally satisfactory, as shown by the graph in Figure 9, in which values for each radial family are averaged. Certain individual units still showed small deviations from the target, and by now we had developed a pretty dependable correlation of change in orifice size to change in flow. Accordingly minute corrections were applied to the diameters of the third test plate in making up the final recommendations.

The final step in the experimental program was to work out the proper sizes for the holes feeding the lattice passages, using the thermistors to observe the flow in a representative number of passages.

Fig. 8 Results of Initial Velocity Survey

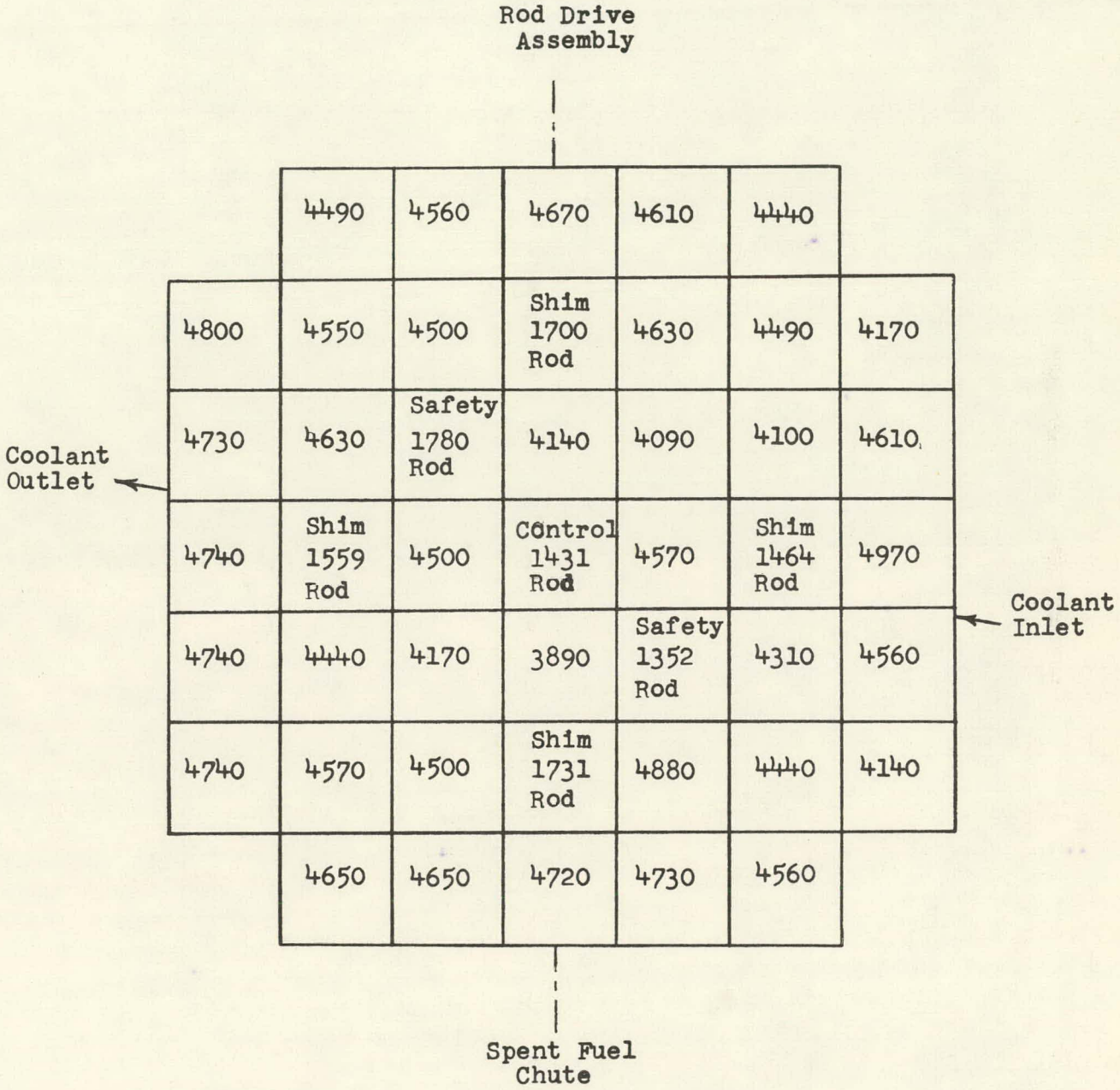

(Top view; Velocities in ft^3/min)

Fig. 9 Effect of Tailoring in the APPR-1 Flow Rig Model

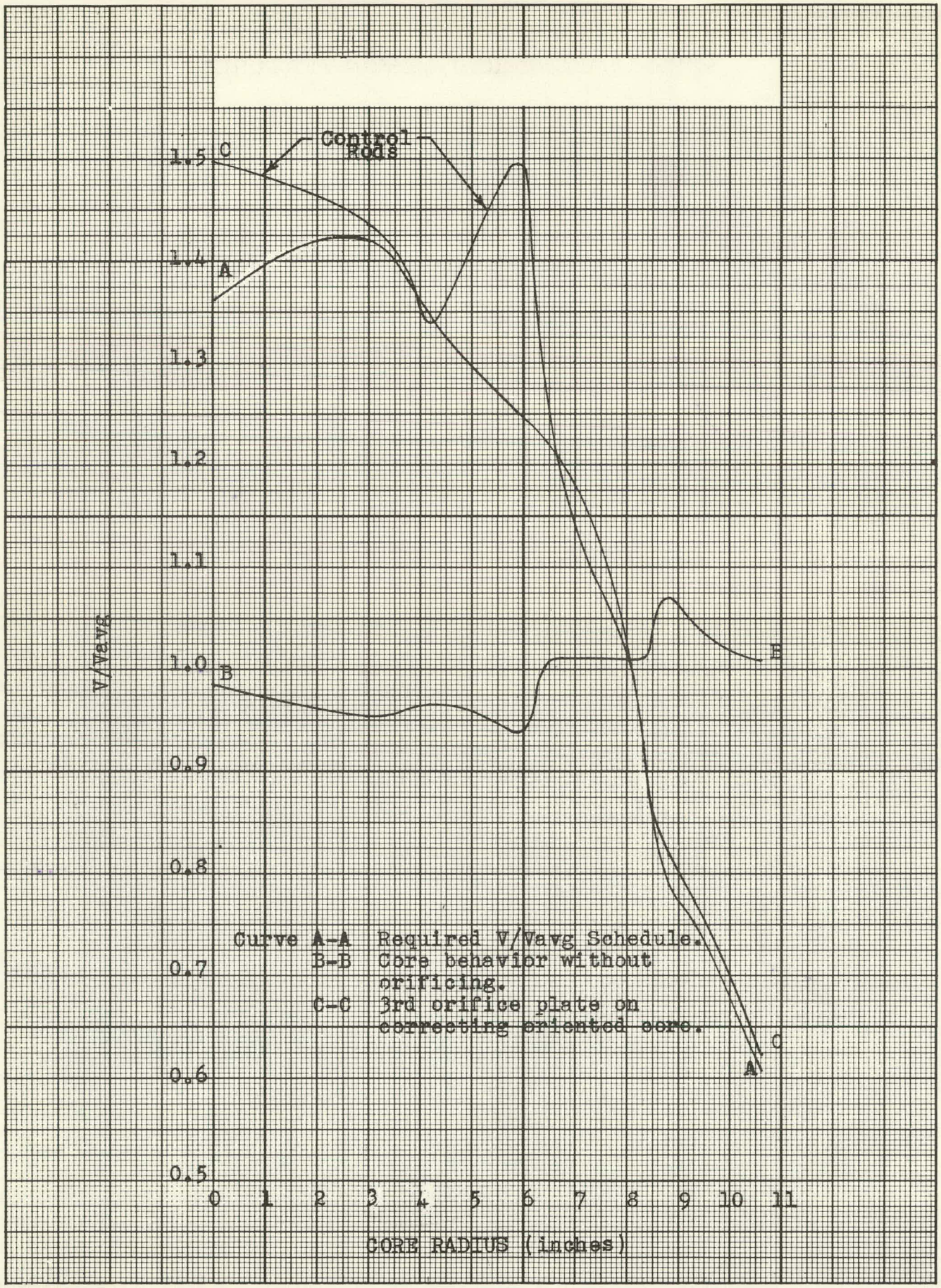

APPR-1 MECHANICAL DESIGN FEATURES

BY

J. F. Haines

J. P. Tully

Presented at the Second Winter Meeting of
The American Nuclear Society on October
28, 1957 in New York City,

LIST OF FIGURES

MECHANICAL FEATURES OF THE APPR-1

I. General Design Philosophy

The design of the major operating components of the APPR-1 primary system was influenced to a large extent by factors peculiar to its role as a prototype of power plants suitable for operation in remote areas. Among these factors were the importance of minimizing the time required for maintenance operations and the need for self-sufficiency of both the plant and its normal operating crew.

Contract requirements specified a time limit of 24 hours for a complete fuel change, exclusive of cooling down and heating up of the primary system. A maximum of 24 hours for removal and replacement of all control rods and drive units was also imposed. Time limits on other maintenance operations were similarly stated in the contract.

Since a remotely located plant is called upon to operate for considerable periods without assistance from outside sources of material or manpower, maintenance of equipment must be performed by the normal operating crews. It is obviously undesirable to require the services of highly specialized personnel to perform maintenance functions only. Therefore, considerable stress was placed upon such units as control rod drives, seals etc. to break them down into sub-assemblies which could be handled as replaceable units rather than attempt to repair components in place. Because radioactivity levels near the primary system after shutdown could not be predicted accurately, an additional premium was placed upon the ability to remove and replace these sub-assemblies with a minimum of personnel exposure inside the vapor container.

Certain components within the reactor vessel such as core support structure, control rods and parts of the control rod drives become highly radioactive after relatively short periods of power operation. Servicing of these components is, therefore, quite difficult. Accordingly, such units were designed very conservatively, and extensive testing was carried out in order to minimize the possibility of mechanical troubles in these areas.

Particular attention was paid to simplifying and fool-proofing the refueling operation for two reasons. First, damage to fuel elements or internal parts of the reactor structure would be extremely costly and time consuming to repair. Second, crews cannot be expected to keep in practice on this operation since it is performed only at intervals of approximately two years. The means by which these ends were obtained will be discussed in this paper.

II. Primary System

Although the APPR-1 has been described many times before, the following brief description of the primary system may not be out of order here.

4000 GPM of water at 1200 psi and 450^{o}F leave the reactor vessel after picking up heat in the core at the full power rate of 10,000 KW. It flows through the 12" pipe to the steam generator where it converts secondary water to steam at 200 psi and 25^{o} of superheat. The pressurizer is connected to the main pipe run between these two vessels by means of a 4" pipe.

From the steam generator the water, now at 431^{o} F, goes through one of two canned rotor pumps and back to the reactor vessel. A 2-way swing valve, of Alco design and manufacture, prevents major back-flow through the inoperative pump, but by-passes enough water to keep the dead leg hot. This is the

only large valve in the system, and its operating requirements permit very simple rugged design, only one moving part and no requirement of internal leak tightness.

The criteria for selection of materials for the primary circuit was an engineering balance between important properties necessary for satisfactory operation and service life on one hand and availability, cost, weight and ease of fabrication on the other. On this basis, type 304 stainless steel was selected as the corrosion resistant material of construction as it offered the best balance between resistance to operating conditions and the economic and practical factors associated with fabrication. The operating conditions of greatest importance are corrosion by 450°F water in all areas and the effects of irradiation in some particular areas of the primary circuit. On the same basis, carbon silicon steel, type A-212 Grade B, was selected as the strength material of construction. The important factors are the effects of irradiation in the reactor vessel shell, allowable stress levels and a satisfactory history in the same or similar application.

Clad material is used for all primary system vessel walls and covers primarily for saving of weight and secondarily for cost reduction.

A number of irradiation samples of the reactor vessel shell material are placed around the top of the core support structure. These samples are encapsulated in stainless steel and are in the form of multiple notched sub-size impact test specimens, permitting up to twenty-one impact tests to be run on the contents of each sample container. The flux in this area ranges from approximately three-fourths to one and one-half the maximum experienced

by the reactor vessel wall. These samples will be removed one container at a time and tested at each fuel change in order to maintain a running check on the vessel pressure shell material to detect any changes in mechanical properties, resulting from irradiation, which might have a bearing on the safety of the reactor vessel.

III. Pressure Vessel and Core Structure

Figure 1 shows the reactor vessel and its contents. Design of the vessel itself presented no major new problems. The ASME unfired pressure vessel code was used as the design basis for the reactor vessel and for all other pressure vessels in both the primary and secondary systems. Thermal stresses in the reactor vessel walls were calculated and the total stress kept within code limits. The combination of a two inch thick stainless steel thermal shield and approximately eight inches of water limits thermal stress in the wall to approximately 12.5% of total allowable stress. Flow is downward around the core and past the thermal shield and then upward through the core itself.

An octagonal section stainless steel ring gasket provides the seal at the closure point between the cover and the vessel shell. The cover is clamped in place by studs and nuts. Here, however, the difficulty of replacement and the necessity for regular removal and re-installation of the cover made itself felt in the selection of materials and treatment of the closure nut and stud threads. Since the vessel cover is immersed in water during operation, the use of corrosion resistant materials was mandatory. Type 410 stainless steel, heat treated, is used in the studs and type 304 in the nuts. These materials are admittedly not the best from the standpoint of thread galling, but experience

has indicated that by lapping the threads and allowing quite large thread clearances, this combination of materials operates satisfactorily.

Removal of the cover weighing approximately one ton is accomplished by means of a manually operated chain fall. The shield tank water, which is approximately 12 feet deep protects the operator during removal of the cover and fuel elements. A small hand operated ratchet hoist permits tilting the cover into a vertical position after removal, for storage in a rack provided on the inside of the shield tank. Storage racks in the form of dummy studs are provided to hold the nuts while the cover is off. The nuts are held in the removal tool by a spring detent to prevent their being inadvertently dropped.

The core support structure consists of a lower plate machined to accept the fuel element lower end boxes, an upper plate in the form of four hinged doors which locate the upper ends of the fuel elements and guide the control rods, a skirt to control water flow through the core, and the control rod drive pinion supports below the lower grid plate. The orifice plate controlling flow distribution is attached to the bottom surface of the lower plate. All components of the core support structure are independently fabricated and finish machined, and assembled by means of appropriate mechanical fastenings.

The use of doors rather than free removable sections of the upper grid plate greatly facilitates fuel handling. The doors are clamped down by captive nuts so that no loose pieces need be handled inside the vessel to gain access to the fuel elements. As in the case of the closure nuts and studs, dis-similar materials are used in the clamping nuts and studs. In this case, the materials are 304 and 17-4 PH. Threads are again lapped and large clearances used.

The core contains 45 fuel elements, 38 of which are of the fixed type shown in Figure 2. The fuel is incorporated as a UO_2- stainless steel dispersion in the form of 18 plates clad with type 304 stainless steel and brazed to inactive side plates. End boxes, of which one is shown here removed to expose the fuel plates to view, complete the assembly. They are welded to the fuel element proper.

The remaining seven places in the core are occupied by control rods as shown in Figure 3. The rod structure is a square tube with the actuating rack rigidly attached to the bottom. A fuel element is loaded into the rod tube through its open upper end and an absorber placed on top of it. They are retained by a positively locking cap.

IV. Fuel Handling Tools

The light weight of the APPR-1 fuel elements, approximately 16 lbs. each, permits the use of manually operated tools for core loading and unloading. A simple hanging weight type of coutergalance is provided to facilitate tool handling. The same tools are used for reactor loading and unloading as are used for transferring the elements to the spent fuel pit through the spent fuel tube. A second identical set is provided to load the spent fuel into storage racks and shipping casks and to serve as a spare set for the primary tools. The gripping elements are so designed that once a fuel element or absorber section has been picked up, it is held positively until intentionally released. The operator has good feel of the locking and unlocking operation to minimize the possibility of accidental release of a fuel element.

The tools telescope from a minimum length sufficient to reach from the operating platform down to the core, to a maximum length permitting an

element to be lowered to the bottom of the spent fuel tube or to be picked up at the bottom of the tube for reloading.

An additional tool handle with interchangeable tools is provided to handle the reactor cover nuts, the upper grid door locking nuts and the control rod caps. Particular care was given to the handling of the control rod caps to prevent the possibility of their being installed on the rods without having an absorber element and fuel element in each rod in their proper positions. The cap will not release from the tool unless this installation is properly made. Storage of the caps when off the rod is provided on dummy holders in the shield tank.

A manually operated geared wrench is provided for tightening and breaking loose the reactor cover hold-down nuts. These nuts are tightened to a prescribed torque range. While this is not the most satisfactory way of establishing proper tightness, it is simple to use and it is felt that the chances of improper tightening are minimized by this means assuming average operating crew personnel to be doing the work.

A complete fuel change cycle was demonstrated at Fort Belvoir to meet the contract requirements. Total elapsed time was 23 hours and 40 minutes.

V. Control Rod Drives

Figure 4 shows the control rod drive train. The drive, of Alco design and manufacture, consists of a rack and pinion, associated bearings and shafting, a seal to control leakage at the point of penetration at the reactor vessel wall, a scram clutch assembly, instrumentation assembly and a drive motor with integral reduction gear. All bearings outside the reactor vessel are

standard commercially available components, conventionally lubricated by pre-packing. The drive is mounted below the reactor to simplify fuel handling. By use of this arrangement, stationary fuel as well as control rod fuel elements and absorber sections can be removed and replaced without interfering with the control rod drives in any way.

All external drive components, including the seal, can be removed and replaced with the primary system hot and pressurized. This is achieved by a valve-like arrangement on the pinion drive shaft which is used to seal off the penetration before removal of the seal. The time required to completely remove and replace all drive components, including seals, was demonstrated at Fort Belvoir to be 45 minutes per drive or a total of 5-1/4 hours. Replacement of the pinion with its associated stellite bearings and the pinion shaft require draining of the system. The control rod and rack can be removed through the vessel cover opening with the system open, but not drained.

As noted before, the seal, clutch, motor and instrumentation are made up of completely independent assemblies bolted together. All components are pre-adjusted and pre-tested on the bench before installation to minimize shut-down time and time of personnel in the rod drive pit. Quick disconnect fittings are used throughout for all electrical connections.

The entire assembly of control rod drives, rods, core support structure and fuel elements were run in the Zero Power Experiment in Schenectady at room temperature before installation at Fort Belvoir.

The seal consists of a series of close fitting metallic rings floating on a shaft. These rings seat on lapped faces of mating diaphrams to prevent leakage around the rings, but permit radial float. A series of very close clearance

annular leakage paths result from this design which gives a low and very constant rate of leakage. Figure 5 shows leakage measurements taken over a period of 2000 hours of both intermittant and continuous operation. A total of seven seals were tested under operating pressure and varying temperature for a cumulative total of approximately 7900 hours during which some 60,000 scram cycles were accumulated. No seal malfunction or significant mechanical malfunction developed during this period. Leakage rate is rather sensitive to temperature as indicated on the curves, but very insensitive to operating cycles and time.

Low temperature make-up water is introduced to the inner ends of the seals so that such leakage as does occur is purified make-up water rather than possibly radioactive primary coolant. Failure of this make-up system would simply result in a slight increase in seal temperature and leakage rate and a small amount of short life radioactivity in the scal effluent. Normally this leakage water amounting to approximately 3 gallons per hour total is reprocessed and returned to the system along with the primary blowdown water. If necessary, however, it can be diverted to the hot waste tank.

Figure 6 shows the results of control rod drop tests taken at Fort Belvoir under operating conditions of temperature, pressure and flow. Gravity is used as the only accelerating force during a scram and provides sufficient acceleration to shut down the reactor before any serious rise in energy resulting from a reactor excursion can occur. A scram is initiated by de-energizing the magnetic scram clutch. Clutch release requires approximately 40 to 50 milliseconds and free fall acceleration is of the order of .4g under normal

operating conditions. Downward motor drive is provided through a mechanical over-running clutch in case of possible rod sticking, which has not occurred during either testing or well over 2000 hours of plant operation which has been accumulated to date.

VI. Closing

Major attention was given throughout the design and test program to developing components having a high degree of reliability and requiring a minimum of maintenance time. Simplicity of fuel handling tools and techniques was stressed. Development testing of components was as extensive as felt necessary to insure satisfactory plant operation. The fuel handling tools, for example, underwent a minimum of testing prior to their use at the site. On the other hand, control rod drives were given exhaustive endurance tests on a multiple rig permitting simultaneous operation of six drives, in addition to performance tests on a single rig. The swing check valve was given a brief functional test at operating pressure and temperature.

The freedom from difficulties encountered in the reactor and primary system components would indicate that the philosophy followed in the design and testing is a sound one.

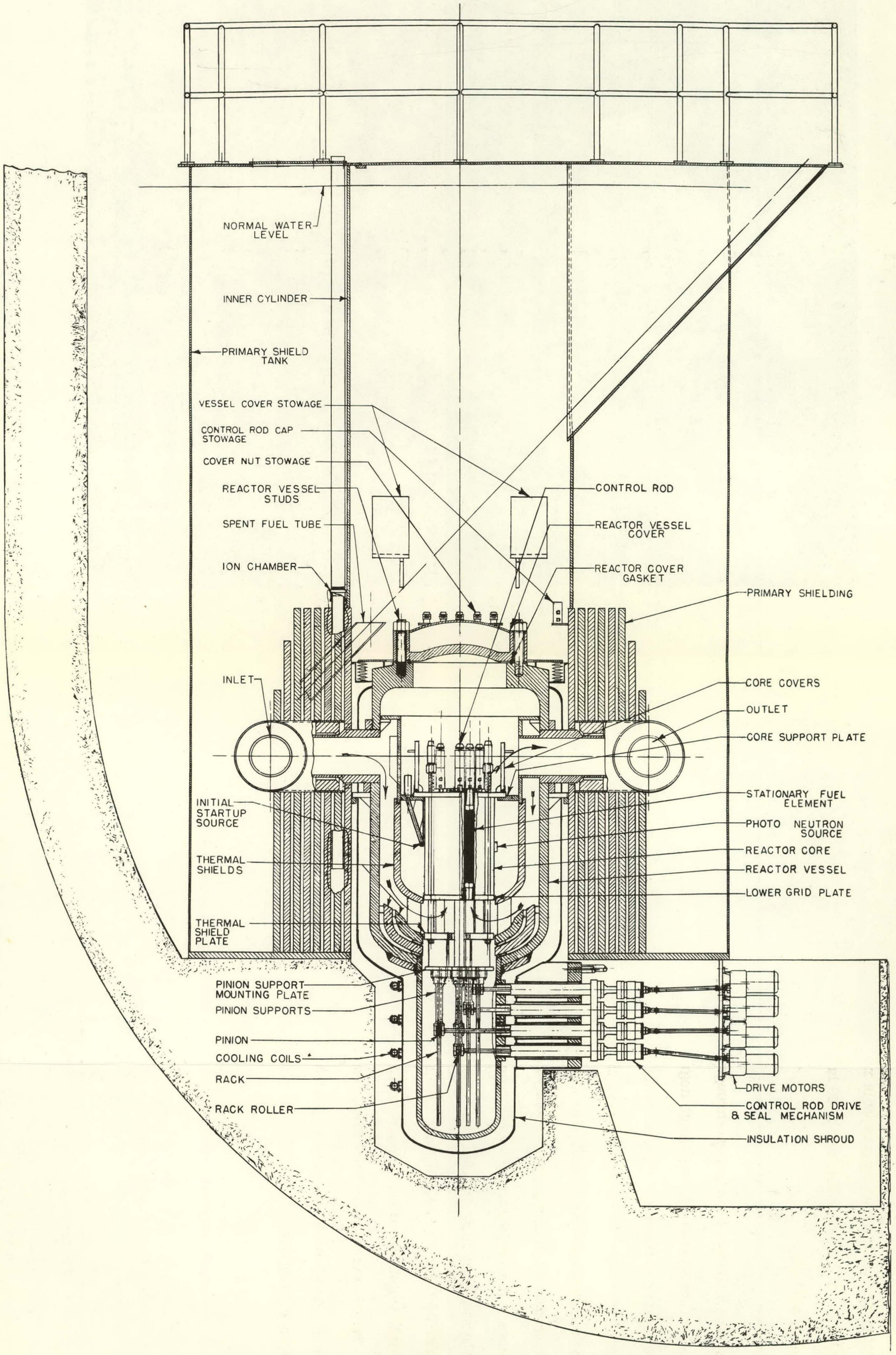

Fig. 1 Reactor Layout

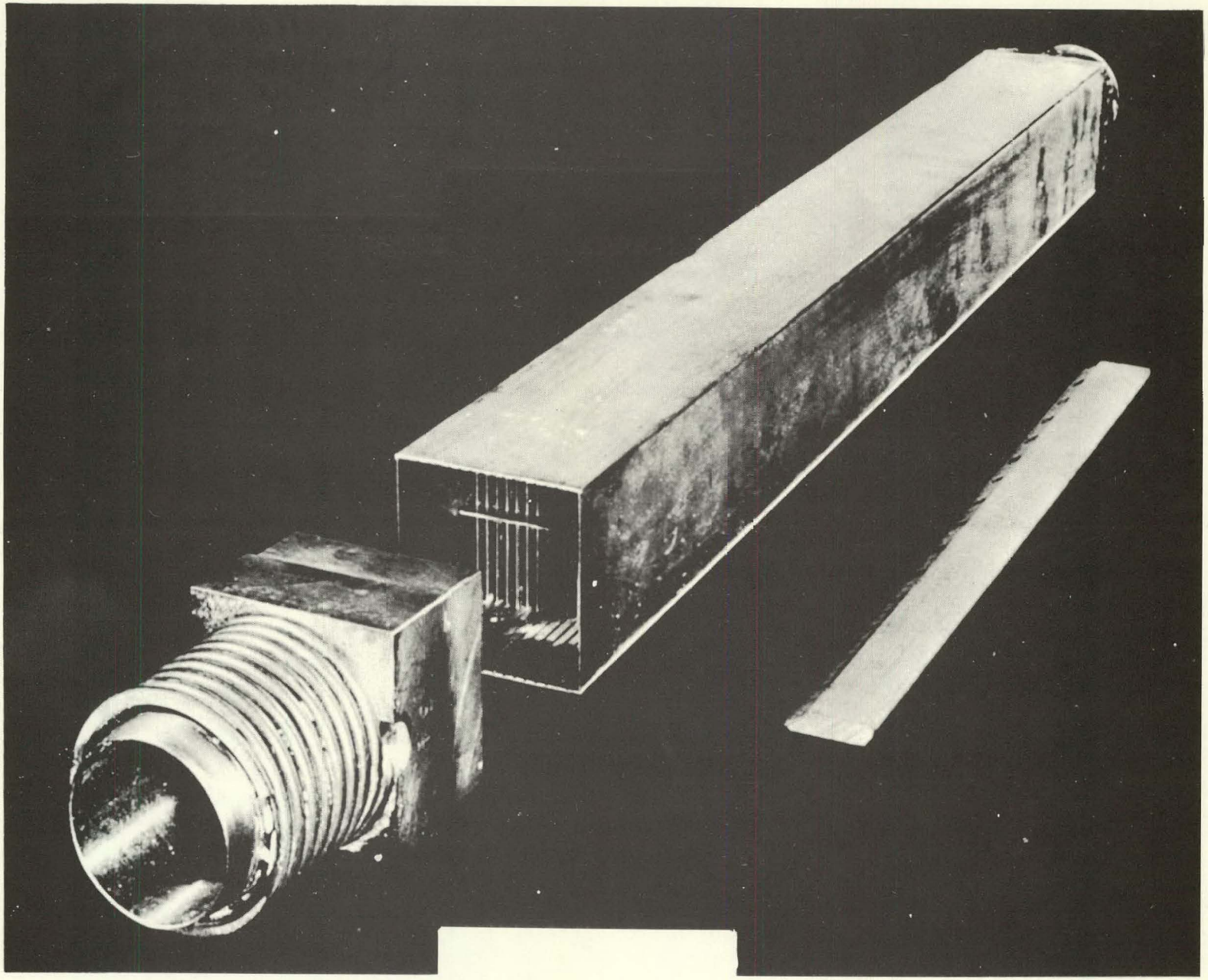

Fig. 2 APPR-1 Fuel Element

Fig. 3 Control Rod Assembly

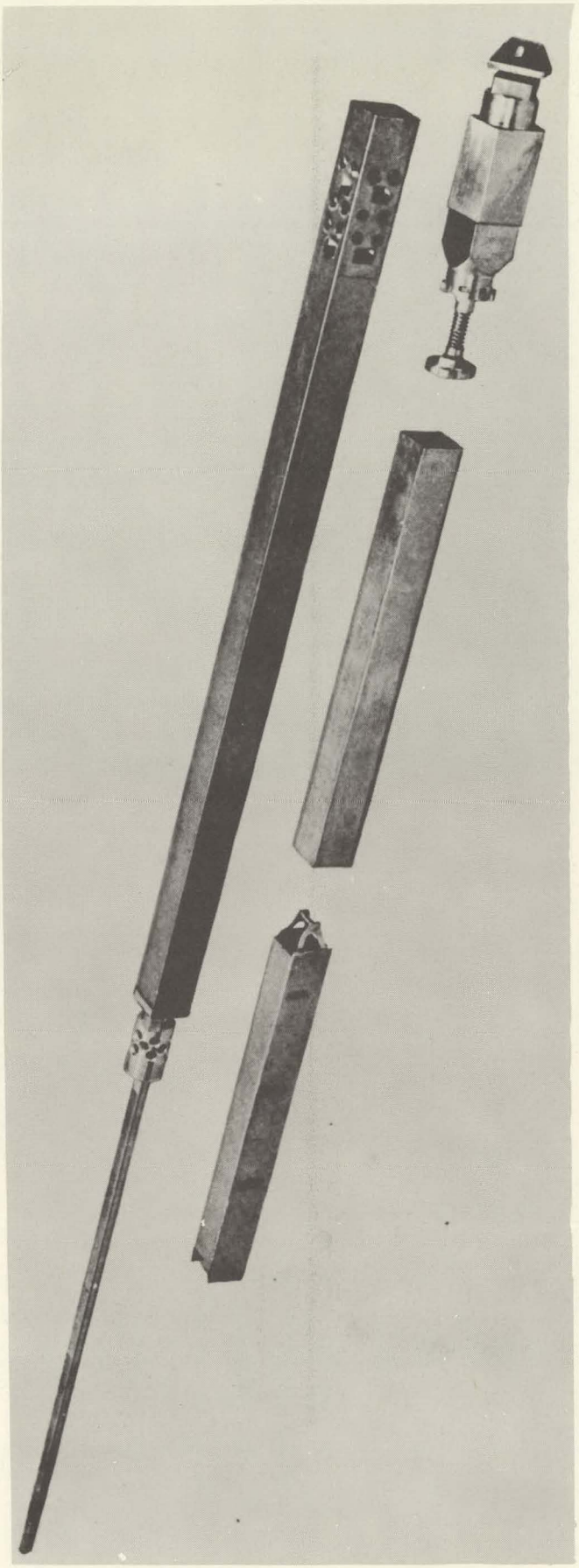

ALCO CONTROL ROD DRIVE MECHANISM

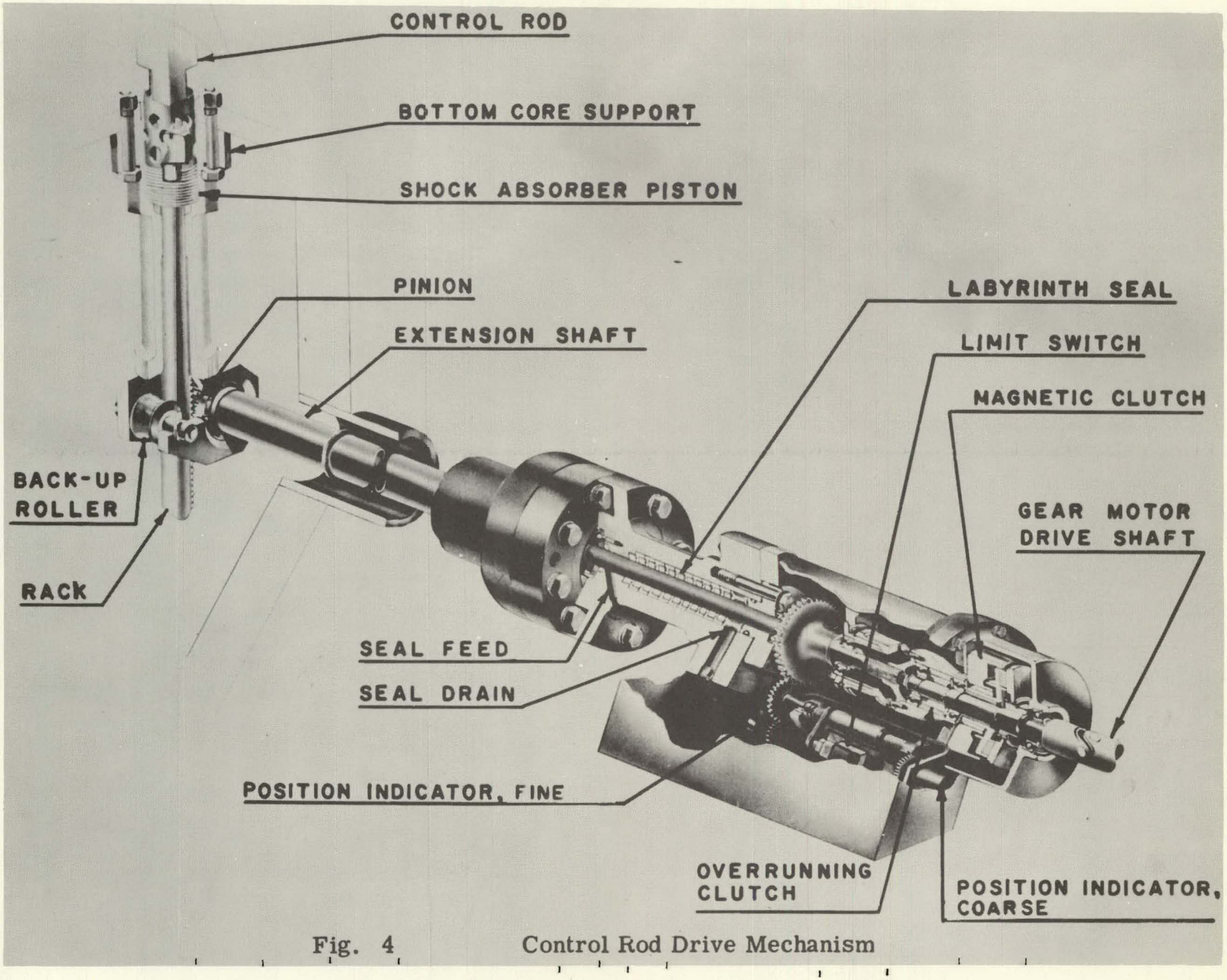

Fig. 4 Control Rod Drive Mechanism

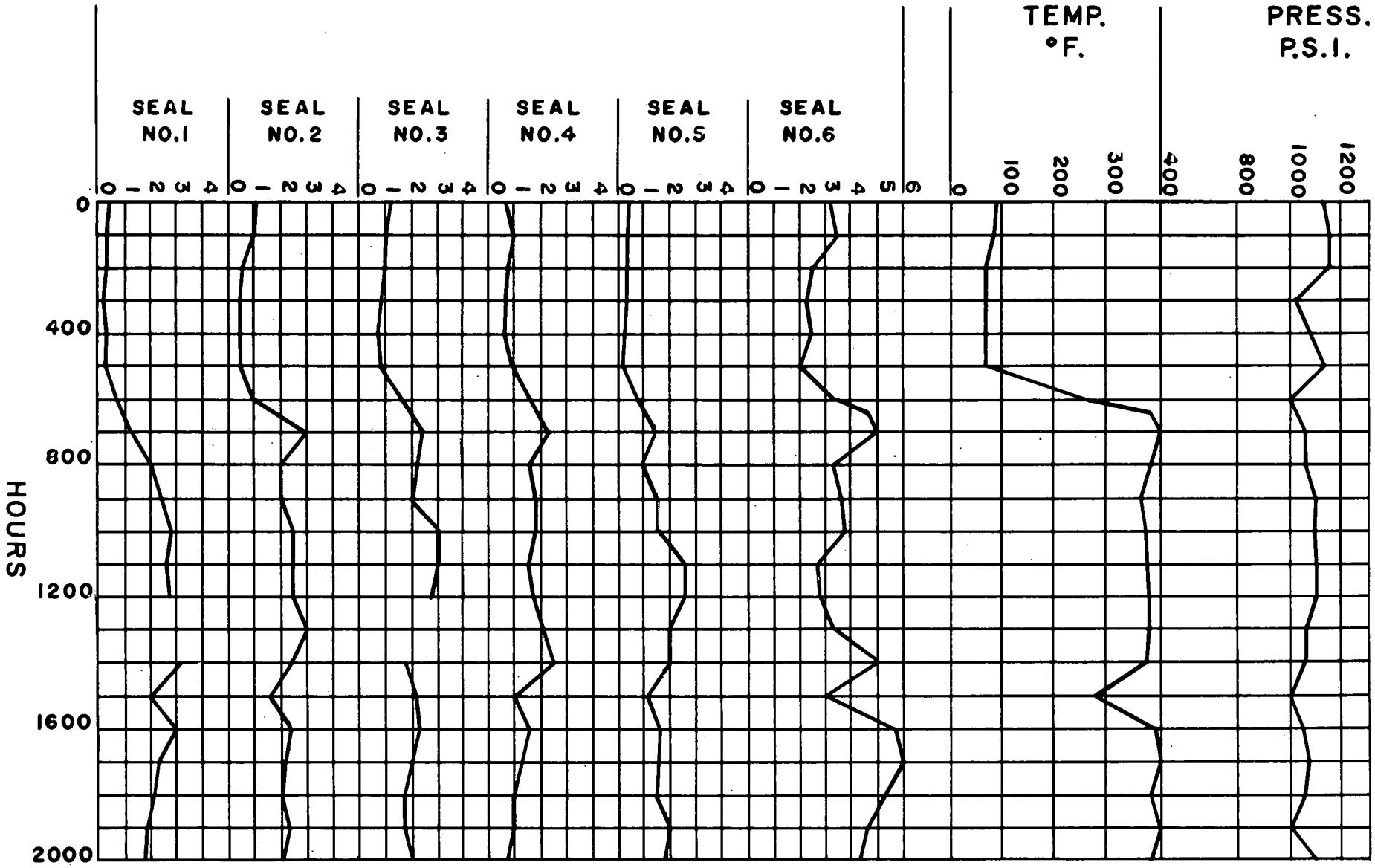

Fig. 5 Average Seal Leakage - Lbs. Per Hour

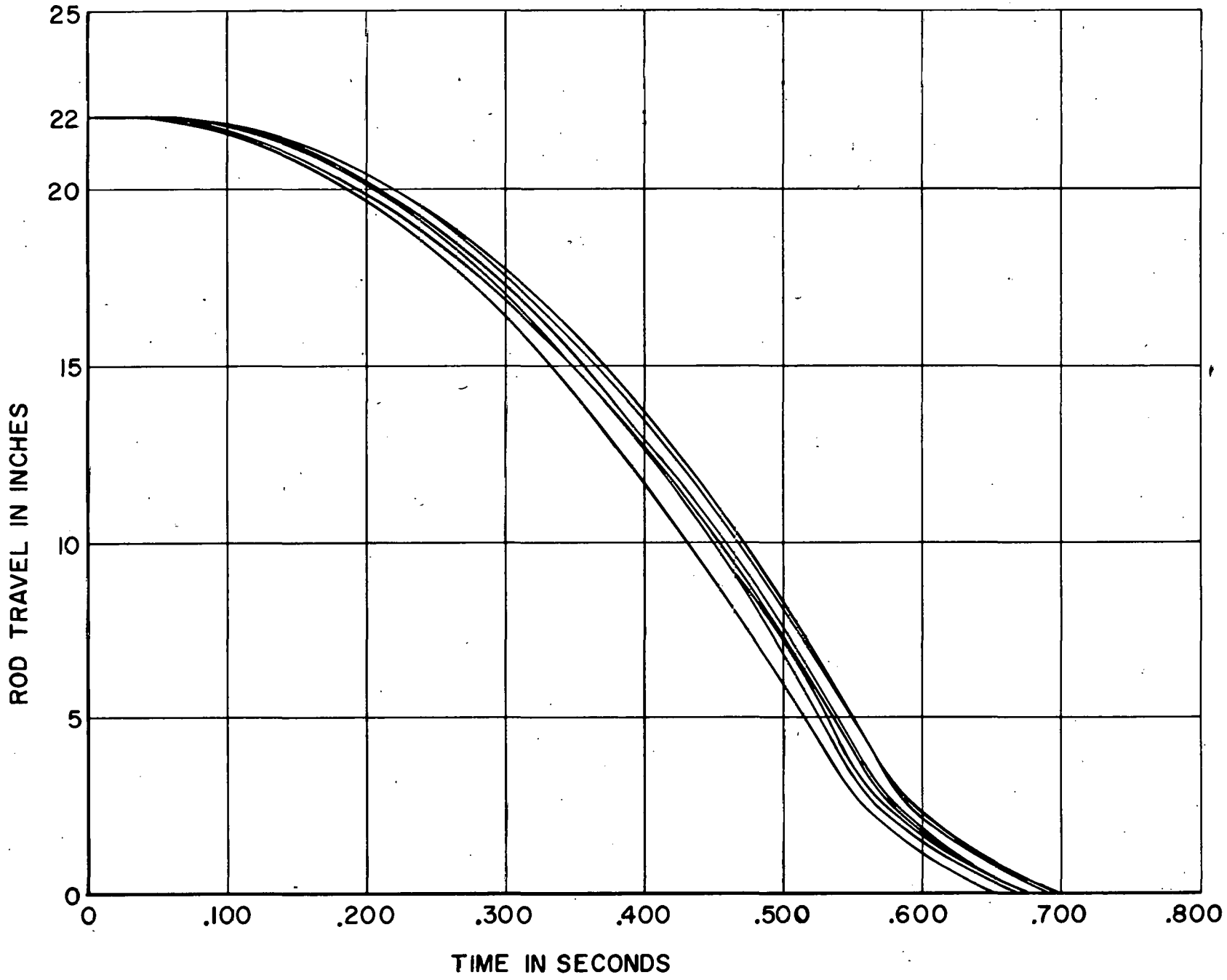

Fig. 6 Control Rod Scram Tests APPR-1 at Fort Belvoir, Va.

APPR-1 SHIELD DESIGN AND MEASUREMENTS

BY

F. B. Fairbanks

W. R. Johnson

Presented at the Second Winter Meeting of The American Nuclear Society on October 28, 1957 in New York City.

LIST OF FIGURES

APPR-1 SHIELDING DESIGN AND MEASUREMENTS

I. Shield Requirements

The Army Package Power Reactor (APPR-1) is a prototype of a reactor designed to meet the requirements and site conditions of a remote military base. Since the prototype reactor is constructed at a site in the United States, some of the design requirements have been changed to meet these needs. In particular, containment of the maximum credible accident is provided.

In designing the APPR-1 shielding, the objective has been to provide sufficient shielding to meet the standards accepted throughout the Atomic Energy Commission program. Under normal conditions, radiation doses for operating personnel are restricted to a fraction of the permissible 300 mr per week. In certain areas, above-tolerance levels are permitted where infrequent access is required for periods of controlled short duration. Taking advantage of this fact permits somewhat greater flexibility of design and operation, but at no expense in terms of increased hazard to the operating personnel.

As the reactor is located at Fort Belvoir, it is necessary to provide a facility which can be approached at any time and from any direction without being unwittingly exposed to excessive radiation levels. Thus the radiation existing at any point around the building is no higher than the permissible continuous exposure level.

II. Shield Design

The concept of separate primary and secondary shields has been used. A

primary shield enclosing the reactor pressure vessel reduces the gamma radiation from the core during operation and after shutdown, and provides neutron attenuation sufficient that there is no activation of equipment outside of the shield. To protect plant personnel during normal operation, the secondary shield enclosing the entire reactor system provides attenuation of gammas from the activated reactor coolant and of direct core radiation which penetrates the primary shield.

The primary shield, consisting of eight 2"-thick iron concentric cylinders around the pressure vessel in a water-filled tank, and the secondary shield, composed of five feet of concrete in and outside the vapor container, have been described previously. The iron-water primary shield was adopted to permit fast erection and low transported weight for remote locations. The concrete secondary shield, serving also to provide missile protection for the vapor container, permitted economical construction. The shielding layout is shown in Figure 1.

III. Shield Testing

During the initial operation of the APPR-1, radiation survey measurements were made to demonstrate the effectiveness of the primary and secondary shields, and to obtain data for future shield optimization. The instruments used were conventional Health-Physics gamma, and fast and slow neutron survey instruments.

A series of measurements were taken inside the vapor container (secondary shield) with the reactor operating at low power (1 to 100 kw) to determine the effectiveness of the primary shield and to investigate the radiation source due to reactor coolant in pipes and equipment. This data was extrapolated to

give approximate values of radiation levels at full power (10 mw).

With the reactor at full power, a complete survey was made of areas outside of and adjacent to the secondary shield to prove the adequacy of this shielding under normal operating condition.

IV. Primary Shield Performance

The dose rates outside the primary shield are indicated in Figures 2 and 3. The dose rate at the surface of the shield tank is 1.7 r/hr. At one location which is slightly above a direct line with the reactor outlet pipe, a full power dose rate of 15 r/hr is determined. For a single streaming path, this is a reasonable value.

The primary shield was designed to give a maximum dose rate at the surface of the tank of 60 r/hr at the full reactor power of 10 MW. The design was calculated using BSR and Lid Tank data, with an effort to make corrections for the APPR-1 core capture gamma spectrum and geometry. The significent difference between the design and actual performance can primarily be accounted for by two factors:

1. The source correction factor which was applied, based on evaluation of the relative high energy capture gamma production in the BSR and APPR-1 cores, was probably conservative.
2. The use of Lid Tank data for determining the attenuation of gammas by replacement of water with iron was conservative for the APPR-1 configuration, but unfortunately no other experimental data was available.

The dose rate at the surface of the primary piping during full power opera-

tion is 12 r/hr. This is almost entirely due to gammas from the 7 - second N^{16} produced by the O^{16} (n, p) N^{16} reaction. Above the reactor, where excess shielding has been provided because of fuel transfer requirements, the dose rate is 0.1 r/hr.

As thermal neutron fluxes are generally less than 1000 n/cm^2 - sec at full power, there should be no problem with induced activity in components.

V. Secondary Shielding Performance

The secondary shield has been designed such that at any point outside the vapor container up to the full height of the power plant building, radiation penetrating the primary shield and radiation from the primary coolant combined would not give more than 1.5 mr/hr - which is two-tenths of laboratory tolerance for a 40-hour week. The radiation levels at full power are indicated in Figure 4.

Measurements made with the reactor at full power indicated a gamma dose rate of 0.01 mr/hr in working plant areas adjacent to the vapor container. This value is slightly above normal background. This low result is probably accounted for by several factors:

1. Conservative primary shield design reduced the radiation level inside the vapor container.
2. The magnitude of the primary coolant source strength was conservatively calculated, using the available experimental information at the time of the design.
3. There is a considerable amount of steel reinforcement in the vapor container and outside concrete, which was not included in the design calculations.

4. The concrete may have a density greater than that assumed in the calculation.

5. Geometric factors were chosen on a conservative basis.

VI. Shutdown Radiation

Surveys taken eight (8) hours after shutdown following the 700-hour performance test indicated the radiation levels shown in Figures 5 and 6. The dose rate immediately adjacent to the primary coolant piping was 60 mr/hr 8.7 hours after shutdown, 40 mr/hr at 13.9 hours, 26 mr/hr at 30.5 hours, and 19 mr/hr at 80 hours. The reactor had been operated at or near full power for several days prior to shutdown. The magnitude of these radiation levels will probably increase slowly as long-lived activity builds up.

VII. Summary of Shield Performance

In view of this experience with shield design and construction, it is certainly possible to design adquately safe shields. However, the existence of additional reliable data is necessary to achieve an optimum design of minimum size, weight and cost.

Fig. 1 Reactor Core, Pressure Vessel and Shield

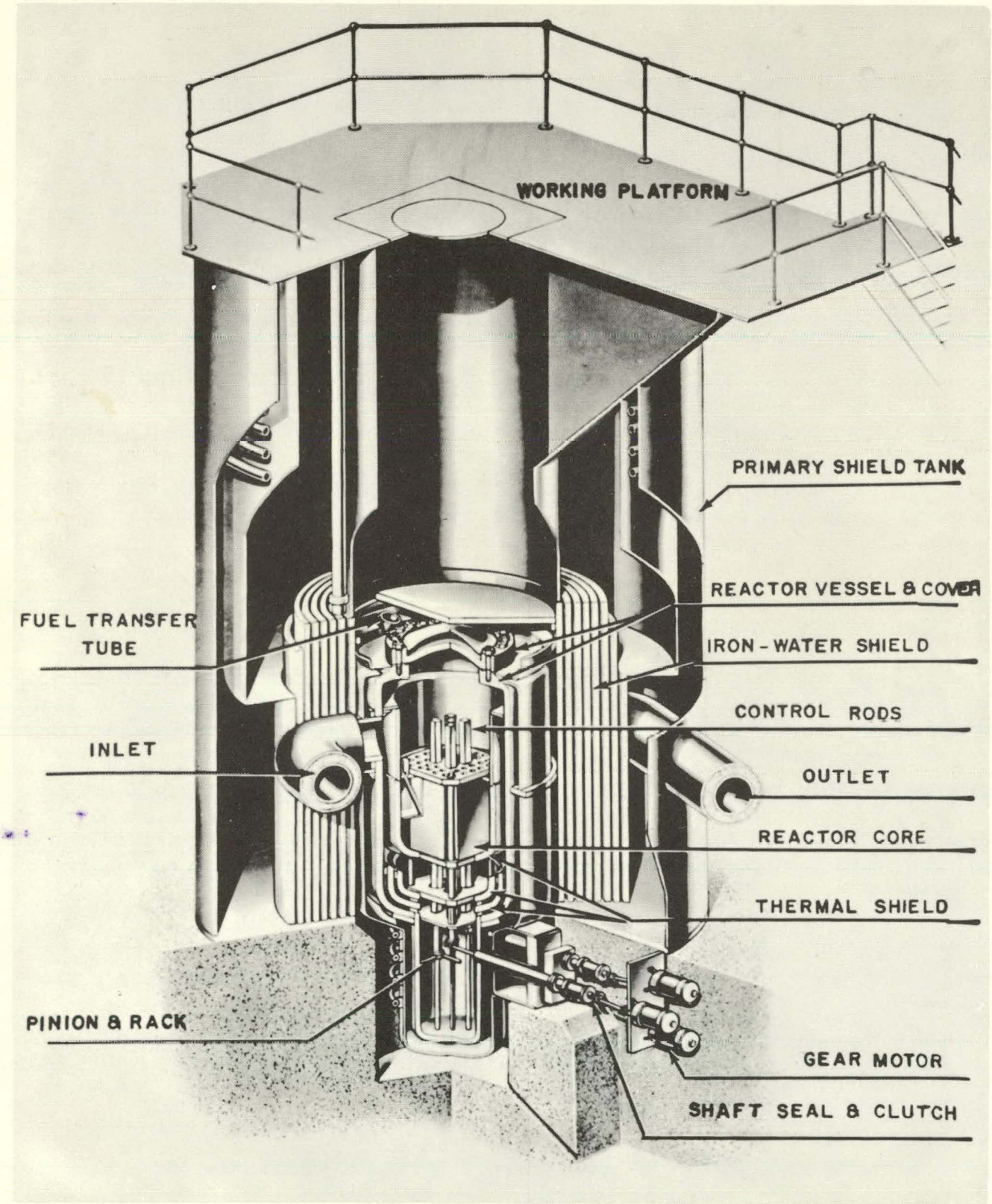

Fig. 2 **Vapor Container Elevation View Showing Gamma Dose Rates in R/HR at Full Power**

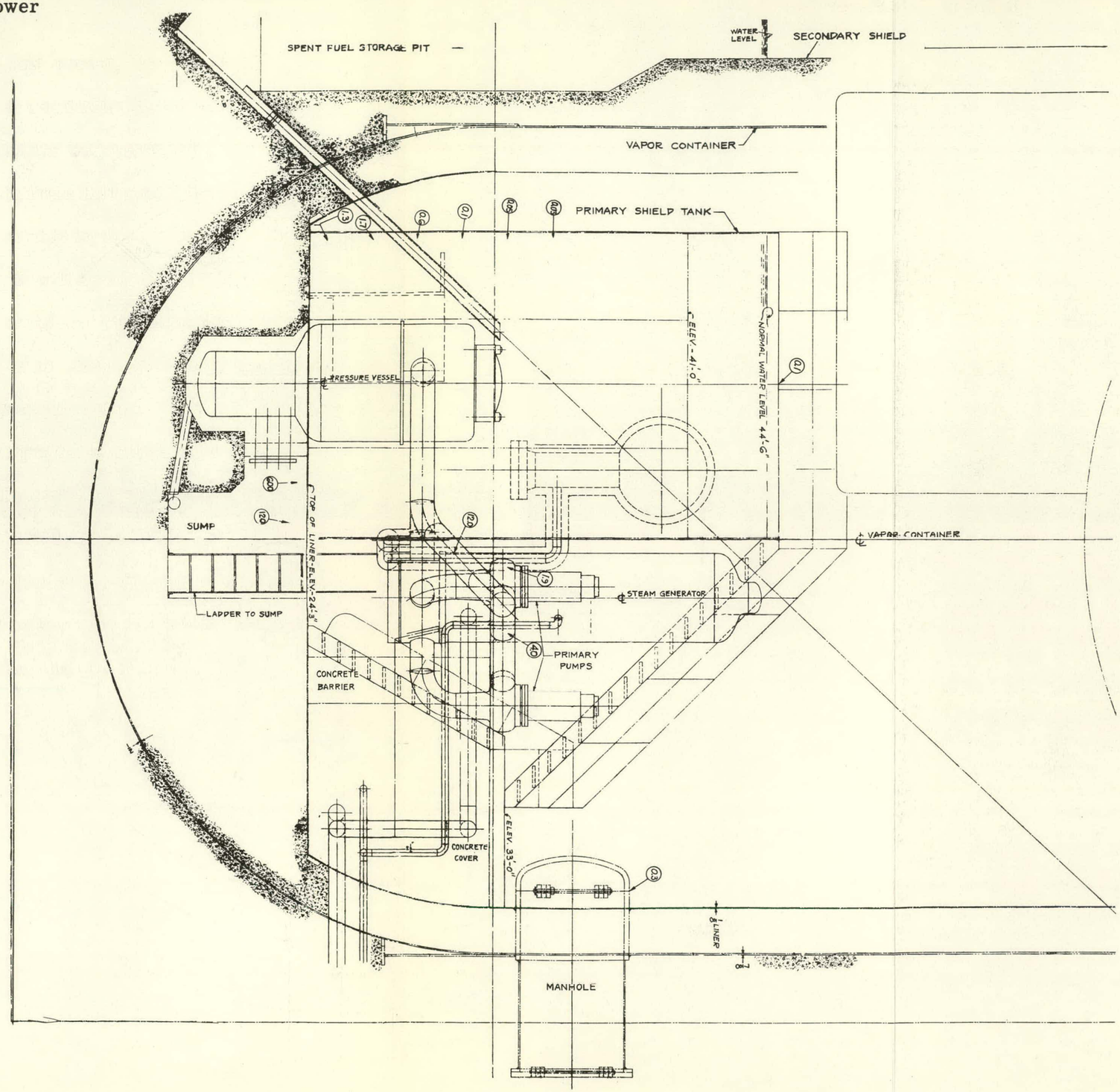

Fig. 3 Vapor Container Plan View Showing Gamma Dose Rates in R/HR at Full Power

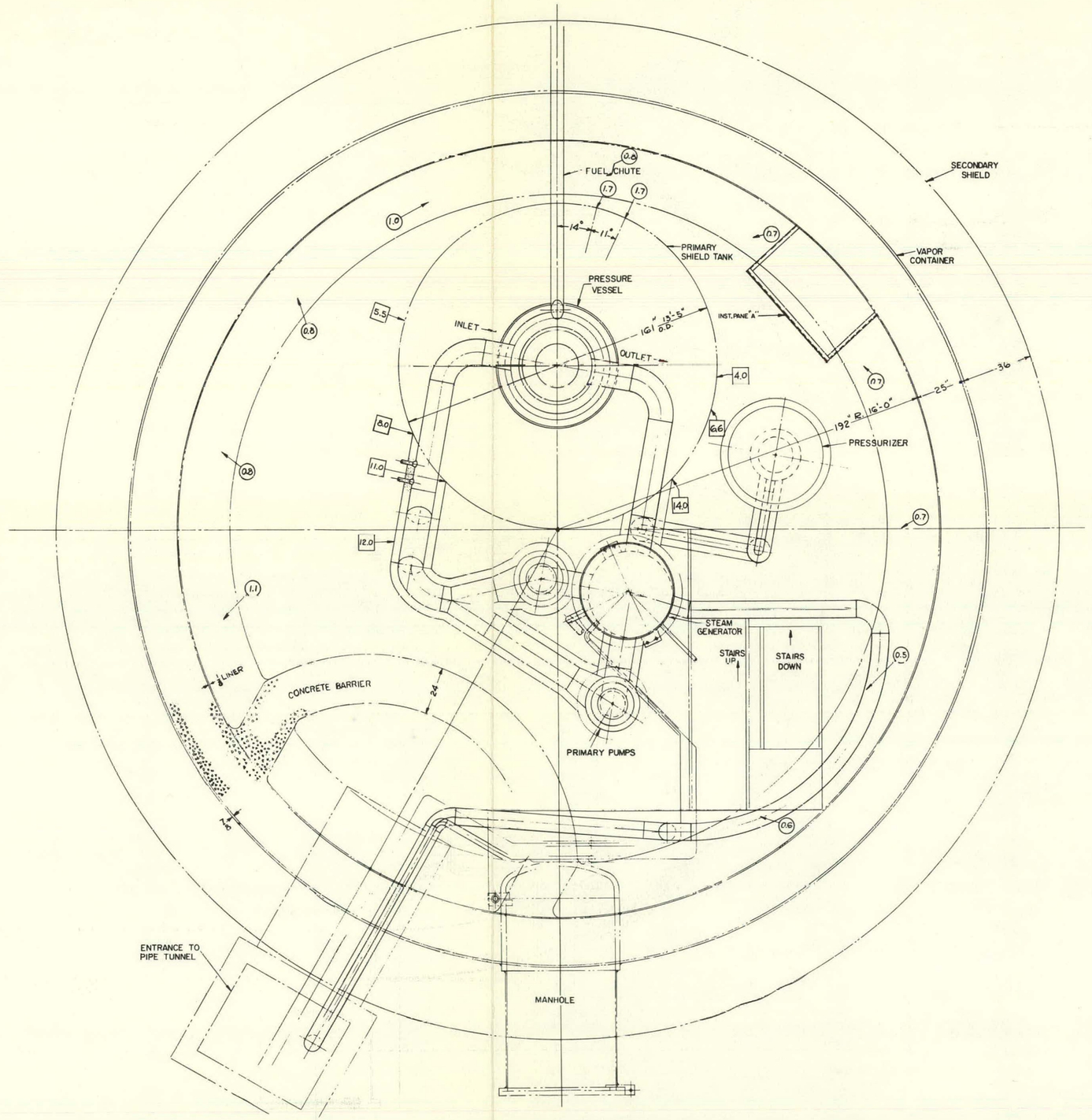

Fig. 4 **Vapor Container Elevation View Showing Gamma Dose Rates in MR/HR at full Power.**

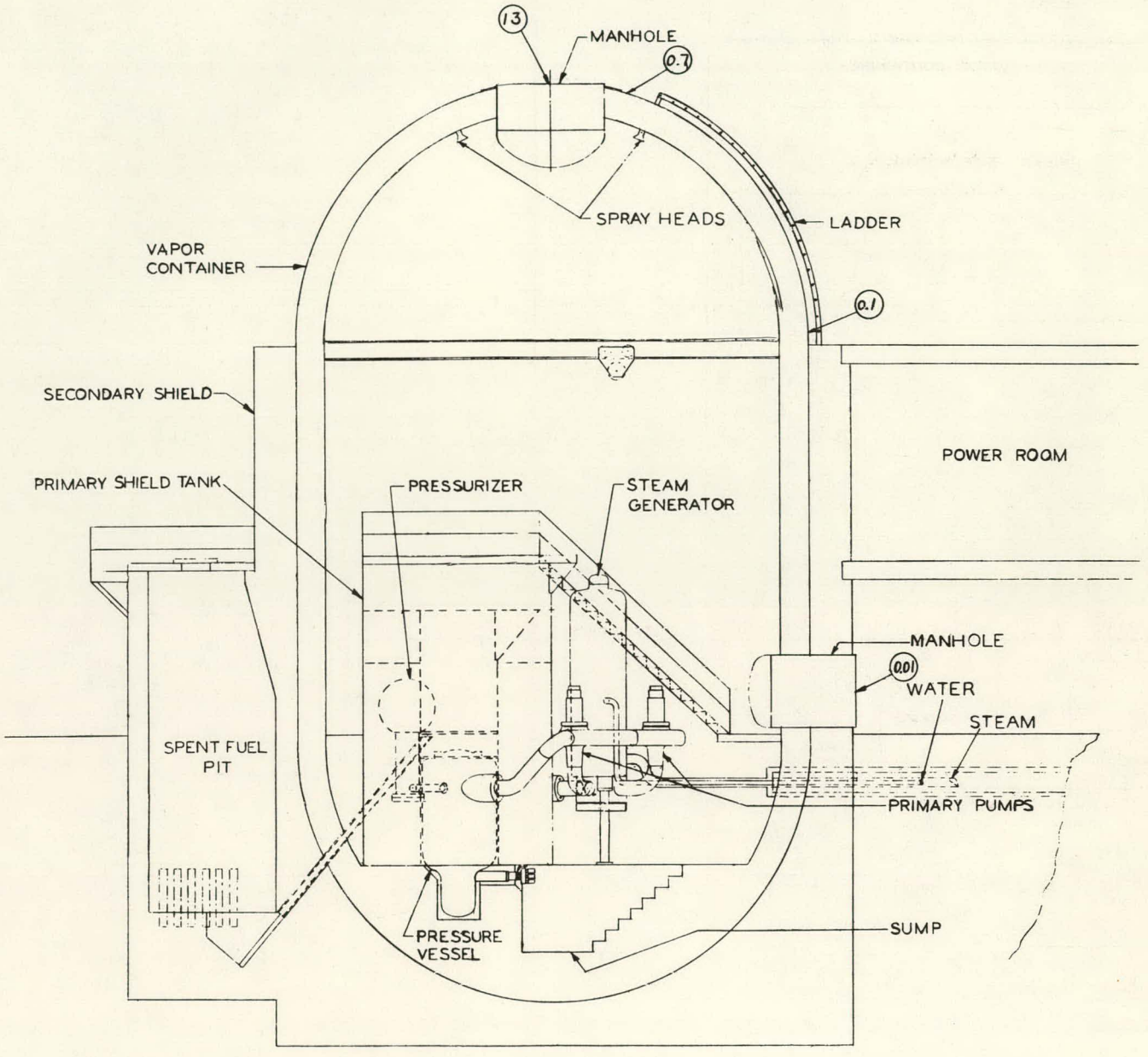

Fig. 5 Vapor Container Elevation View Showing Shutdown Gamma Dose Rates in MR/HR 8.7 Hours after Shutdown.

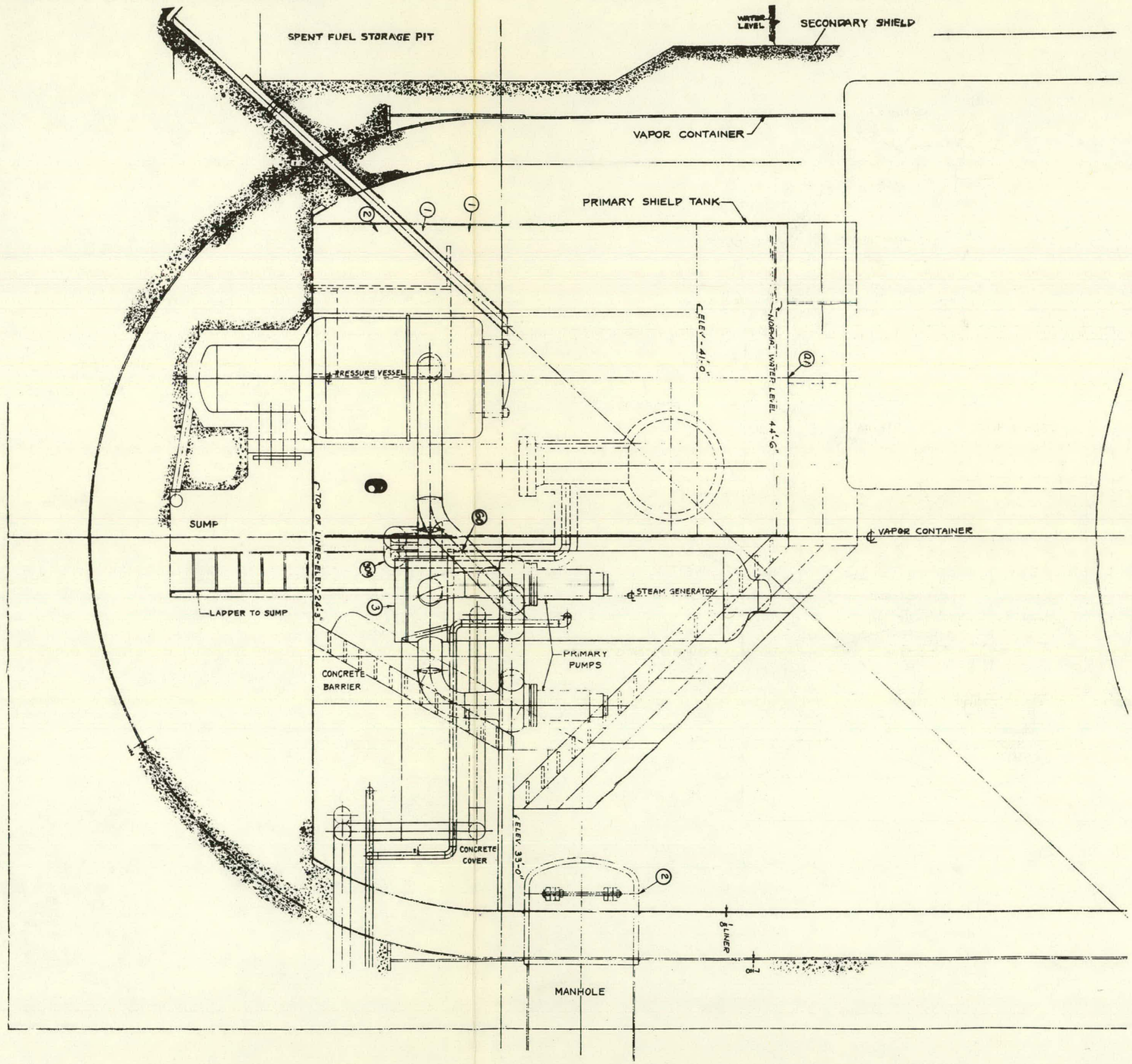

Fig. 6 Vapor Container Plan View Showing Shutdown Gamma Dose Rates in MR/HR 8.7 Hours after Shutdown

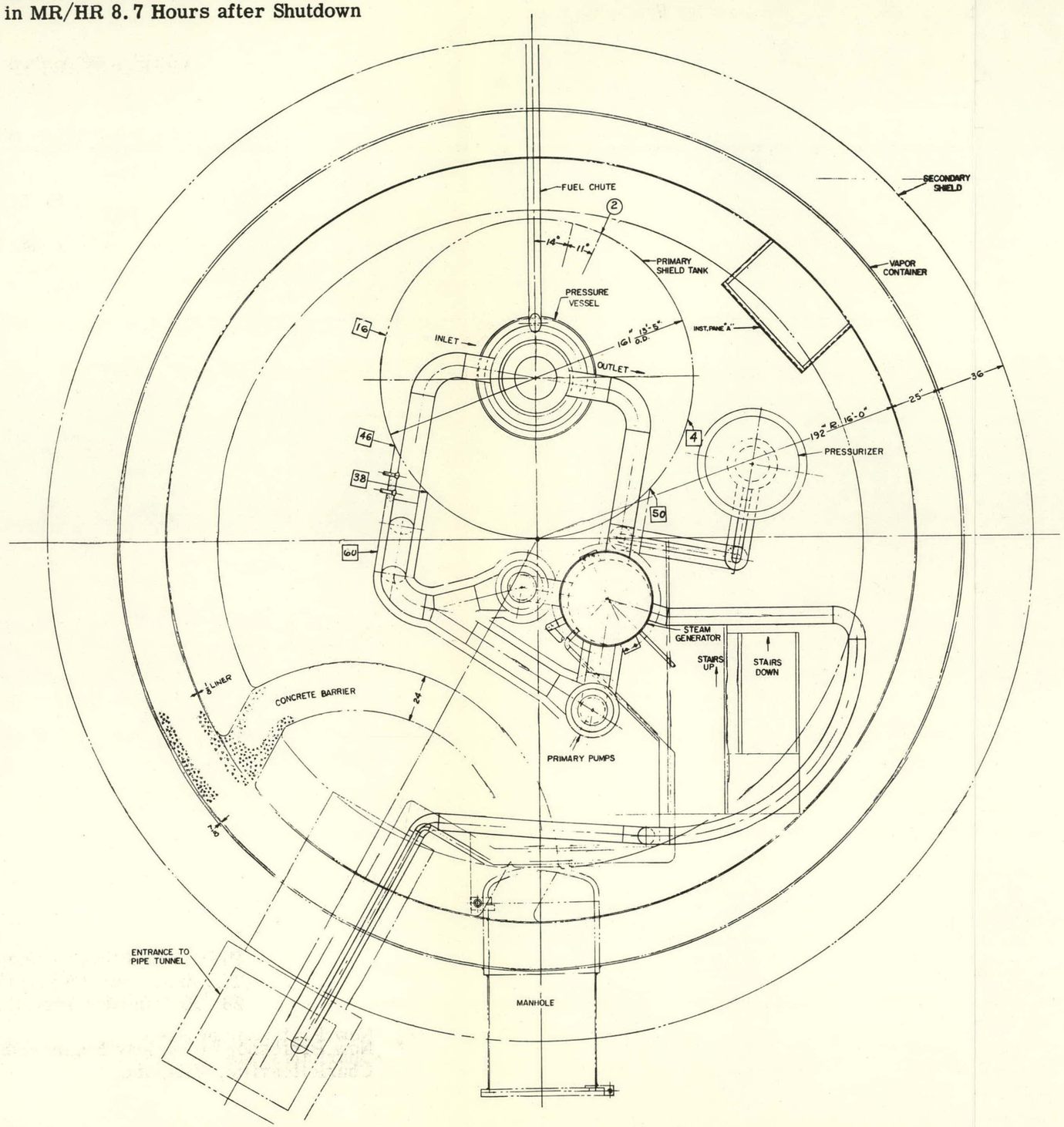

APPR-1 STARTUP AND OPERATION

BY

J. L. Meem*

J. K. Leslie

Presented at the Second Winter Meeting of
The American Nuclear Society on October
28, 1957 in New York City

* Now Professor of Nuclear Engineering, University of Virginia, Charlottesville, Virginia.

LIST OF FIGURES

OPERATION OF THE APPR-1

I. Introduction

The APPR-1 went critical on April 8, 1957, and since practically all of the zero power work had been performed in Schenectady as has been described in a previous paper, it was possible to go to power within a week.

While still at zero power, measurements were made of the temperature and pressure coefficients of reactivity. These were $-2.3 \times 10^{-4}/^{o}F$ and 2 to 4×10^{-6}/psi respectively, at the operating conditions of $450^{o}F$ and 1200 psi.

As the reactor power was increased to succeedingly higher levels, shielding measurements were made as described in another paper, and tests were run to demonstrate that the reactor would be cooled by thermal convection in the event of loss of primary coolant flow.

Numerous tests were performed on the reactor after it was operating at power, and on June 2 the plant was started on a 700 hour endurance test. By July 2, the plant had operated for 700 hours with less than 14 hours of down time. Less than 8 hours of this down time was due to equipment malfunctioning.

The most interesting aspect of the APPR-1 operation is the remarkable response to load demand of the power plant. It had been planned in the test procedures to subject the APPR-1 to a number of load transients. On April 20, the reactor first reached its full power rating of 10 megawatts of heat, and shortly thereafter

a faulty circuit breaker connecting the APPR-1 to VEPCO opened. The plant output dropped from full load to station load smoothly and without any adjustment of the reactor controls. The plant performance was so smooth that it was about a minute before the operators realized that the plant was disconnected from VEPCO and was operating on its own power. The APPR-1 was subjected to this sudden drop to station load many times. A more severe transient, however, consisted of tripping the turbine off the line. In this case the electrical output dropped from full load to zero load instantaneously. This transient is described in this paper. Also described is a load increase where the generator output was increased from 200 kw. to 2000 kw. in 70 seconds. It was found that the reactor would follow a load increase as fast as the load limiter on the turbine generator would allow. No adjustment of any of the reactor controls was necessary.

II. Discussion

In Figure 1 is shown the Log N recording on the loss of load transient. At time "0", the reactor was at 10.6 MW (heat) with an electrical output of 2000 kw. The turbine throttle valve was tripped and the electrical load dropped to zero. Since heat was no longer being drawn from the primary system, the reactor quickly went on a negative period because of the increase in temperature. The neutron level dropped about six decades but after 25 minutes neutron multiplication began to appear. The primary system was beginning to lose heat through the insulation. The reactor went critical and then on a positive period as the temperature dropped below the original mean temperature of 445^{o}F. However after 65 to 70 minutes the reactor power had reached several hundred kilowatts and began to heat up the primary

system water again, hence driving the reactor subcritical. At this point the test was terminated.

In Figure 2 is shown the primary system temperatures. The average of the two temperatures is the mean temperature of the primary coolant system. When the turbine was tripped the temperature spread across the reactor quickly decreased. However the mean temperature went up hence driving the reactor subcritical. The maximum temperature was about 456°F. and this temperature dropped to 445°F. after about 35 minutes when the reactor went from subcritical to super critical. After 70 minutes it can be seen that the water was being heated again as mentioned in Figure 1.

Figure 3 shows the reactor ΔT and the primary system pressure during the transient. The cycling in the pressure trace was caused by the heaters going on and off. When the turbine was tripped the pressure rose from 1210 to 1300 psi and then dropped off.

In Figure 4 are shown the secondary system conditions, namely steam pressure and temperature. The pressure rose from 200 to 435 psi when the throttle valve was tripped and the secondary pressure relief valve lifted briefly. This was not unexpected. The steam temperature rose to 460°F. as shown.

The next series of Figures shows the increase in load transient test. Figure 5 shows the recording of the electrical generator output. At time "0" the load was a little over 200 kw. Increased load was applied by opening the load limiter on the generator. The generator output was increased a factor of 10 in 70 seconds. Since this is a conventional generator it was not felt advisable to overload it more drastically than this.

The reactor response is shown in Figure 6. The overshoot in neutron level is hardly visible and the reactor power stabilized immediately. The reactor outlet and steam generator outlet (same as reactor inlet) temperatures are shown in Figure 7. As can be seen the temperature quickly stabilized.

Figures 3 and 4 should be referred to again but this time the traces on load increase are to be observed.

On July 9, a demonstration was held for some prominent European visitors. With the plant at full load of 2000 kilowatts (electrical) the main breaker was opened and the plant output allowed to drop to station load of 200 kilowatts. The generator was then resynchronized and the load increased to 2000 kilowatts in the same fashion as described in the previous figures. This dropping to station load and increasing to full load was repeated five times in less than an hour and a half. Figure 8 shows the trace from the generator wattmeter and Figure 9 shows the reactor Δ T recording for the five demonstrations. During this entire time (hour and a half) the only controls that were manipulated were those for the electrical switch gear. In particular the reactor control rods did not move.

The next Figures will show the emergency cooldown tests. The APPR-1 was designed so that it would cool itself by thermal convection of the water in the primary loop through the reactor and steam generator and back again. Calculations indicated that the maximum temperature from after-heat would appear in 20 to 30 minutes after pump failure at full power. The reactor was designed so as to permit no boiling under such conditions.

During the initial tests while approaching full power, the primary coolant pump was turned off at succeedingly higher power levels. On turning off the

pump the rods drop an a low flow scram within a fraction of a second. The procedure was then to withdraw the rods and return to critical at zero power as soon as possible after the scram. Observations were then made for the reactivity fluctuation characteristic of boiling reactors.

The Log N recording is shown in Figure 10 for the final test of this series. The reactor had been at 10 megawatts for 10 hours before stopping the pump. The reactor scrammed immediately and was brought critical at 100 watts within 10 to 15 minutes. In Figure 11 is shown the reactor outlet temperature. This temperature began to rise after about 20 minutes and continued to rise for about 1/2 hour due to afterheat. The system heat losses then amounted to more than the afterheat and the temperature started to drop. If boiling due to afterheat had not occurred up until the time that this temperature began to drop it may be concluded that it would not occur thereafter.

In Figure 12 is shown the linear power recording. The figure shows the trace after about 7 minutes. Prior to this time, numerous rod movements and scale changes were made, and the record was meaningless. This range is around 100 watts. At 13 minutes the reactor was super critical and on a positive period, but leveled out and went on a negative period until there was a rod withdrawal sufficient to make the period positive again. Again the period leveled out and became negative so that further rod withdrawal was required. This pattern repeated for a number of times. See Figure 13 which is a continuation of the previous figure.

III. Conclusion

Throughout the record a slight oscillation in the trace can be observed. This is no more pronounced at one time during the experiment than during another,

and when compared with previous traces taken at low power, was found to be typical of the instrumentation. No large amplitude oscillation in the trace of the neutron level recorder as is typical of boiling reactors was observed. Accordingly, it was concluded that after pump failure and scram from full power the APPR-1 will cool itself by thermal convection without detectable boiling.

Returning to the discussion of the record, it will be observed that the last rod withdrawal was required at 53 minutes after shutdown. Up until this time it had been necessary to repeatedly withdraw the rods to compensate for a decreased reactivity because of the temperature increase from afterheat.

After this last rod withdrawal, the reactor power levelled off in about 3 minutes and stayed level for 7 minutes. At 63 minutes after shutdown, the reactor started to indicate increased reactivity. This obviously meant that the peak in temperature had been passed and the primary system was beginning to cool down. From that time on, rod insertions were required to keep the reactor from going on to short a period as shown. The experiment was then terminated.

Fig. 1 Log N Chart, Loss of Load Transient Test

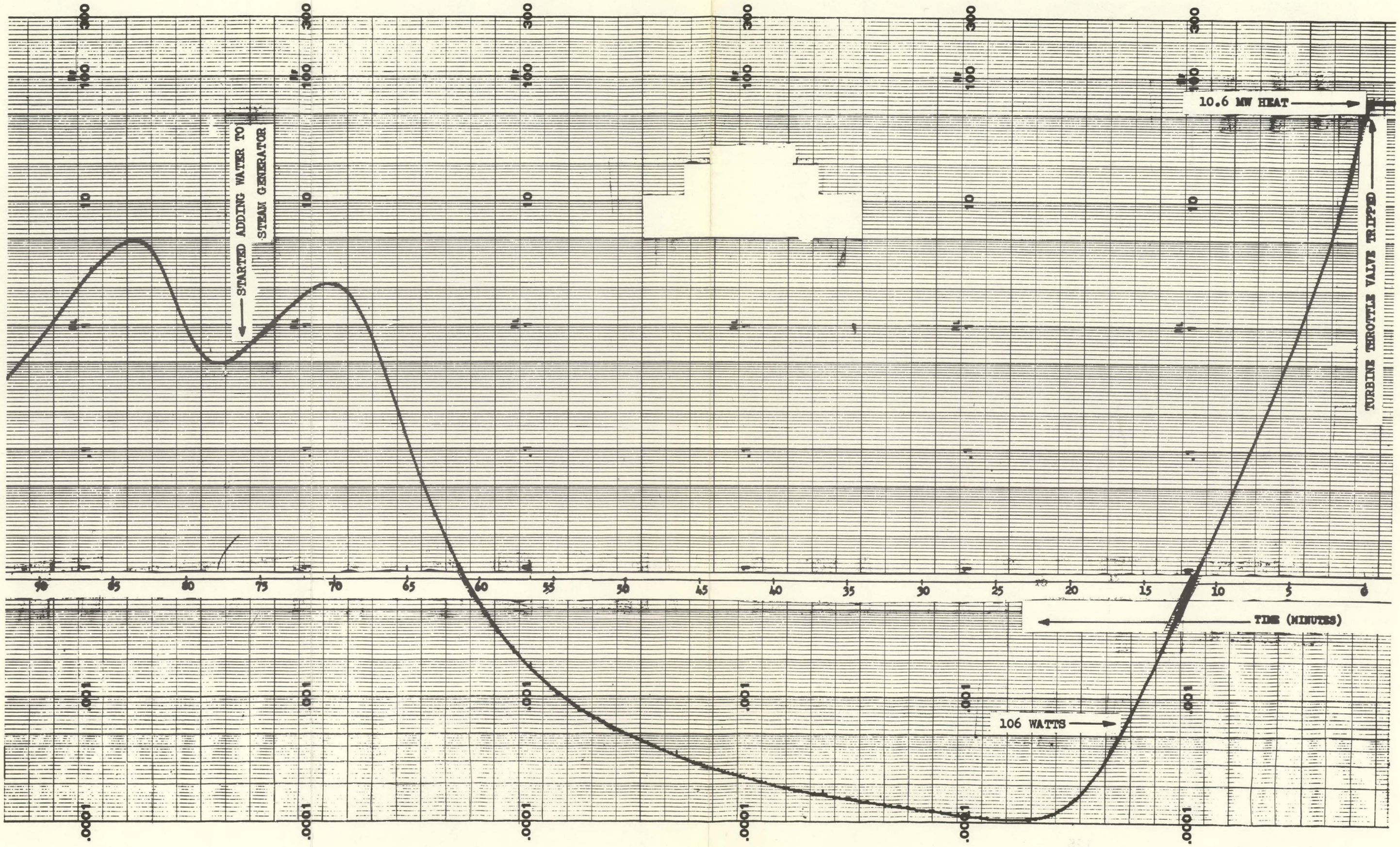

Fig. 2 Reactor and Steam Generator Outlet Temperature, Loss of Load Transient Test

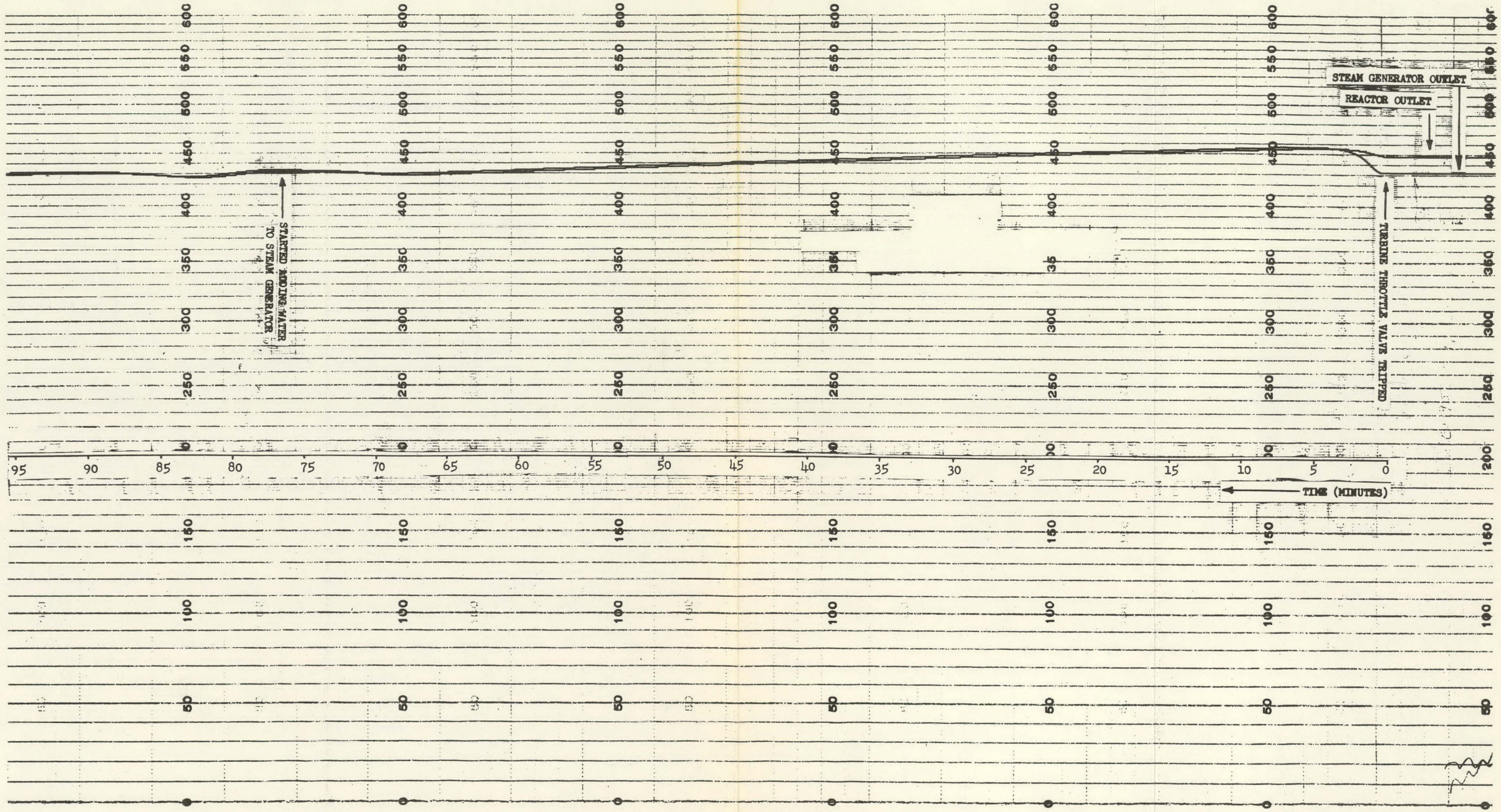

Fig. 3 Reactor T and Primary System Pressure Vs Time

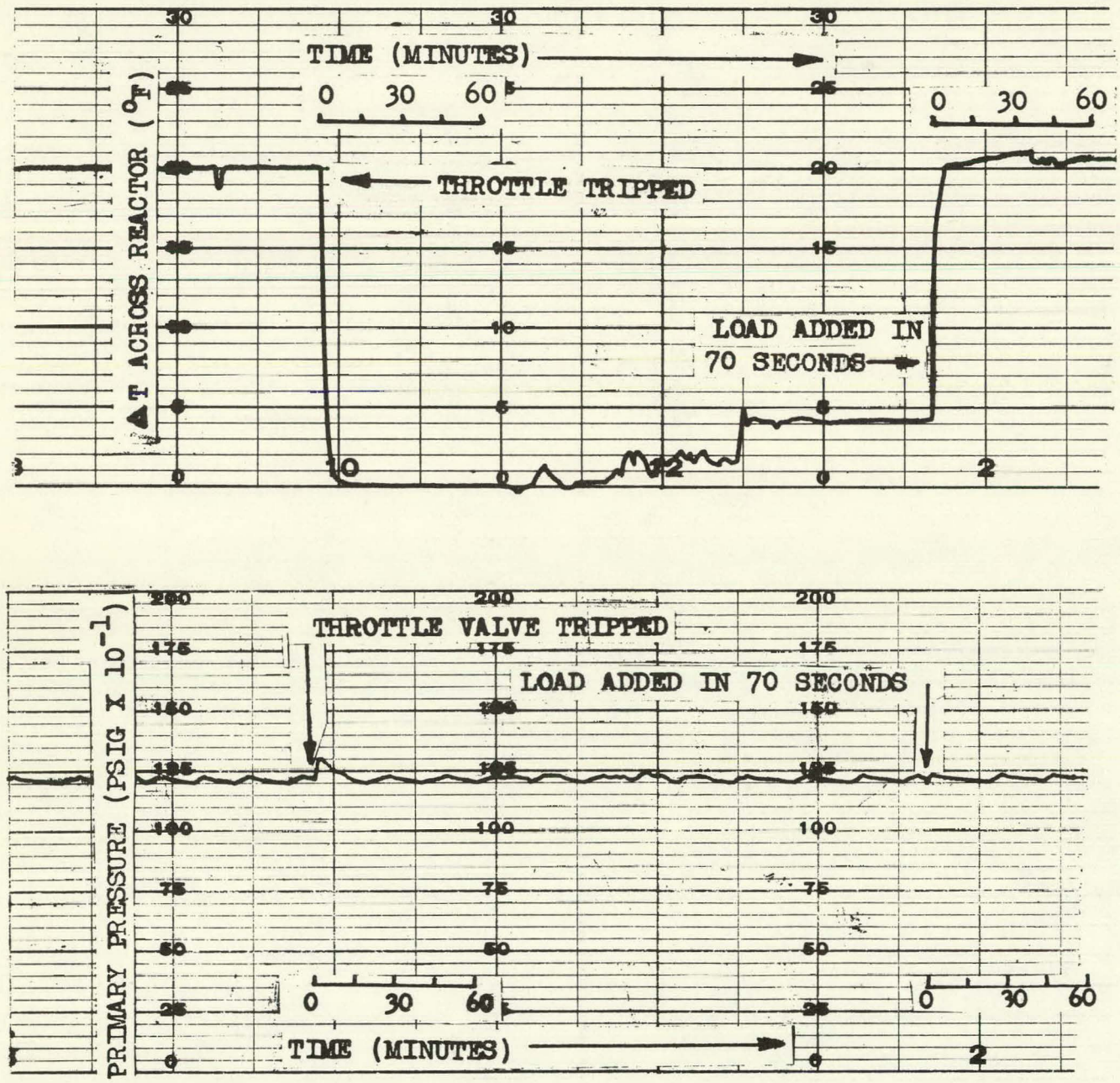

Fig. 4 Steam Pressure and Steam Temperature VS Time

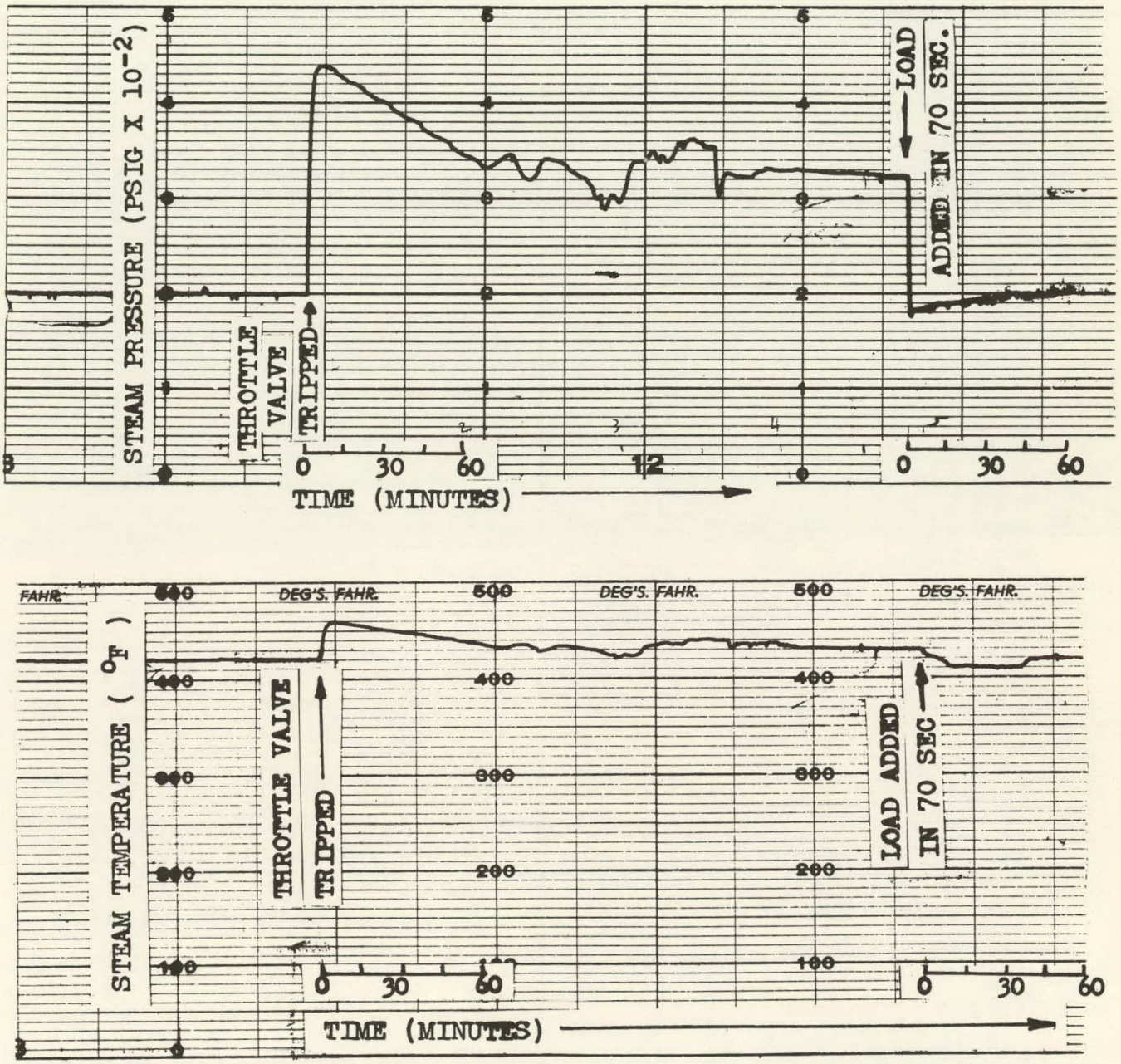

Fig. 5 Generator Watt Meter, Increase of Load Transient Test

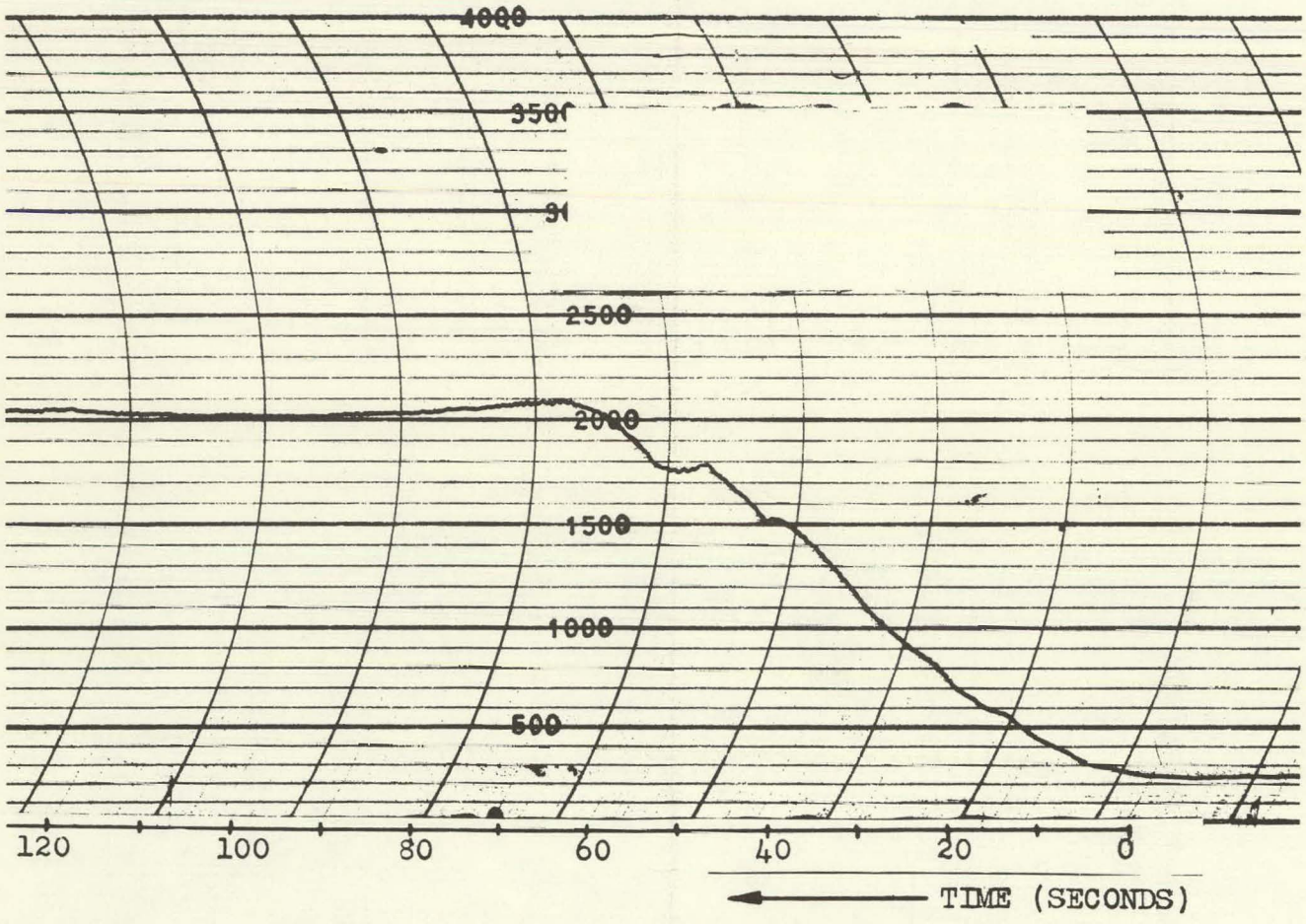

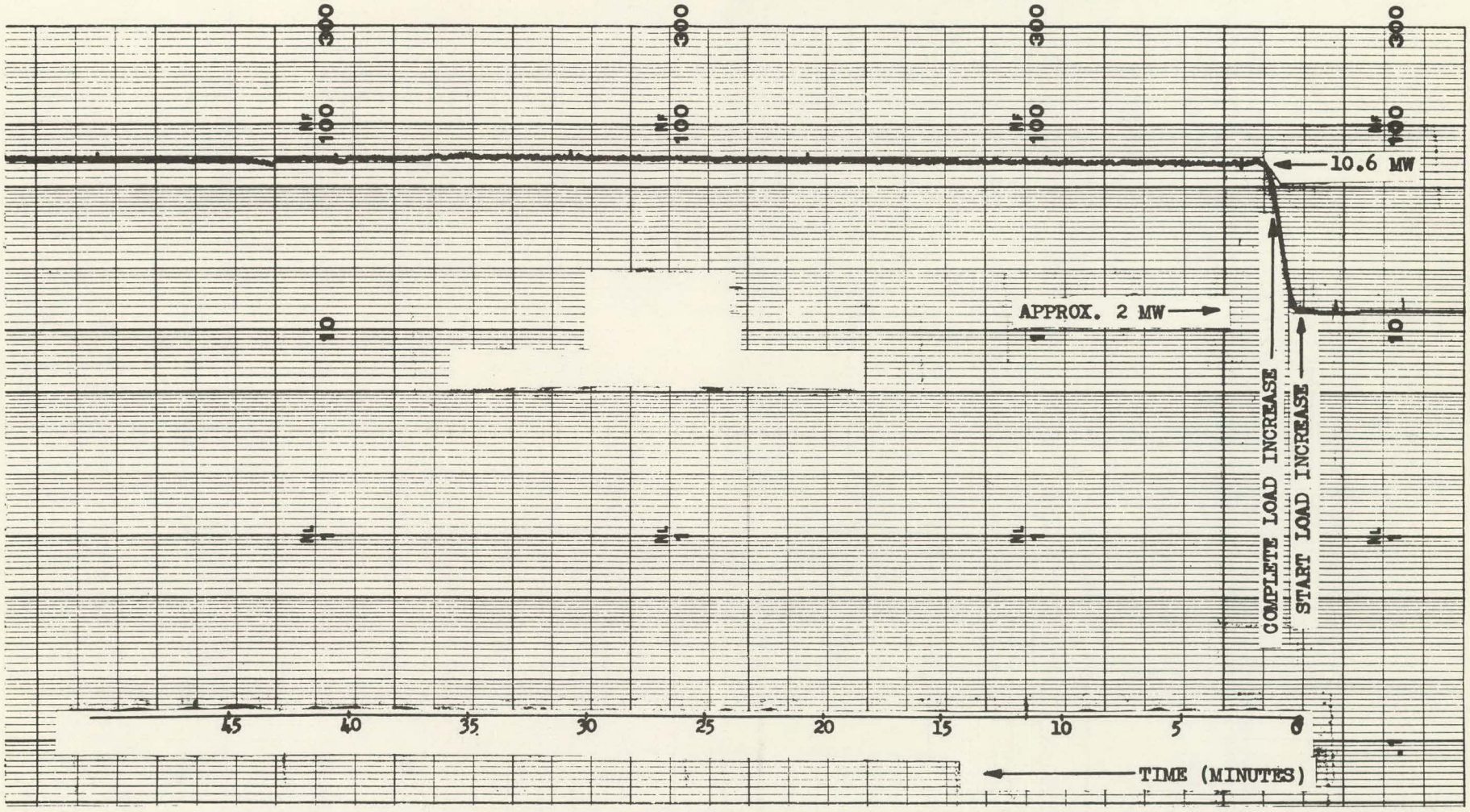

Fig. 6 Log N Chart, Increase of Load Transient Test

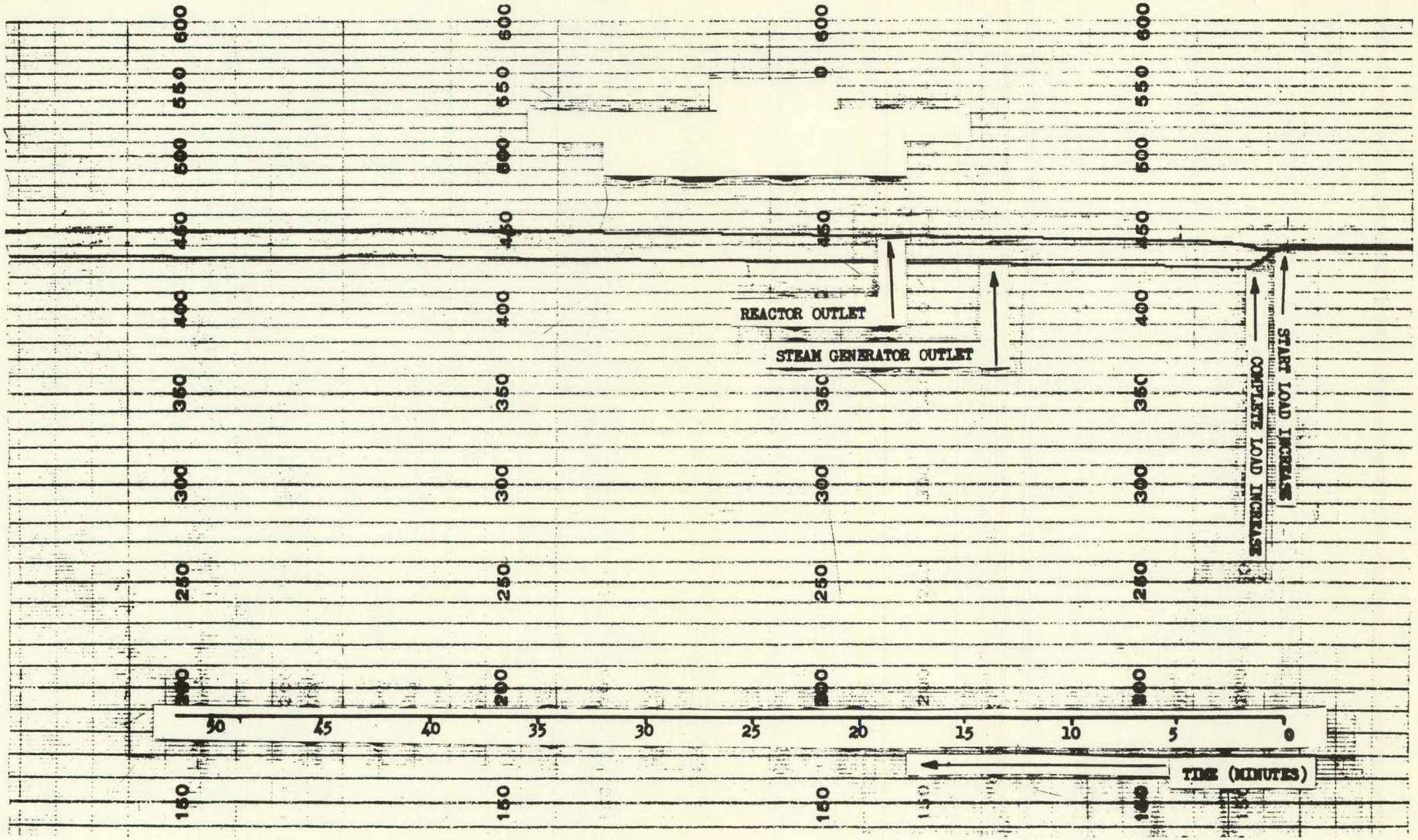

Fig. 7 Reactor and Steam Generator Outlet Temperatures Increase of Load Transient Test

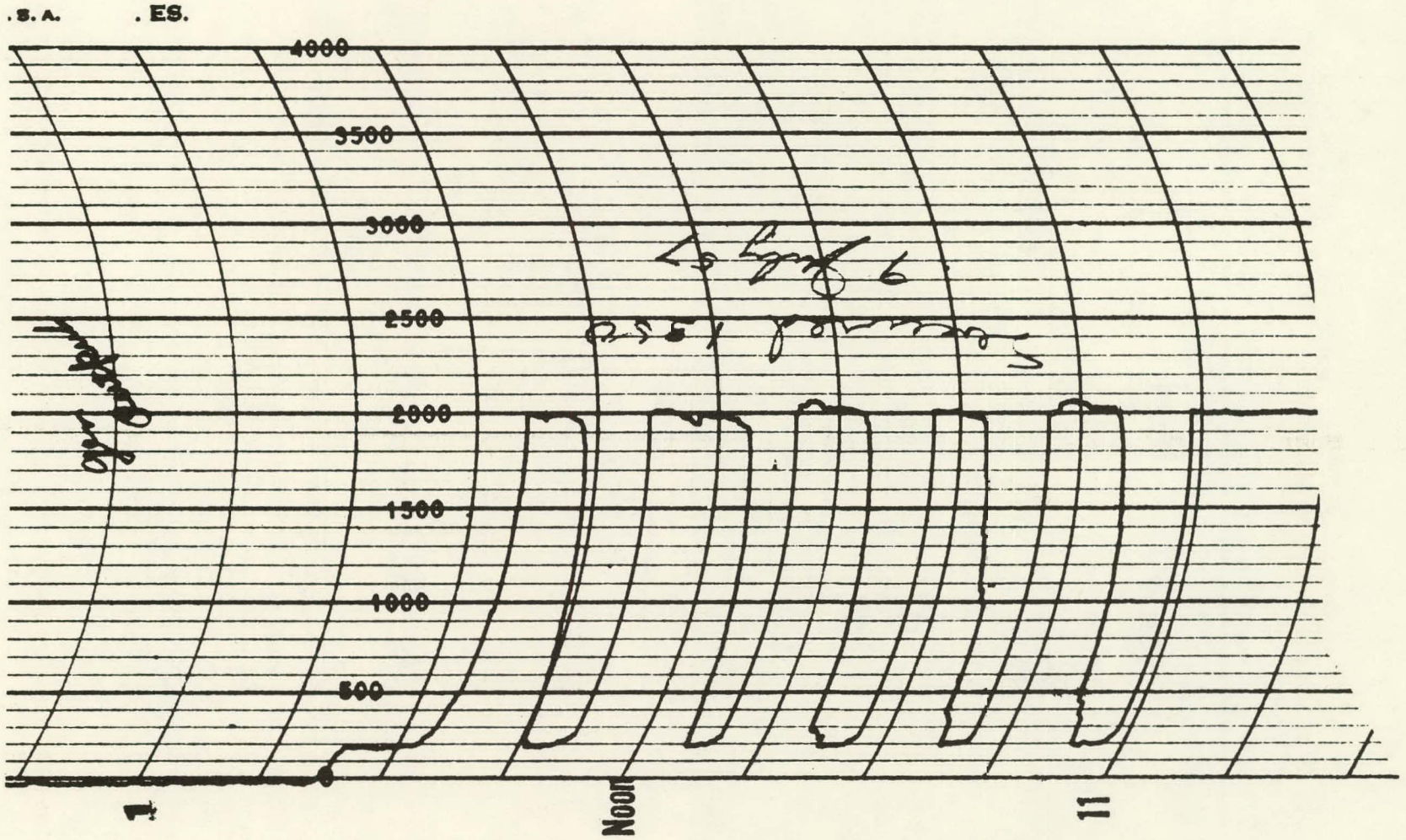

Fig. 8 Trace From Generator Watt Meter

Fig. 9 Reactor T Recording

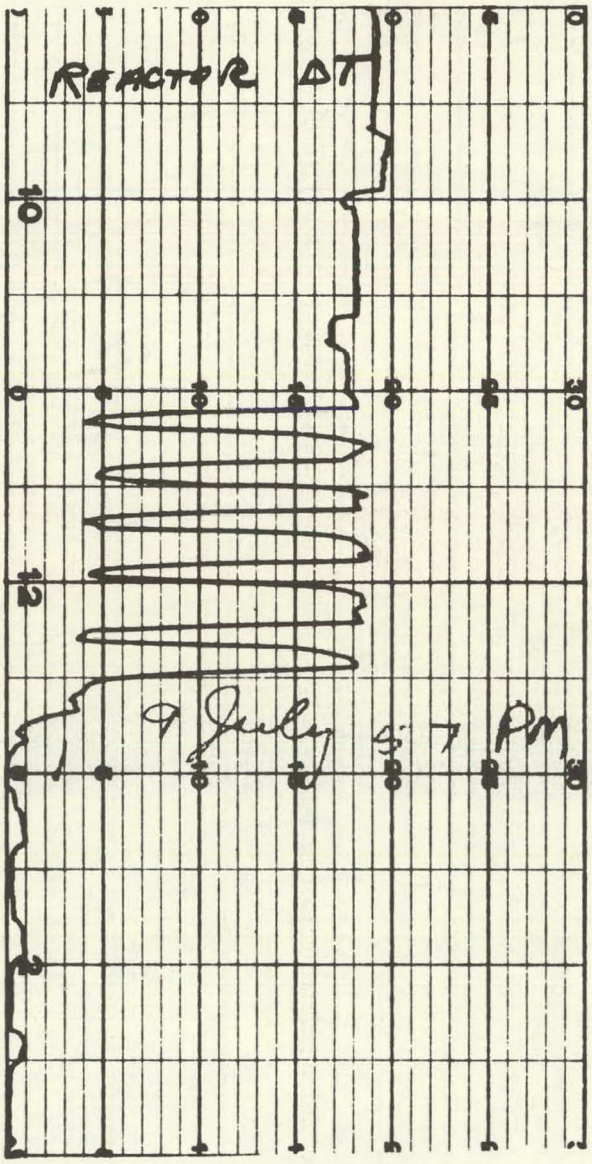

Fig. 10 Emergency Cooling - Log N Chart

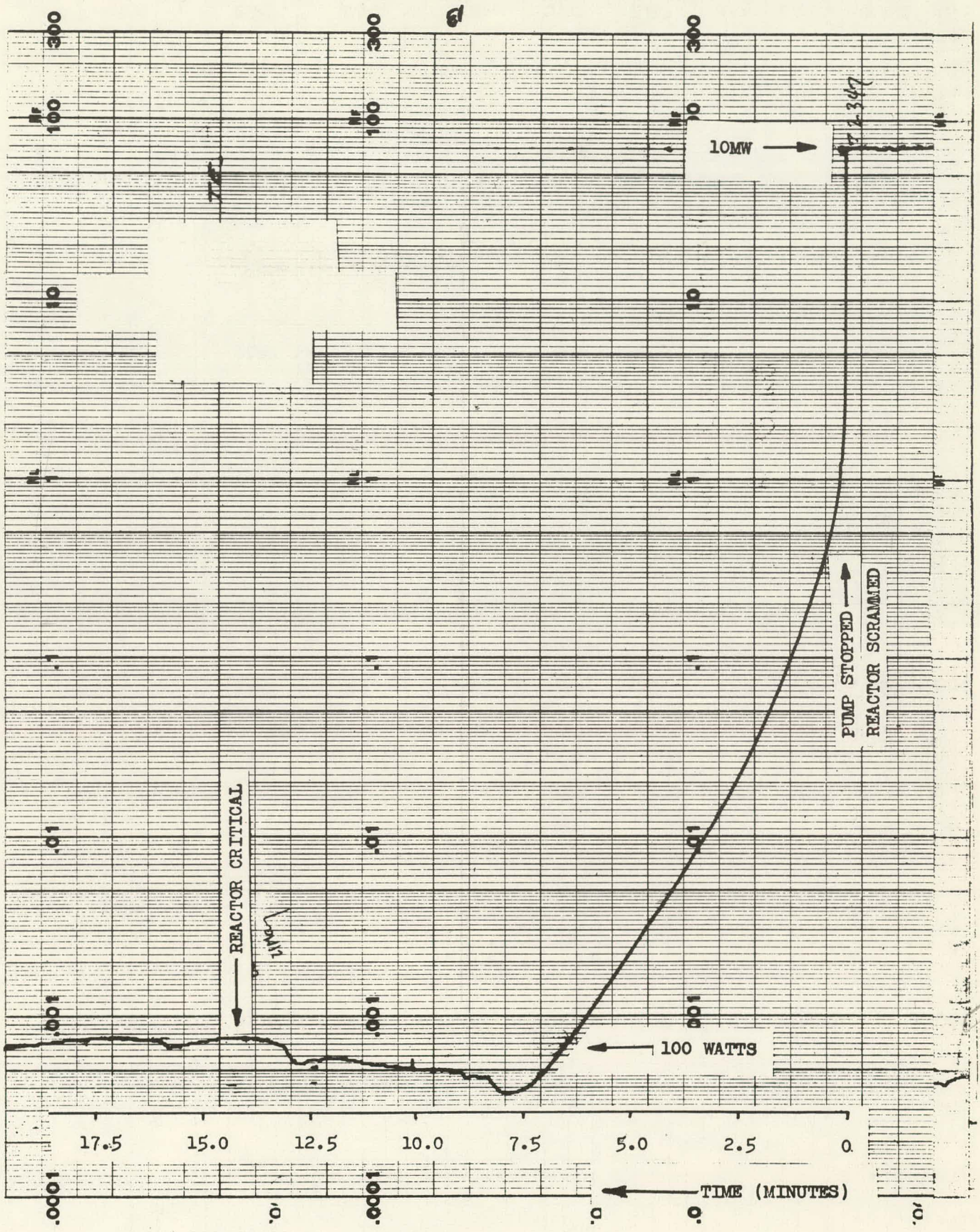

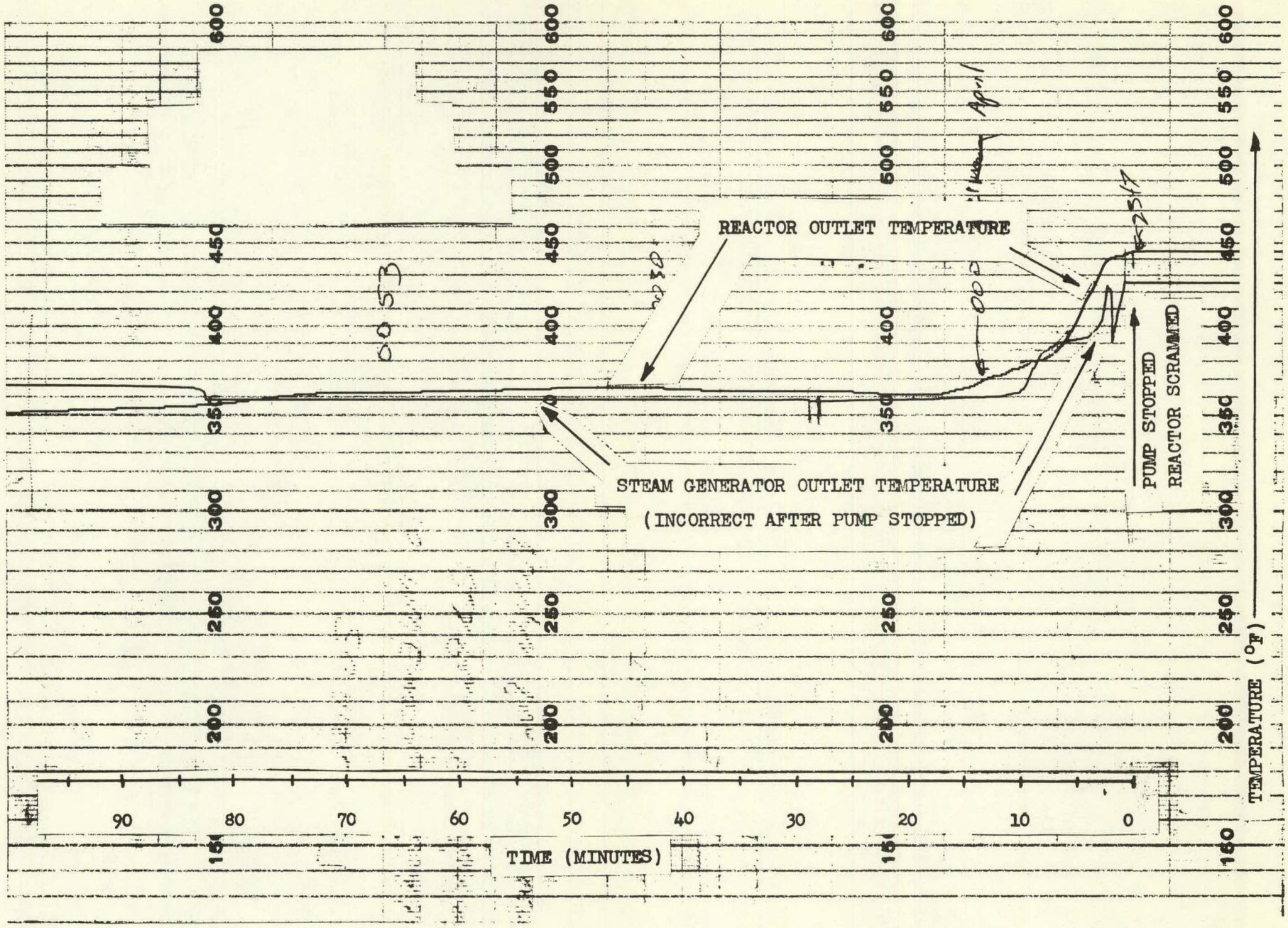

Fig. 11 Emergency Cooling - Reactor Outlet Temperature

Fig. 12 Emergency Cooling - Linear Power Chart (Part 1)

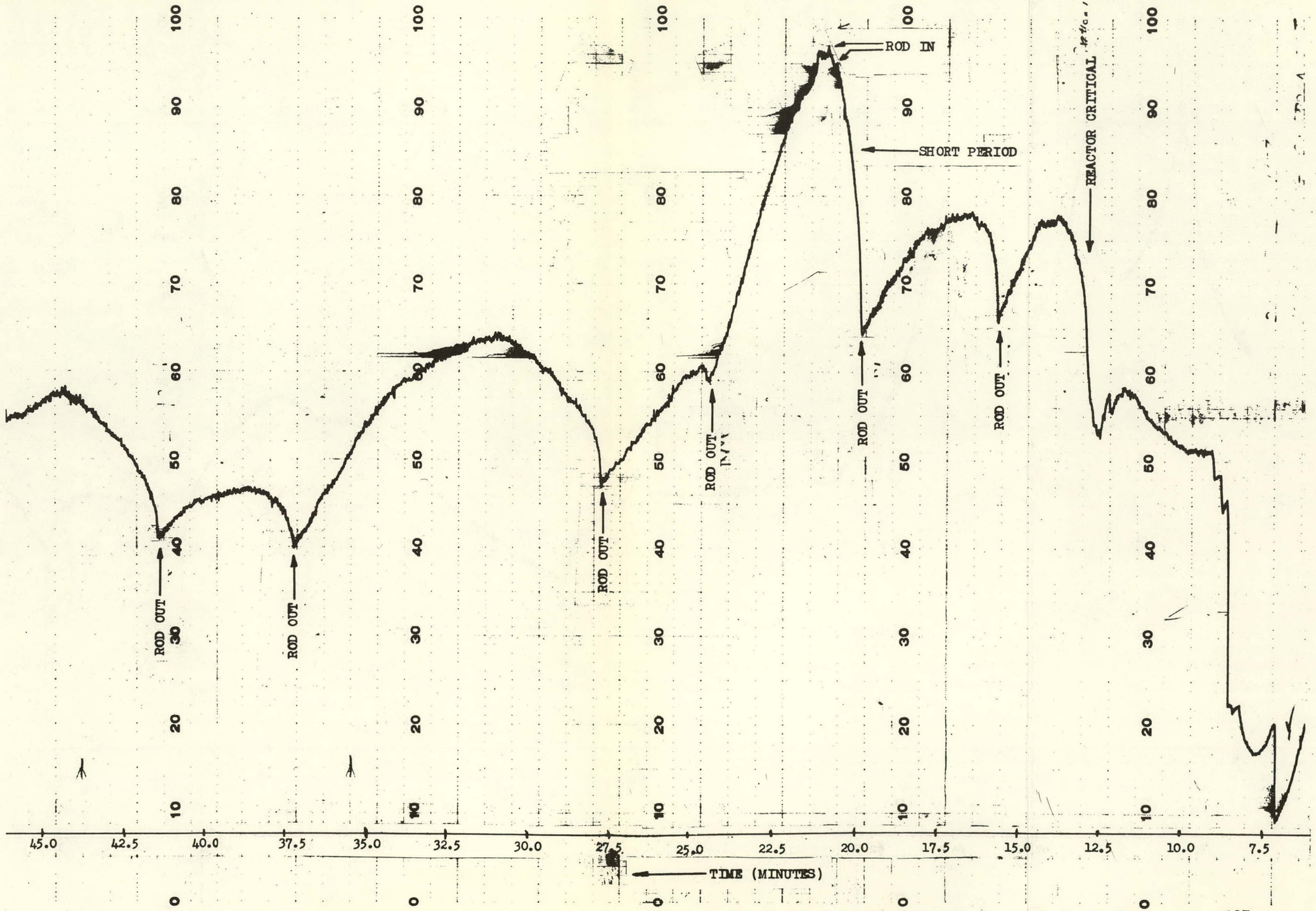

Fig. 13 Emergency Cooling - Linear Power Chart (Part 2)

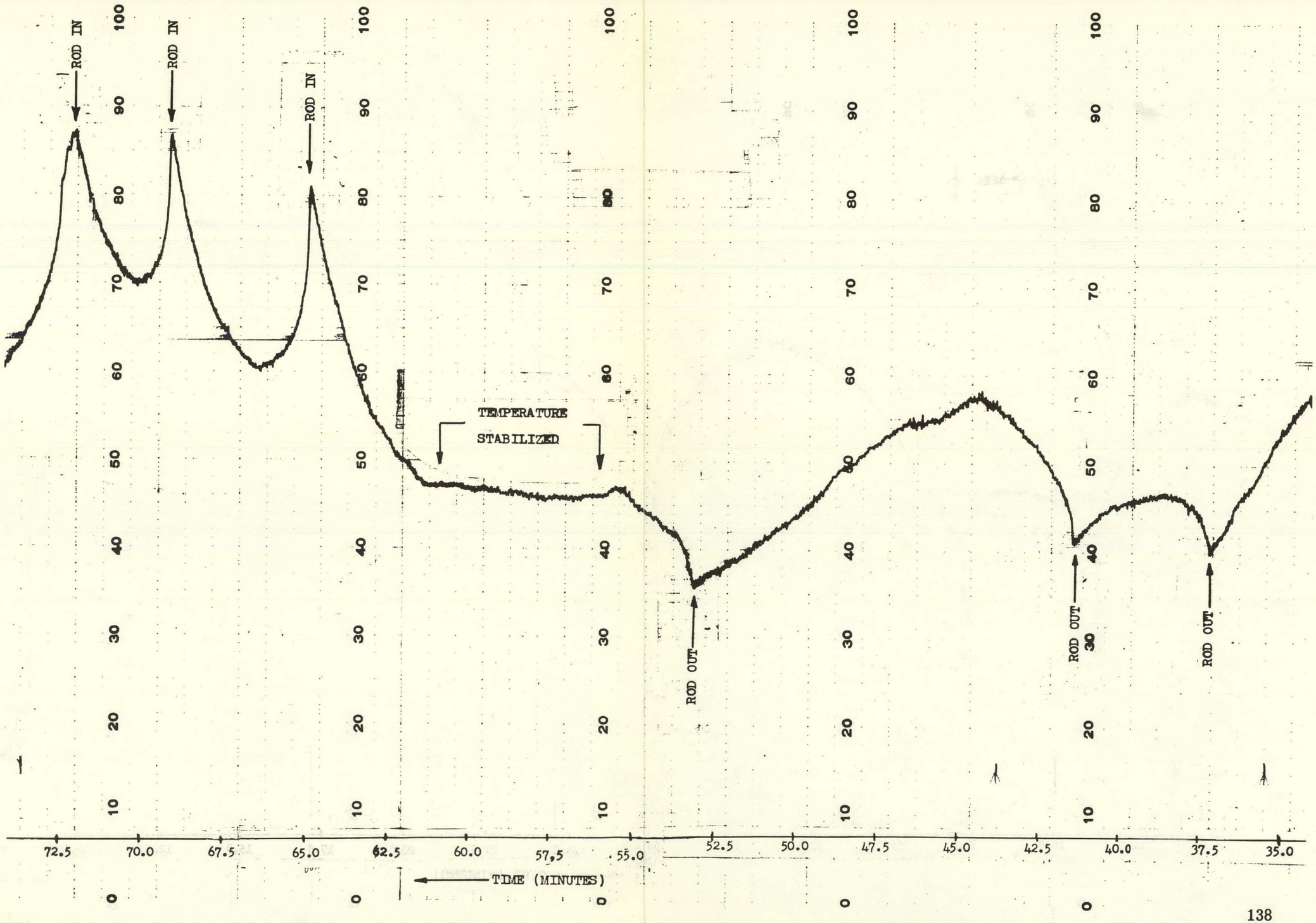

APPR-1 WATER TREATMENT AND WASTE DISPOSAL

BY

A. L. Medin

W. S. Brown

R. J. Clark

L. H. Heider

Presented at the Second Winter Meeting of
The American Nuclear Society on October
28, 1957 in New York City.

LIST OF TABLES

LIST OF FIGURES

APPR-1 WATER TREATMENT AND WASTE DISPOSAL

I. Introduction

The design and operation of the APPR-1, a pressurized water reactor, involves many phases of chemical technology. Of major importance are the water treatment and waste disposal requirements. This paper will give a brief description of these systems along with some operating results.

Among the reasons necessary for the control of the primary water purity are included the following:

1. Reduce build-up of excessive radioactivity.
2. Minimize large scale deposition of solids on fuel elements.
3. Minimize possible clogging of close tolerances from deposition of solids.
4. Minimize corrosion due to oxygen.

For these reasons, the primary water purity is maintained below 2 ppm total solids and oxygen is essentially eliminated. To maintain this purity, continuous purification of the primary water is performed. As shown in Figure 1, a portion of the primary water is removed, purified and recirculated back to the primary system.

The blow-down water is removed from the primary system at a temperature of approximately 430°F. River water is used in the blow-down heat exchanger to reduce the temperature of the primary water to less than 120°F. This reduction in temperature is necessary to protect the demineralizer resins from serious thermal damage. A motor operated throttling valve reduces the

pressure from 1,200 psi to less than 100 psi. Should a leak develop in the blow-down cooler, or should the unlikely event of a fuel element rupture occur, radiation monitors will automatically divert either the primary blow-down or the contaminated river cooling water to an underground hot waste tank.

The blow-down water is then passed through one of two mixed bed demineralizers for purification, and then through a micro-metallic filter which serves to collect any resins that are lost from the demineralizer.

Leaving the filter, the water is collected in a 5,000 gallon Type 304 stainless steel hold-up tank from which it is recirculated back to the primary system by means of one of two positive displacement pumps. Hydrogen is injected into this tank to scavenge the oxygen in the primary system during reactor operation.

The purification rate is dependent upon the release rate of corrosion products into the primary coolant. The purification system design is based on the maximum possible release rate which is the corrosion rate. For Type 304 stainless steel, the corrosion rate is approximated at 0.05 mg/cm^2-mo.

II. Precritical Operation

Before the reactor became critical, a series of non-nuclear tests were performed with dummy fuel elements in the core. During this test period it was demonstrated that satisfactory water purity in the primary system could be maintained.

The primary system was filled with distilled water from a portable distilling unit. The system was heated to 450°F. by passing steam from an auxiliary boiler into the secondary side of the steam generator. Pressure was maintained

at 1,200 psi on the primary side with the pressurizer or the make-up pumps.

During the dummy core test, hydrazine was used to scavenge dissolved oxygen. A dilute solution of hydrazine was injected into the primary system by means of a small chemical feed pump feeding to the suction side of the primary make-up pumps. Hydrazine feed concentrations varied from 0.04% to 1% at feed rates up to 14 ml/min maximum. Of particular interest is the rate at which the dissolved oxygen in the initial fill water was removed. Figure 2 indicates the dissolved oxygen concentration dropped from 5.4 ppm to less than 0.01 ppm in 12-1/2 hours. The system was being heated up at this time, with the mean temperature during this period about 325^{O}F. Because of the intermittent operations and frequent shutdowns during this period, hydrazine feed rates could not be held constant, causing difficulty in maintaining a definite hydrazine residual. Generally, an excess of 0.05 to 0.1 ppm N_2H_4 was strived for. However, in spite of the erratic conditions, oxygen concentrations were usually kept below 0.1 ppm.

The initial quality of the distilled water used to fill the system was rather poor, with a specific resistance of about 120,000 ohm-cm and a chloride concentration of about 0.5 ppm. After about one weeks operation with normal purification, the resistivity was raised to 300,000 ohm-cm and the chlorides dropped essentially to 0. The demineralizer performed effectively, with the effluent from the unit consistently reading 2 to 4 meg-ohm-cm. The pH of the system remained relatively constant, in the range of 6.2 to 6.8. The demineralizer effluent averaged about pH 6.5.

III. Plant Start-up and 700 Hour Test

At the completion of the dummy core tests, the primary system was drained. The water remaining in the primary make-up tank was purified by recirculation through the primary demineralizer using temporary hose connections and a small portable pump.

After removal of the dummy elements and inspection and cleaning of the inner shield tank, the primary system was filled with demineralized water, and the uranium fuel elements loaded. When the reactor was brought up in power, hydrazine addition was suspended and hydrogen added to maintain zero oxygen residual.

Hydrogen control in the system was excellent and was easily accomplished. Hydrogen is added only to the primary make-up tank and reaches the primary system in the water being added by the primary make-up pump. The rapidity with which the hydrogen concentration in the system reaches equilibrium with the concentration in the tank is shown in Figure 3. Maintaining an approximate gauge reading of 15 to 20 psig from the hydrogen feed tank was adequate to maintain a concentration of 30 to 45 cc H_2/liter of water in the primary system. The effectiveness of the hydrogen was proved in that no oxygen of consequence was detected during the duration of the phase of plant operation. Initially, analyses for oxygen were performed every shift, but since no oxygen was appearing in the system, frequency of analyses was reduced.

The control of chlorides was never a problem. The initial fill water was analyzed at less than 0.1 ppm, and daily analyses showed that the chloride concentration did not exceed this value.

Frequent determination of total solids in the system indicated that the buildup of circulating solids was small and remained within specifications. The demineralizer performed very satisfactorily. During the two month operating period, the specific resistance of the primary system generally exceeded 600,000 ohm-cm as shown in Table 1. Resistivity of the effluent from the demineralizer was generally in excess of 2 meg-ohm-cm. Measurements were made with a dip-type cell in an open breaker and the actual downstream resistivity was probably higher than these measured values.

Primary coolant pH varied between 6.4 and 9.0 as shown in Figure 4. The pH of the demineralizer effluent remained in the range 6.5 to 7.0. The alkaline pH of the primary water was primarily due to the presence of ammonia as shown by chemical analysis. The ammonia is synthesized from nitrogen and hydrogen in pressurized water reactors by the action of radiation. The source of nitrogen was probably due to residual hydrazine decomposition, the dissolved air in water at startup and possible in-leakage of air into the make-up system. It was demonstrated that the ammonia concentration could be reduced and the pH dropped by increasing the purification blowdown rate.

Chemical analysis for corrosion products circulating in the system indicated that insignificant amounts of iron, chromium, nickel, manganese, or cobalt were present. Analysis by colorimetric methods on samples concentrated 10-fold by evaporation showed undetectable amounts of all these metals with the exception of iron. Iron concentration varied from 0.01 to 0.05 ppm.

A slight residual of oxygen was detected at times, usually to the extent of 0.01 to 0.04 ppm, as shown in Table II. Analysis of the water in the primary

make-up tank showed oxygen concentrations of about 0. 1 to 0. 3 ppm. Source of the oxygen in this tank was not conclusively determined. A limited number of tests indicated that in-leakage of air may have been occurring at the seal leak-off collection tank.

IV. Secondary System

The principal difference between the APPR-1 secondary system and that of a normal power plant is the structural material of the steam generator. Whereas most conventional power plants have carbon steel boilers, Type 304 stainless steel was employed here because of the primary system requirements. With an austenitic-type stainless steel steam generator, chloride and oxygen control became extremely important because of possible stress corrosion problems. Unfortunately, the threshold amounts of either oxygen or chlorides that cause cracking have not been well defined. Consequently, at the APPR, the maximum oxygen concentration was established at 0. 03 ppm and the maximum chloride concentration at 0. 5 ppm. These limits were felt to be severe but practical.

Two chemicals primarily have been used to minimize corrosion of secondary system components: hydrazine to eliminate oxygen and morpholine to control pH. Although provisions are available for adding phosphate, it has not been used since the pH was easily maintained within the desired range by morpholine alone. In general, a 1% solution of both chemicals has been fed to either the boiler feedwater line or to the hotwell, depending on evaporator operation. Oxygen concentrations in the boiler water and steam were reduced to essentially zero and in the hotwell to about 0. 01 ppm. With minor exceptions, the same oxygen levels were maintained throughout the entire full power run. Table III shows typical oxygen residuals.

Since the secondary system had been filled with demineralized water prior to start-up, chlorides were very low throughout the full power run, even in the steam generator blowdown. As shown in Table IV, chloride concentrations were well within the specifications of 0. 5 ppm maximum chloride concentration.

The pH of the secondary system was easily maintained at 8. 5 to 9. 0 by feeding morpholine either to the boiler feed or to the hotwell. Since morpholine carries over with the steam, both the steam and condensate systems were protected by the alkaline pH.

V. Waste Disposal

The employment of the closed purification system has precluded extensive waste disposal facilities. Unlike most nuclear power plants, the APPR-1 waste disposal system has been so minimized that extensive appropriations have not been necessary for this operation.

The principal source of radioactive wastes is the demineralizer resins in the primary purification system. In the process of purification, radioactive as well as non-radioactive substances are removed. The buildup of radioactivity on the resin beds is significant at the time of the exhaustion of these resins. To facilitate simple disposal, a satisfactory but extremely economical unit was designed and constructed as shown in Figure 5. This unit is twelve inches in diameter by thirty-six inches high. Upon exhaustion, the complete unit, that is, the resin and housing, will be removed from the APPR-1, placed in a lead shipping cask and sent to a designated burial facility.

Other waste disposal features at the APPR-1 include a 5, 000 gallon underground carbon steel tank. This tank is designed to collect primary water due to a

large buildup of activity from the unlikely event of a fuel element rupture.

Two laboratory waste tanks, each of 250 gallon capacity, are provided to receive waste fluids from the laboratory and the sampling in the demineralizer room.

TABLE I

RESIN PERFORMANCE (700 HOUR TEST)

DATE	UPSTREAM DEMINERALIZER RESISTIVITY (MILLION OHM-CM)	DOWNSTREAM DEMINERALIZER RESISTIVITY (MILLION OHM-CM)	UPSTREAM pH	DOWNSTREAM pH
4/12	0.45	2.5	6.4	6.4
4/16	0.7	3.0	7.9	6.2
4/20	0.4	2.0	8.5	7.0
4/28	0.75	2.0	7.7	7.4
4/30	0.9	2.0	7.6	6.7
6/2	1.3	4.0	7.6	7.1
6/6	2.5	4.0	7.2	6.8
6/10	0.7	4.0	8.4	6.9
6/12	0.6	4.0	8.8	6.3
6/16	0.55	2.0	8.6	7.1

TABLE II

OXYGEN RESIDUAL (700 HOUR TEST)

DATE	OXYGEN, PPM
6/1	0.0
6/2	0.0
6/3	0.0
6/4	0.0
6/6	0.0
6/9	0.01
6/10	0.04
6/11	0.03
6/14	0.02
6/15	0.01
6/16	0.01
6/29	0.04
7/1	0.03

TABLE III

OXYGEN RESIDUALS (HOTWELL)

DATE	SAMPLE NUMBER	OXYGEN CONCENTRATION (PPM)
6/3	896	0.0
6/5	958	0.0
6/7	988	0.03
6/9	1042	0.11
6/16	1258	0.02
6/22	1488	0.009
6/26	1581	0.013

TABLE IV

STEAM GENERATOR CHLORIDE CONCENTRATION

DATE	SAMPLE NUMBER	CHLORIDE CONCENTRATION
6/3	882	0. 25
6/5	935	0. 30
6/7	964	0. 10
6/9	1, 000	0. 14
6/11	1, 030	0. 13
6/12	1, 057	0. 0
6/14	1, 193	0. 25
6/15	1, 230	0. 34
6/17	1, 301	0. 17
6/19	1, 366	0. 13
6/22	1, 466	0. 10

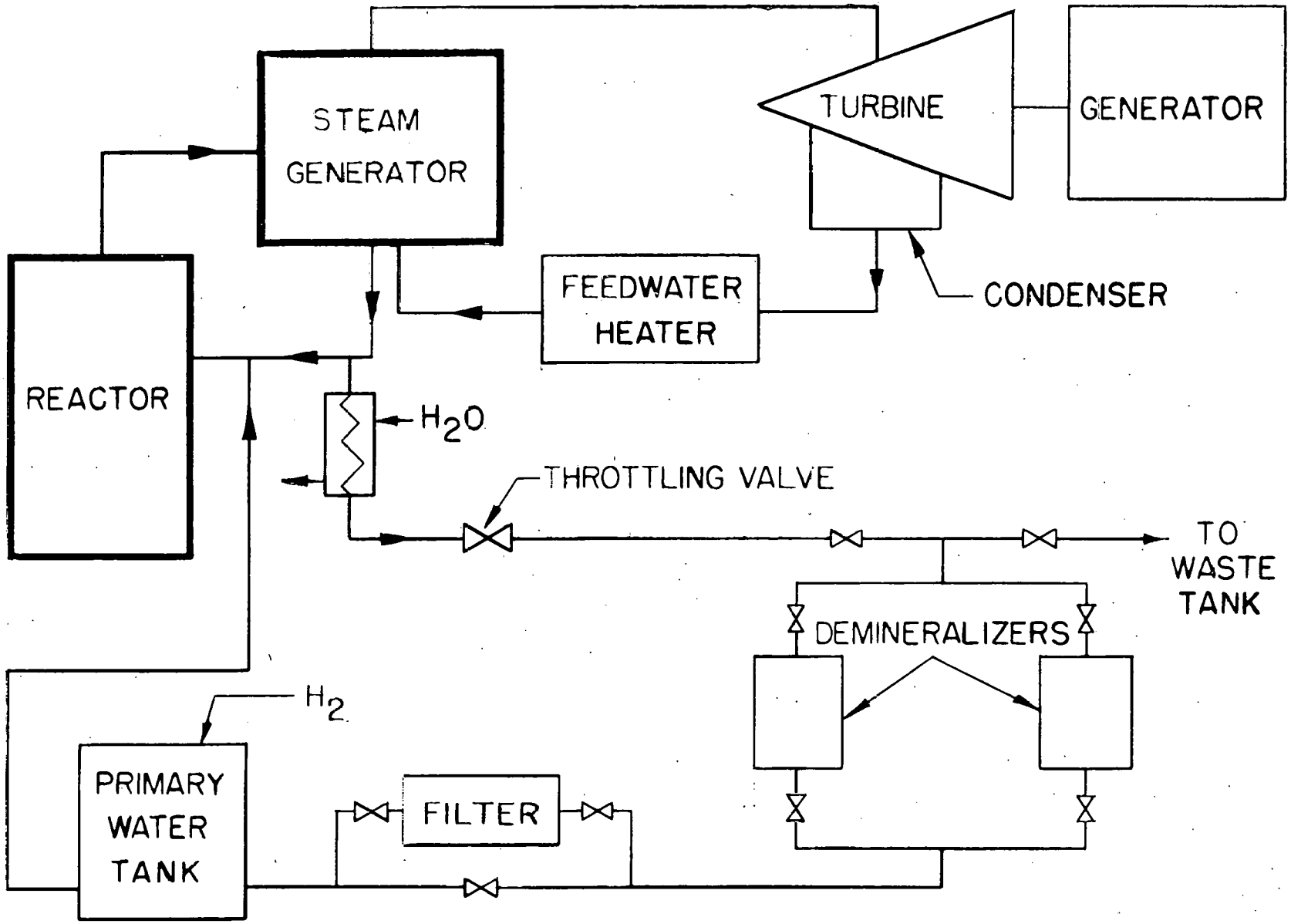

Fig. 1 Simplified Flow Diagram

Fig. 2 Oxygen Scavenging with Hydrazine

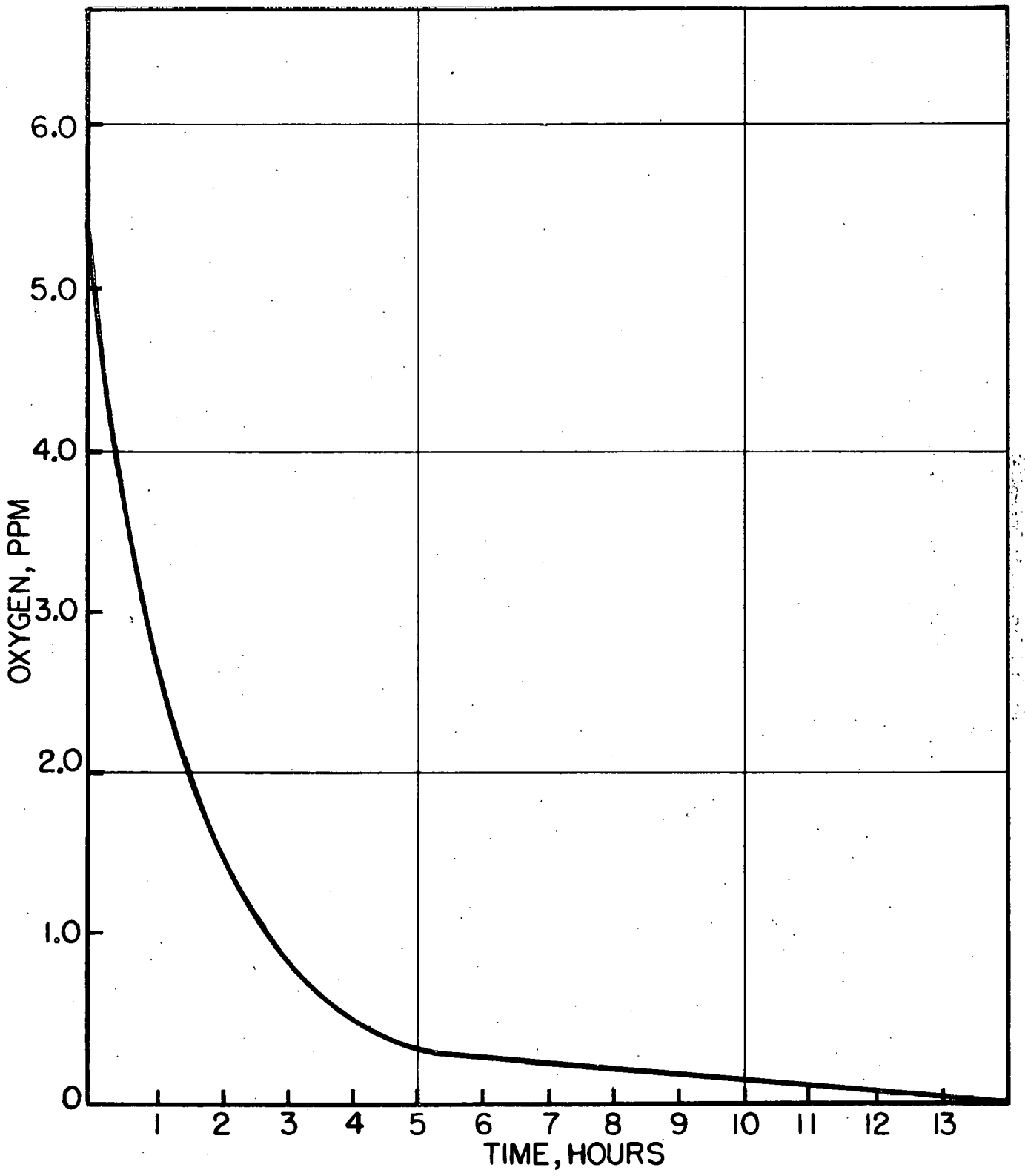

Fig. 3 Hydrogen Concentrations in Primary Make-up Tank and Primary Circulating System

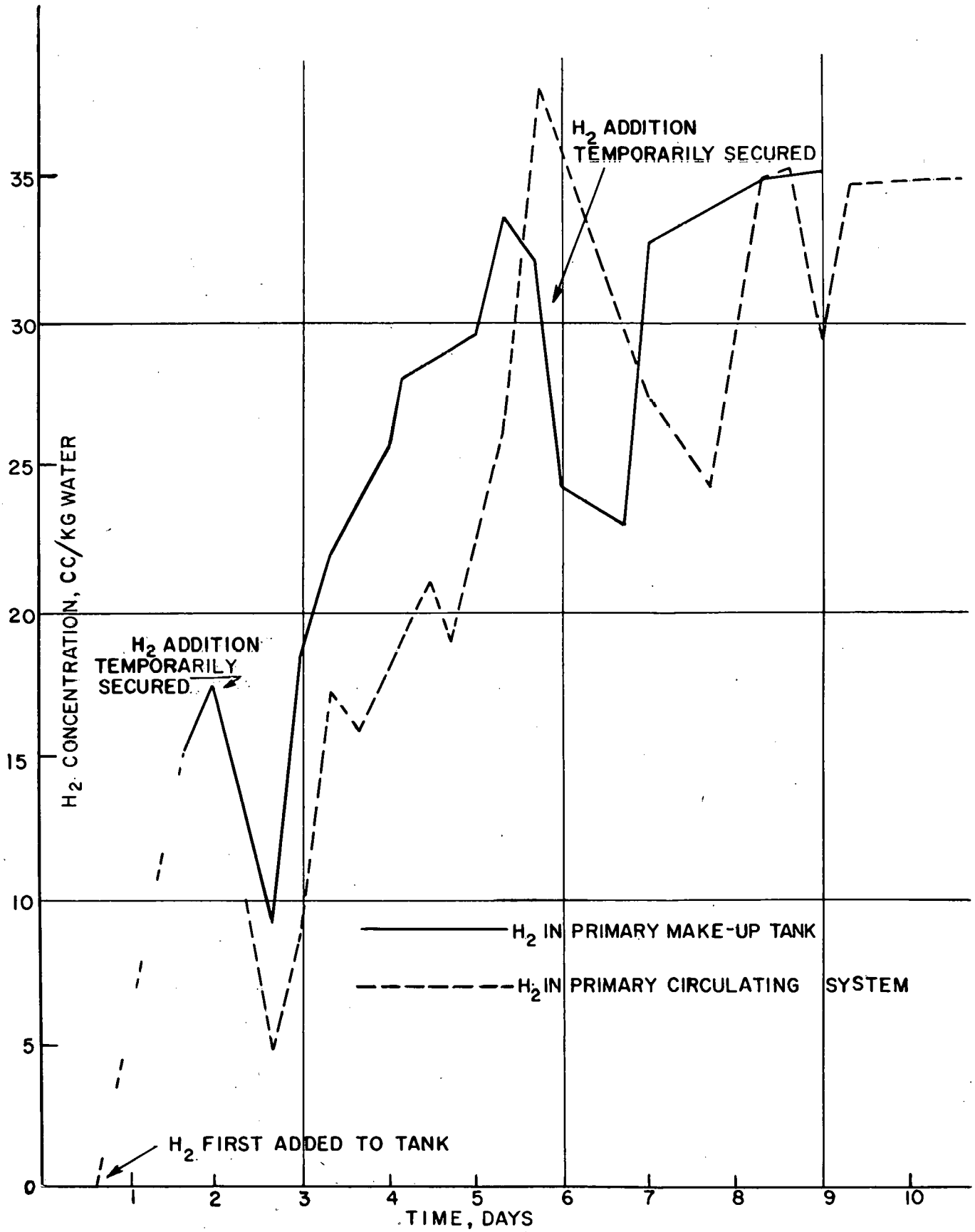

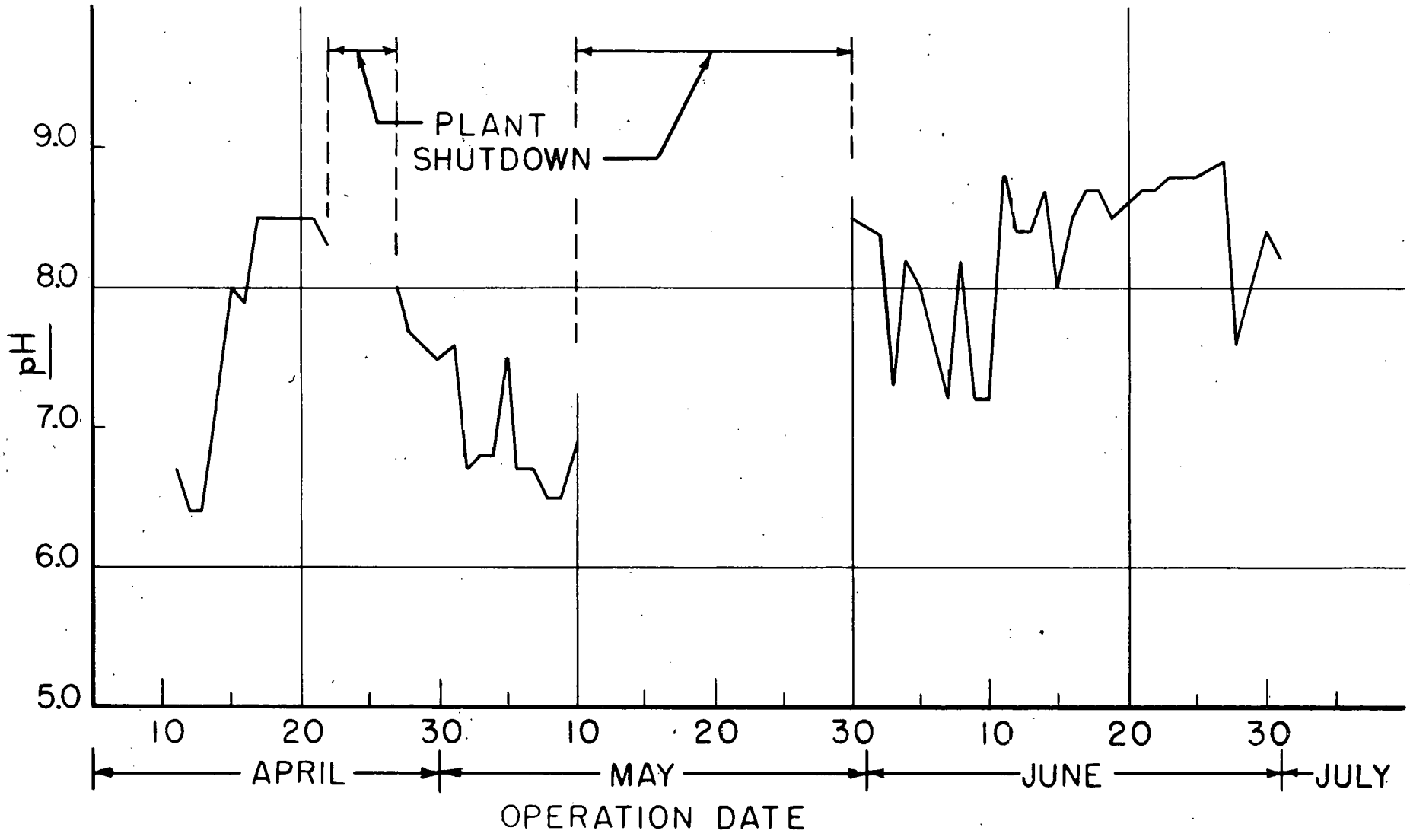

Fig. 4 Primary Coolant pH

Fig. 5 APPR Demineralizer

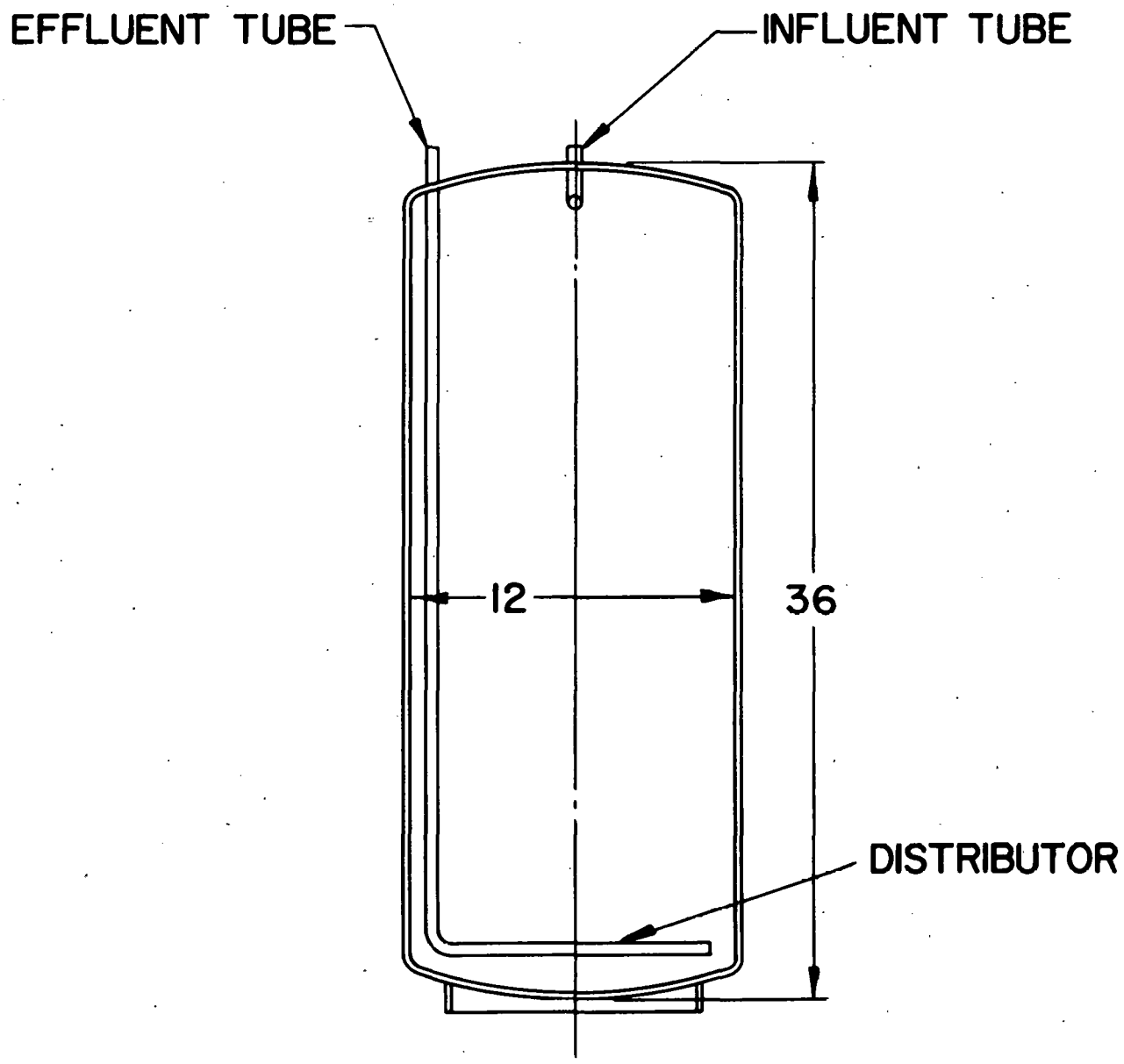

APPR-1 RADIOCHEMICAL DATA

BY

W. J. Small

J. L. Zegger

A. L. Medin

Presented at the Second Winter Meeting of The American Nuclear Society on October 28, 1957 in New York City.

LIST OF FIGURES

APPR-1 RADIOCHEMICAL DATA

I. Introduction:

The Army Package Power Reactor, located at Fort Belvoir, Virginia, is a heterogeneous, water-cooled and moderated reactor which employs enriched uranium fuel clad in stainless steel. The reactor is capable of producing 10,000 KW of heat while generating about 2,000 KW of electricity. An extensive testing program has been conducted at the APPR-1 including a 700-hour power performance test. Prior to and during this test a study was undertaken to obtain information concerning short-lived nuclides in the primary system. Work involved measuring gross beta-gamma activity with a Geiger-Muller counter and was directed toward obtaining information on the following:

1. Identification and characterization of short-lived nuclides (less than 6 hours).
2. Determination of absolute activity to ascertain the equilibrium values of short-lived nuclides at full power.
3. Decontamination values of the demineralizer system.

A long-lived nuclide program, performed in conjunction with this particular study, indicated that the nuclides $Co^{58,60}$, $Fe^{59,55}$, Mn^{54}, and Cr^{51} were present and accounted for approximately 80% of the long-lived activity. From a consideration of structural and cladding materials, together with experiences at other reactors, it was expected that among the principal short-lived nuclides would be Mn^{56}, Ni^{65}, Si^{31}, N^{16}. Fig. 1 lists the characteristics of these particular nuclides. It is true that A^{41} has been reported in the primary coolant of other systems. However, in a deaerated system like the APPR-1, the possibility for the formation of this nuclide is very small.

II. Sampling Procedure:

The sampling procedure involved initially collecting samples upstream of the demineralizer. From these samples aliquots were then taken, evaporated to dryness in a planchet, and counted for beta-gamma activity with a mica window G. M. detector. This procedure naturally excluded detection of any volatile nuclides, i. e., N^{16}.

III. Nuclides Detected:

Decay and beta energy results indicated the presence of Mn^{56} and/or Ni^{65} as the major components. On the basis of lead absorption data, the unknown nuclide was believed to be Mn^{56}. Fig. 2 compares the known nuclear properties of these nuclides with the observed values. The Si^{31} with a half-life of 2. 6 hours has been omitted because of its 1. 5 Mev beta particle and weak gamma. The beta energies are too close to be separated by the usual aluminum absorption techniques and half-lives may only be differentiated by extremely precise measurements. If the two nuclides do occur together, they could best be resolved on the basis of a radio-chemical separation or by gamma spectrometry methods.

Subsequent data corroborated the earlier conclusion that the principal short-lived nuclide was chiefly Mn^{56}. Upstream samples showed a 3-hour component which represented approximately 90-95% of the total activity. Fig. 3 represents a typical decay curve of an upstream sample. The curve is a two component system with a 2. 5 hour half-life together with a 19. 5 hour half-life. The chart of isotopes lists no applicable nuclide with a half-life of 19. 5 hours; consequently this component probably represents a composite of several nuclides.

It is interesting to note that within 48 hours there was a hundredfold decrease in the primary upstream activity from 10^{-1} to 10^{-3} uc/cc. Fig. 4 lists the results of beta energy determinations on another upstream sample taken 24 hours after the sample shown in Fig. 3. The energy values, i. e., 3 Mev, 1 Mev, 0. 5 Mev are consistent with Mn^{56}. The change in percentages of the components as a function of time after sampling illustrates the importance of correcting samples to the time of sampling.

IV. Sampling Corrections:

This is perhaps an obvious point yet a necessary one which occasionally produces some interesting results as will be shown shortly. Decay correction factors were obtained by extrapolating all the gross decay curves to the time of sampling. The fraction of activity remaining after various intervals was then calculated for the upstream samples, i. e.

$$\text{Decay Factor} = \frac{\text{Activity (counts/minute) @ } t_1}{\text{Activity (counts/minute) @ } t_2}$$

Fig. 5 presents all the results for upstream samples from 4 June through 25 June. The mean of the decay factors after each time interval has been calculated and the standard deviations show only slight dispersion. The composite decay curve is given as a function of time in Fig. 6 and shows a half-life of exactly 2. 5 hours. These results indicate that during this period the gross circulating activity before purification contained nuclides with the same half-lives and in the same proportions. This is in spite of the fact that during this period the gross activity varied by a factor of 3-4! It is logical therefore to interpret this to mean that the short-lived nuclides in this system had reached their equilibrium specific activity (dpm/mg.)

by 4 June or within 48 hours after the start of the 700-hour test.

V. Circulating Activity:

The upstream circulating activity, expressed as uc/cc, during this period is given in tabular form in Fig. 7. Assuming the specific activity (dpm/mg) of the short-lived nuclides had reached their equilibrium value and this level completely masked any contribution from long-lived nuclides, a straight line parallel to the abscissa would be predicted. Since the power level and the specific activity (dpm/mg) remained constant during this period, the deviation from this expected behavior is explained on the basis that the concentration of crud varied (mgs/ml).

The downstream samples, on the other hand, showed a different non-reproducible decay pattern. Fig. 8 represents one particular decay curve. No long-lived activity was apparent and all the samples decayed to background within 24 hours. There is no apparent explanation for this behavior. Perhaps it is channeling of solids through the resin or desorption of the monovalent ions from the resin. The 84 minute half-life is in the neighborhood of F^{18} (110 minute half-life); this nuclide is suspected in other reactor systems. It is important to note that counting rates are decidely lower than for upstream samples. Therefore reliable points on the decay curves require either longer counting times or more elaborate techniques. Nevertheless within 15 hours the sample had decayed to such a point (10^{-5} uc/cc) that a dilution factor of 100 would reduce the activity to M. P. C. levels.

VI. Demineralizer Efficiency:

This brings us to a consideration of the purification system. This function is performed by one of two mixed bed demineralizers consisting of a mixture of a

strong sulfonic acid type resin in the H^+ cycle and a strong basic type resin in the OH^- cycle. One of the major functions of the demineralizer is to remove radioactive nuclides from the blowdown water. The bulk of the activity should be removed whether it is present as suspended or dissolved material in the primary blowdown system since the demineralizer acts as both a filter and an exchanger. Consequently, a valid measure of the demineralizer efficiency is the decontamination factor, which is the ratio of the radioactivity in the influent to the effluent both corrected to instant of sampling (t_o).

Efficiencies across the demineralizer were determined by sampling both the up and downstream at approximately the same time. No samples were taken more than one minute apart and all samples were corrected to instant of sampling by the correction factors presented in previous sections. Each downstream sample was corrected with its own decay curve since these were all non-reproducible. Fifty-five minutes was the longest time between sampling and assaying. The decontamination values are plotted as a function of time in Fig. 9. During the period covered by the data blowdown was maintained at 1 gpm. The semilogarithmic plot gives an equilibrium decontamination value of approximately 360, reached after 600 e.f.p.h. or about 24 days after the start of the 700-hour test. This would mean that the demineralizer was removing 360/361 or 99.72% of the activity in the influent or primary blowdown.

Normally a straight line parallel to the abscissa would be expected. This would continue until the resin was exhausted at which time the decontamination factor would drop sharply. There is no apparent explanation for the observed behavior. Since the nuclides in the influent were shown to be different than those

in the effluent, the G. M. data would be subject to some correction. However, these would be small.

VII. Conclusion:

In conclusion then,it appears that the activity of the non-volatile short-lived nuclides entirely masks contributions from long-lived nuclides in the APPR-1 circulating water. These short-lived nuclides are probably Mn^{56} and/or Ni^{65} and account for about 90-95% of the non-volatile short-lived activity. They reached an equilibrium specific activity within 48 hours after the start of the 700-hour test and did not change throughout the remainder of the test in spite of an increase in overall circulating activity. The circulating activity in the primary blowdown water is being effectively removed by the demineralizer.

Fig. 1 Short-Lived Nuclides

NUCLIDE	HALF LIFE (HOURS)	PARENT	REACTION
Mn^{56}	2.58	Mn^{55}(100)	n-γ
		Fe^{56}(91.7)	n-p
Ni^{65}	2.56	Ni^{64}(1.16)	n-γ
Si^{31}	2.62	Si^{30}(3.05)	n-γ
		P^{31} (100)	n-p
N^{16}	0.002 (7.5 SECS.)	O^{16} (99.8)	n-p

Fig. 2 Mn^{56} Nuclides

NUCLIDE	HALF LIFE (HOURS)	BETA ENERGY MEV	%	GAMMA ENERGY (MEV)
Mn^{56}	2.58	2.81	50	2.06
		1.04	30	1.77
		0.65	20	0.82
Ni^{65}	2.56	2.10	57	1.49
		1.01	14	1.12
		0.60	29	0.37
UNKNOWN	2.7-3.0	2.6-3.0	55	2.0
NUCLIDE		1.0-1.1	45	

Fig. 3 Primary Water Decay Upstream Demineralizer June 10, 1957

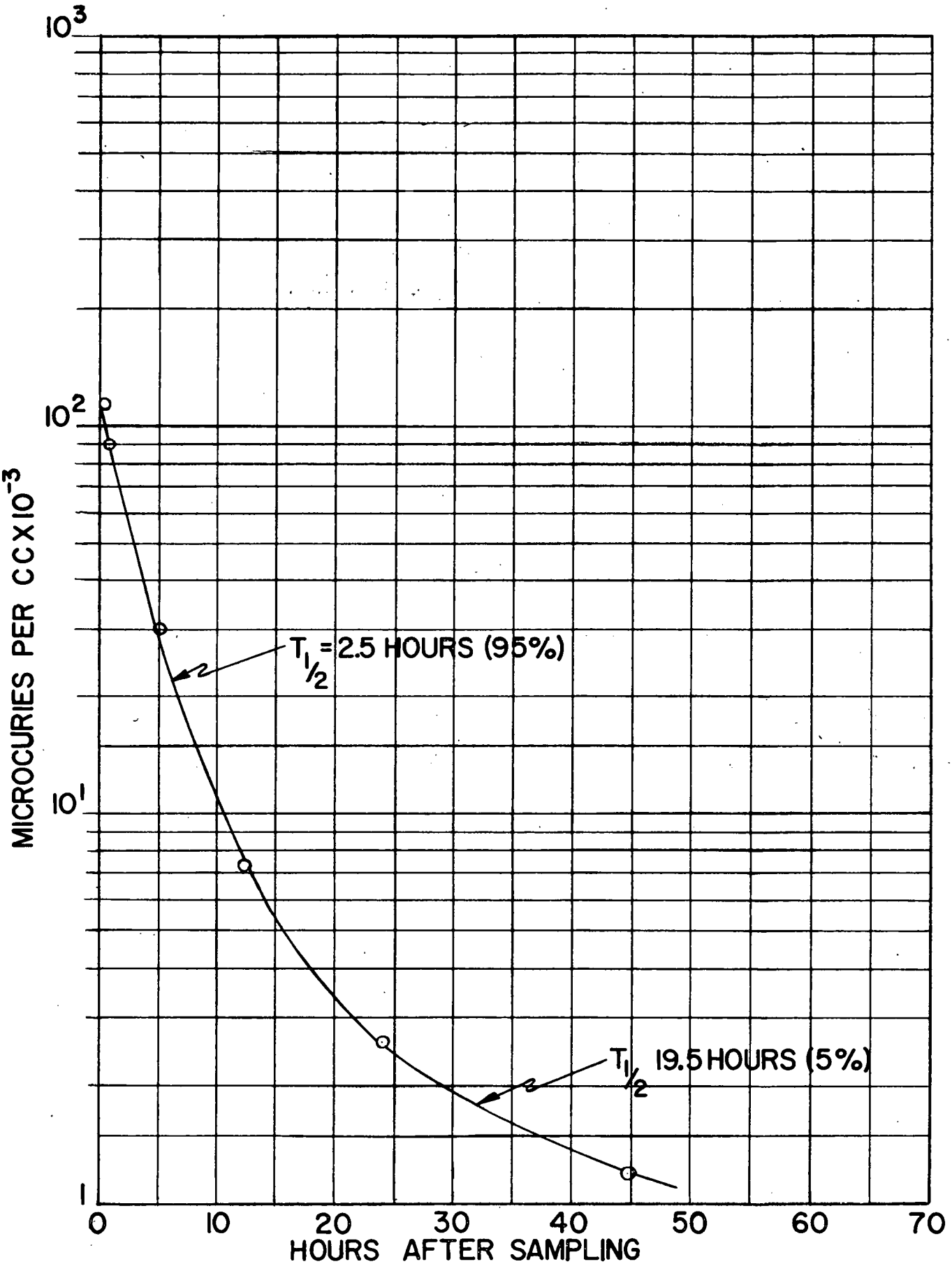

Fig. 4 Beta Energy Values - Upstream Demineralizer June 11, 1957

HOURS AFTER SAMPLING	BETA ENERGY	
	MEV	PERCENT
1.5	3.0	28.1
	1.3	38.9
	0.5	33.0
9.8	3.0	17.4
	1.0	44.3
	0.3	38.3

Fig. 5 Upstream Decay Factors

	HOURS AFTER SAMPLING							
DATE	0.5	1.0	1.5	2.0	2.5	3.0	3.5	4.0
JUNE 4	.89	.78	.67	.58	.50	.44	.39	.33
JUNE 10	.89	.77	.66	.57	.50	.44	.38	.34
JUNE 11	.89	.78	.66	.60	.52	.46	.41	.36
JUNE 14	.88	.74	.63	.54	.43	.38	.32	.27
JUNE 22	.89	.78	.71	.63	.57	.51	.45	.40
JUNE 26	.86	.74	.64	.55	.47	.41	.35	.30
MEAN	.88	.77	.66	.58	.50	.44	.38	.33
S.D.	0.01	0.02	0.03	0.03	0.04	0.04	0.04	0.04

Fig. 6 Upstream Decay Factors

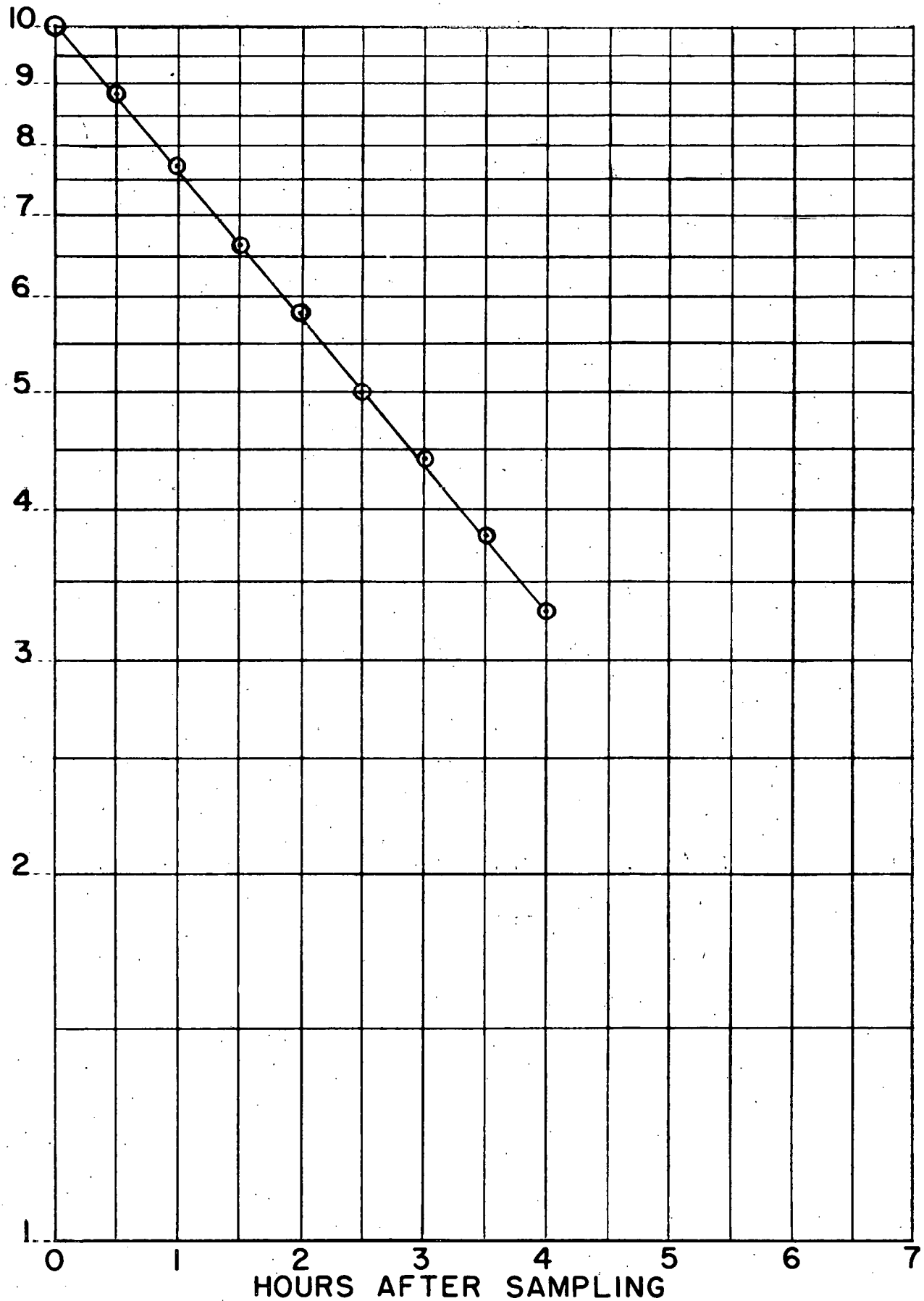

Fig. 7 Gross Activity - 700 Hour Test

DATE	efph	uc/cc x 10^{-2}
3 JUNE	150	7.6
4 JUNE	154	7.9
10 JUNE	221	12.6
11 JUNE	241	12.7
11 JUNE	245	15.1
14 JUNE	319	17.8
22 JUNE	491	22.8
24 JUNE	539	21.3
26 JUNE	589	15.3

Fig. 8 Primary Water Decay Downstream Demineralizer June 4, 1957

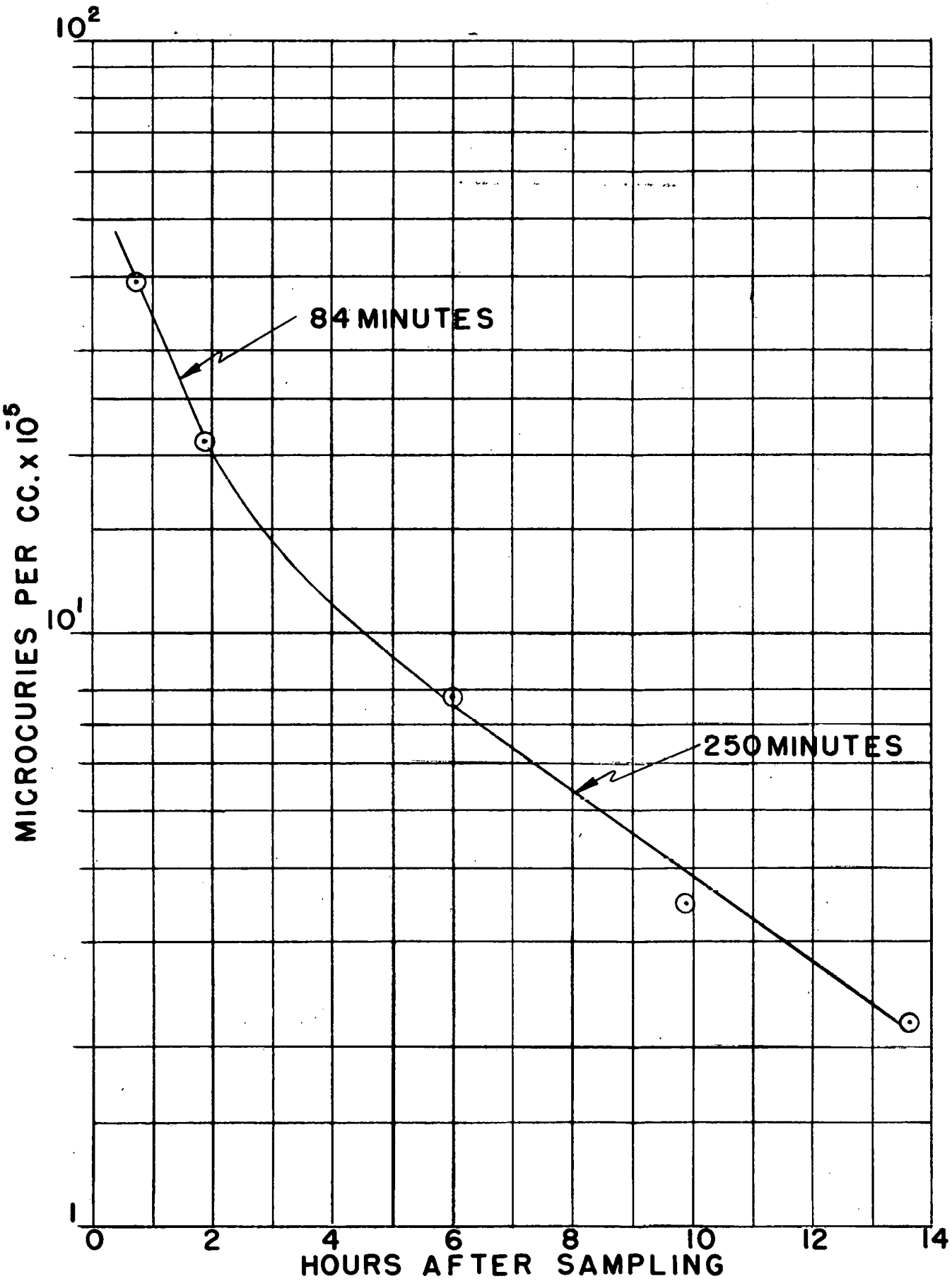

Fig. 9 Decontamination Factors - 700 Hour Test